UC Berkeley
SEMM Reports Series

Title

Evaluation of Discrete Methods for the Linear Dynamic Response of Elastic and Viscoelastic Solids

Permalink

https://escholarship.org/uc/item/7vj1x3dc

Author

Goudreau, Gerald

Publication Date

1970-06-01

REPORT NO. 69-15

EVALUATION OF DISCRETE METHODS FOR THE LINEAR DYNAMIC RESPONSE OF ELASTIC AND VISCOELASTIC SOLIDS

by

G. L. GOUDREAU

JUNE 1970

EVALUATION OF DISCRETE METHODS FOR THE LINEAR

DYNAMIC RESPONSE OF ELASTIC AND VISCOELASTIC SOLIDS

by

G. L. Goudreau

Graduate Student in Civil Engineering
University of California at Berkeley

ACKNOWLEDGEMENT

This work was submitted in partial fulfillment of the requirements for the degree of Doctor of Philosophy in Engineering in the Graduate Division of the University of California at Berkeley.

The author wishes to thank Professors K.S. Pister, C.D. Mote, and Chairman R.L. Taylor who served on the dissertation committee. Also, the assistance of Shirley Edwards who did the typing, and William Kot and Elizabeth Winkler who drew the figures, is gratefully acknowledged.

The author's introduction to problems of wave propagration is credited to Dr. Yalcin Mengi, who has been an inspiring colleague. The assistance of graduate students Paul Smith and Thomas Hughes with the numerical examples is appreciated.

The deepest gratitude is reserved for the author's wife and his four children whose patience, love and understanding these past five years were essential to the completion of this work.

CONTENTS

1. INTRODUCTION

The approximation of the motion of solid continua by a finite number of degrees of freedom is classical [1]. The essence of Lagrangian mechanics is representation of the kinetic and potential energy of a body in terms of a finite number of generalized coordinates. Extremization of Hamilton's principle yields Lagrange's equations of motion. If the motions of a body are restricted to small excursions from a state of equilibrium or rigid body motion, the linear theory of small oscillations is generated.

For some problems, the configuration of a mechanical system leads naturally to the idealizations of concentrated masses, springs, and linkages. In these cases, the selection of the generalized coordinates is simplified, and no further refinement is sought. For the more general problem of deformable solids, the intractability of the governing field equations often leads one to accept a finite degree of freedom approximation. In this case there is no obvious set of generalized coordinates. Not only does one need to be able to define a convergent sequence of approximations, but to appreciate the qualitative nature of the errors in the finite model.

There are two approaches to reducing the field problem to a finite number of degrees of freedom. Once the inertia is "lumped" at a finite number of nodal points, the elastic restoring forces may be expressed in terms of the nodal displacements by exact or approximate static relations. Alternatively, the Rayleigh-Ritz procedure [10] may be used to spatially discretize variational principles. Unless the basis functions are orthogonal with respect to the mass or stiffness operators,

the mass and stiffness matrices of the discretized set of equations
will be non-diagonal or coupled.

The finite element method may be regarded as a particular case
of the Ritz method, ideally suited to the spatial discretization of a
linear differential operator defined on an arbitrary inhomogeneous
domain [6 - 11]. In that the basis functions are selected with minimum
support (i.e., the stiffness of a node is directly coupled only with
adjacent nodes), the method leads to an algebraic problem with narrowly
banded coefficient matrices. The equations resulting from the principle
may be regarded as a difference equation, though not necessarily the
same one that would result from conventional discretization of the
differential equation. The superiority of the variational technique for
the generation of difference equations lies in the ease with which
irregular meshes, arbitrary body forces, material interfaces, and natural
boundary conditions can be accommodated. Further, the algebraic system
is symmetric for all self-adjoint operators (an advantage not shared by
conventional finite difference techniques). The variational method
allows an elegant proof of convergence of the approximation in the
energy norm [12], but appears less amenable to a pointwise estimation
of the error in the function than finite difference methods generated
by Taylor series expansion. The extensive application of the finite
element method to linear elasto-static field problems is well documented
[13 - 15].

For linear elastic bodies, the solution of forced vibration
problems is classically obtained by the method of normal modes [16].
The separation of space from time variables leads to an eigen-problem
for the exact or approximate determination of the eigenvalues and eigen-
functions (or vectors). Since the higher modes of the discrete model

are progressively more in error, the number of degrees of freedom must be selected large enough so that the dominant lower modes are sufficiently accurate. The particular integrals of the normal equations are determined exactly or numerically, depending on the input function. In the last few years, the finite element concept has been applied in this manner [14, 17, 18, 19] to vibration problems of elastic media.

In impact problems the peak stress response occurs during the time span of the first few reflections. Reflection from the interface with an acoustically denser medium increases the stress. Reflection of a compressive pulse from a free boundary will produce tension, and for materials weak in tension, the phonomenon of "scabbing" may result. As time progresses, geometric and material dispersion of the pulse occurs, diminishing the peak response. Thus, early time response is critical. In this time range, the lower modes of the overall domain do not dominate the response as at later times after multiple reflection.

Comparison of the solutions of discrete and continuous eigen-problems when they can be found does help evaluate the "consistent" vs "lumped" mass approximations. This evaluation has usually been made in numerical rather than analytic form [19, 20]. In the case of the string (or simple bar) the analytic solution of the lumped mass approximation was obtained by Lord Rayleigh [21], and that for "consistent" mass was presented quite recently by Washizu [22]. Leckie [23] did the same for a finite difference equation for the beam. Although these efforts have been directed toward the lower modes, the analytic solutions of the difference equations permit the display of the errors in the entire discrete spectrum.

Time integration of initial value problems has an extensive literature, and Richtmyer and Morton [54] provides an excellent text. A general family of one step methods which includes several well known special cases was discussed by Newmark [47]. A unique integration scheme was presented by Wilson [50], and applied to the dynamic response of two-dimensional solids. Although the linear problems are capable of a modal analysis, the development of step-by-step methods provides a starting point for integrating the response of non-linear problems.

For viscoelastic solids, space and time variables can be separated only in exceptional cases. If the viscoelastic properties are temperature dependent, and the temperature is a function of space and time, they are definitely not separable and the time solution of the discrete equations must be integrated directly. Such was done for the quasi-static case by Taylor, Pister and Goudreau [29], and for the dynamic case by Nickell [42].

An important feature of the hyperbolic partial differential equations governing motion of elastic and viscoelastic solids, not shared by finite degree of freedom systems, is the existence of solutions possessing surfaces of discontinuity (i.e. the propagation of wave fronts with finite velocity). Although a theoretical treatment is presented by Courant [2], the theory of characteristics has been applied only to problems with one space variable. Important contributions in applying the method of characteristics to elastic wave propagation problems have been made by Chou and Mortimer [56], and by Mengi and McNiven [61] Insight into the two dimensional character of wave propagation solutions was revealed by Bertholf's finite difference study of a bar [57].

Chapter 2 presents the governing field equations of the linear mechanical theory of solids, including the extension of Hamilton's principle to viscoelastic solids by Taylor [3], whose Euler equations are the integro-differential equations of motion. The defect of this principle in generating initial conditions is remedied by the variational principle introduced for elastodynamics by Gurtin [4], and extended to viscoelastic media by Leitman [5]. Through the use of convolutions, a principle is constructed whose Euler equations are the integral equations of motion, containing the initial conditions. Finally, the viscoelastic characterization most suitable for stress analysis is discussed, along with the problems in obtaining it.

Chapter 3 presents the closed form solutions for the lumped and consistent mass finite element models of the simple bar, membrane and beam operators. Further, the spectral approximation to the two radial mode Mindlin-Herrmann bar theory [24, 25] is studied.

To exhibit the errors in the transient solutions introduced by the spatial discretization, simple bar theory is employed to study the early time response of an elastic bar to impact on an elastic spring. The foundation spring constant serves as a parameter defining the transition from an acceleration wave into a shock wave. Exact time solutions for lumped mass, consistent mass, and a higher order finite difference approximation are compared with the exact eigen-expansion truncated to and equal number of terms.

A second impact example of a step stress on a half space is studied. The converged time solutions for finite degree of freedom models for the above three discretizations are compared with the exact solution.

Chapter 4 discusses step-by-step schemes for the time integration of discrete systems. The implications of the Newmark family of methods on early time transient response is emphasized. The methods of Wilson [50] and Nickell [42] are also considered. The concern is not on accurate integration of the discrete system as much as the combined effect of space and time integration errors on the approximation to the hyperbolic problem. The dispersive approximation afforded by discrete systems is compounded by time integration errors. This is revealed by several one-dimensional examples. Finally, the scheme presented in [29] for discretizing the viscoelastic history integral is found to carry over to the dynamic case.

Chapter 5 discuses a property of the explicit time integration scheme which gives it the power to capture discontinuities in the propagation of stress waves. The method embodies the "direct" or "discontinuous step" method of Mehta and Davids [55] and Koenig and Davids [59] in conjunction with a finite element spatial discretization. Excellent results are presented for several one-dimensional elastic and viscoelastic examples. However, stability problem can arise, limiting the generality of the method. Finally, the two dimensional problem of a step stress on the end of a short bar is examined and the detail near the discontinuity front is revealed without the mesh induced oscillations of Bertholf's finite difference results [57].

2. LINEAR MECHANICAL THEORY OF SOLIDS

In fullest generality, the theory of solid continua treats the coupling of mechanical with thermodynamic, electrical, chemical, and other state variables. Such coupled field theories can be consistently linearized with respect to all state variables. However, by the linear mechanical theory of solids shall be meant the general theory of elastic and viscoelastic solids linearized with respect to mechanical variables. The resulting theory may depend on non-mechanical variables (or their histories), which are assumed prescribed. Such variables will be typified by the thermal variable temperature. In uncoupled thermo-mechanics the work done by deformation is neglected in the energy balance equation, which reduces to Fourier's law of heat conduction for the determination of temperatures.

The formulation of a linear mechanical theory of solids has been treated extensively, as a general three dimensional field problem [26, 27, 28], and in the many kinematic and constitutive subclasses of bars, beams, plates, and shells. The basic equations and assumptions of the three dimensional theory will be restated here both as local field equations and as global variational principles.

A. Constitutive Equation for Linear Mechanical Theory

For a simple material, the stress at a particle of the body is determined by the history of deformation and other non-mechanical variables at the particle. The motion of the body will be restricted to small deformations from an unstressed reference state of rigid body motion. If the body is simultaneously subjected to a non-mechanical variable change, (say temperatures), relative to the same reference state,

the stress is given by the equation

$$\underset{\sim}{\sigma}(\underset{\sim}{x},t) = \underset{s=-\infty}{\overset{s=t}{F}} [\underset{\sim}{\varepsilon}(\underset{\sim}{x},s), T(\underset{\sim}{x},s); \underset{\sim}{x}, t] \qquad (2.1)$$

where $\underset{\sim}{\sigma}$, $\underset{\sim}{\varepsilon}$ are the stress and small strain tensors at the particle $\underset{\sim}{x}$ at time t; T is the temperature at $\underset{\sim}{x}$ and F is the thermomechanical response functional of the body. The linear mechanical theory restricts the functional to be linear in strain while still non-linear in temperature. For a non-aging material (2.1) can be replaced by the hereditary integral representation[*]

$$\underset{\sim}{\sigma}(\underset{\sim}{x},t) = \int_{\tau=-\infty}^{\tau=t} \underset{s=0}{\overset{s=t}{C}} [T(s), \underset{\sim}{x}; t-\tau] \frac{\partial}{\partial\tau} [\underset{\sim}{\varepsilon}(\tau) - \underset{\sim}{\theta}(\tau)]d\tau \qquad (2.2)$$

In (2.2) the pseudo-temperature introduced by Morland and Lee [28]

$$\underset{\sim}{\theta}(\tau) = \int_{T_0}^{T} \underset{\sim}{\alpha}(T') \, dT' \qquad (2.3)$$

has been used, where $\underset{\sim}{\alpha}$ is the temperature dependent coefficient of thermal expansion tensor and the kernel

$$\underset{\sim}{C}(\underset{\sim}{x},t,\tau) = \underset{s=0}{\overset{s=t}{C}} [T(s); \underset{\sim}{x}; t-\tau] \qquad (2.4)$$

is a fourth rank relaxation modulus tensor, whose value depends on the temperature history of the material at the particle $\underset{\sim}{x}$.

---

[*] The number of contractions between two adjoined tensors will be implied by the context. For example, since in (2.2) C is a rank four tensor, and $\underset{\sim}{\sigma}$, $\underset{\sim}{\varepsilon}$, and $\underset{\sim}{\theta}$ are of rank two, a double contraction is implied between C and $\frac{\partial\underset{\sim}{\varepsilon}}{\partial\tau}$, $\frac{\partial\underset{\sim}{\theta}}{\partial\tau}$.

For lack of a better thermal characterization, and to simplify the numerical problem, consideration is restricted to thermorheologically simple (TS) materials [28, 29, 30], where

$$\underset{s=0}{\overset{s=t}{\underset{\sim}{C}}} [T(s), \underset{\sim}{x}; t-\tau] = \underset{\sim}{C} [\underset{\sim}{x}, T_0; \xi(t) - \xi(\tau)] \qquad (2.5)$$

and where

$$\xi(\tau) = \int_0^\tau \phi [T(s)] ds \qquad (2.6)$$

is the reduced time and $\phi(T)$ is the temperature shift function assumed to be an intrinsic property of the material, normalized by the condition $\phi(T_0) = 1$. Thus, (2.2) becomes

$$\underset{\sim}{\sigma}(\underset{\sim}{x},t) = \int_{-\infty}^t \underset{\sim}{C} [\underset{\sim}{x}, T_0; \xi(t) - \xi(\tau)] \frac{\partial}{\partial\tau} [\underset{\sim}{\varepsilon}(\tau) - \underset{\sim}{\theta}(\tau)] d\tau \qquad (2.7)$$

Since for any mechanical problem, it is necessary to start the analysis at some fixed time, say $t_0 = 0$, let

$$\underset{\sim}{\sigma}(\underset{\sim}{x},t) = \underset{\sim 0}{\sigma}(\underset{\sim}{x},t) + \int_0^t \underset{\sim}{C}[\underset{\sim}{x},T_0;\xi(t)-\xi(\tau)] \frac{\partial}{\partial\tau} [\underset{\sim}{\varepsilon}(\tau) - \underset{\sim}{\theta}(\tau)] d\tau \quad (2.8)$$

where

$$\underset{\sim 0}{\sigma}(\underset{\sim}{x},t) = \int_{-\infty}^0 \underset{\sim}{C}[\underset{\sim}{x},T_0;\xi(t)-\xi(\tau)] \frac{\partial}{\partial\tau} [\underset{\sim}{\varepsilon}(\tau)-\theta(\tau)] d\tau \qquad (2.9)$$

is a function of the history of deformation and temperature up to time zero and must be known to ensure a well posed problem.

If the body is assumed to be free of stress up to time zero, $\underset{\sim 0}{\sigma} \equiv 0$. For the consideration of the propagation of surfaces of discontinuity, it is then convenient to integrate (2.8) by parts.

$$\sigma(x,t) = C_0 : (\varepsilon(t) - \theta(t)) - \int_0^t \frac{\partial}{\partial \tau} C[x, T_0 ; \xi(t) - \xi(\tau)][\varepsilon(\tau) - \theta(\tau)] d\tau$$

(2.10)

where $C_0 = C[x,0]$ is the instantaneous modulus governing the propagation of wave fronts, and is assumed to be independent of temperature and thus not a function of time. It is now possible to introduce the notation

$$\sigma(x,t) = C_0 : (\varepsilon - \theta) + \dot{C} \circledast (\varepsilon - \theta)$$

(2.11)

where

$$\dot{C} = + \phi[T(\tau)] \frac{\partial}{\partial s} C[x, T_0 ; s] \Big|_{s = \xi(t) - \xi(\tau)} ,$$

(2.12)

the symbol $*$ denotes the convolution of two functions in the sense

$$f * g = \int_0^t f(t-\tau) g(\tau) d\tau$$

(2.13)

and the symbol $\circledast$ denotes the ordinary convolution extended to include reduced time in the left hand function. Note that $*$ is a commutative operation, while $\circledast$ is not. For an elastic material $\dot{C} \equiv 0$.

B. Formulation of the Initial/Boundary Value Problem

For a solid undergoing small deformations, the balance of linear and angular momentum yields respectively, the local field equations

$$\nabla \cdot \sigma + b = \rho \ddot{u}$$

and

$$\sigma = \sigma^T$$

(2.14)

where $\underset{\sim}{b}(\underset{\sim}{x})$ is a prescribed body force vector, $\underset{\sim}{u}$ the displacement vector, $\rho(\underset{\sim}{x})$ the mass density, and $\underset{\sim}{\nabla}$ the gradient operator.

The strain displacement relations are

$$2\underset{\sim}{\varepsilon} = [\underset{\sim}{\nabla}\underset{\sim}{u} + (\underset{\sim}{\nabla}\underset{\sim}{u})^{\mathsf{T}}] \qquad (2.15)$$

To these equations, and the constitutive equation (2.11) are adjoined the boundary conditions,

$$\underset{\sim}{T}(\underset{\sim}{x},t) = \underset{\sim}{n} \cdot \underset{\sim}{\sigma} = \underset{\sim}{\overline{T}} \quad \text{on} \quad S_\sigma$$

$$\underset{\sim}{u}(\underset{\sim}{x},t) = \underset{\sim}{\overline{u}} \quad \text{on} \quad S_u \, , \qquad (2.16)$$

where $\underset{\sim}{\overline{T}}$, $\underset{\sim}{\overline{u}}$ are respectively the prescribed surface tractions and displacements on complementary part S_σ and S_u of the surface of the region of space R occupied by the body, and $\underset{\sim}{n}$ is the unit outward normal to the boundary surface.

An arbitrary specification of initial conditions

$$\underset{\sim}{u}(\underset{\sim}{x},0) = \underset{\sim}{u}_0(\underset{\sim}{x}) \qquad (2.17)$$

$$\underset{\sim}{\dot{u}}(\underset{\sim}{x},0) \equiv \frac{\partial}{\partial t} \underset{\sim}{u}(x,t) \Big|_{t=0} = \underset{\sim}{\dot{u}}_0(\underset{\sim}{x})$$

would imply some non-zero initial history, and the knowledge of $\underset{\sim}{\sigma}_0(\underset{\sim}{x},t)$. In the following, consideration will be restricted to an initial stress free state of rigid body motion, for which $\underset{\sim}{\sigma}_0 \equiv 0$.

Substitution of the constitutive relation (2.11) and kinematic relation (2.15) into the momentum balance equation (2.14) yields the displacement equation of motion

$$\nabla \cdot \underset{\sim}{C}_0 : \nabla u + \nabla \cdot \dot{\underset{\sim}{C}} \circledast \nabla u + \underset{\sim}{p} = \rho \ddot{\underset{\sim}{u}} \tag{2.18}$$

where

$$\underset{\sim}{p} = \underset{\sim}{b} - \nabla \cdot [\underset{\sim}{C}_0 : \underset{\sim}{\theta} + \dot{\underset{\sim}{C}} \circledast \underset{\sim}{\theta}] $$

This integro-differential equation can be transformed into an integral equation, incorporating the initial conditions, which will be needed for the Gurtin type variational theorem discussed later. In the manner of Gurtin [4], let $g(t) = t$ and $\dot{g} = 1$ for $t>0$ and zero for $t<0$. Taking the convolution of (2.14) with g,

$$g * (\nabla \cdot \sigma) + \underset{\sim}{f} = \rho u \tag{2.19}$$

where

$$\underset{\sim}{f} = g * \underset{\sim}{b} + \rho(\underset{\sim}{u}_0 + \dot{\underset{\sim}{u}}_0 t) \tag{2.20}$$

is a known function of the body force and the initial conditions. Substitution of (2.11) into (2.19) yields the displacement integral equation governing motion.

$$g * \nabla \cdot \underset{\sim}{C}_0 : \nabla u + g * \nabla \cdot \dot{\underset{\sim}{C}} \circledast \nabla u + \underset{\sim}{q} = \rho \underset{\sim}{u} \tag{2.21}$$

where

$$\underset{\sim}{q} = \underset{\sim}{f} - g * \nabla [\underset{\sim}{C}_0 : \underset{\sim}{\theta} + \dot{\underset{\sim}{C}} \circledast \underset{\sim}{\theta}] \tag{2.21a}$$

C. Variational Formulation

The power of direct variational methods to discretize an operator motivates the consideration of two principles: Hamilton's principle for non-conservative systems, and a Gurtin type stationary principle developed by Leitman [4,5].

1. Hamilton's Principle

Presented by Taylor [2], Hamilton's principle extended for the linear mechanical theory of viscoelastic solids is

$$\delta \int_{t_1}^{t_2} (T + W)\, dt = 0 \tag{2.22}$$

where

$$T = \int_V \frac{1}{2}\, \rho\, \dot{\underset{\sim}{u}} \cdot \dot{\underset{\sim}{u}}\, dv \tag{2.23}$$

and

$$\delta W = - \int_V [\underset{\sim}{\sigma} : \delta\underset{\sim}{\varepsilon} - \underset{\sim}{b} \cdot \delta\underset{\sim}{u}]dv + \int_{S_\tau} \underset{\sim}{T} \cdot \delta\underset{\sim}{u}\, ds \tag{2.24}$$

If the constitutive equations (2.11) and strain displacement relations (2.15) are assumed embedded, the Euler equation is the displacement equation of motion (2.18). To establish this, the divergence theorem is needed,

$$\int_V \underset{\sim}{\nabla} \cdot \underset{\sim}{F}\, dv = \int_{\delta V} \underset{\sim}{n} \cdot \underset{\sim}{F}\, ds \tag{2.25}$$

Letting $\underset{\sim}{F} = \underset{\sim}{\sigma} \cdot \delta\underset{\sim}{u}$, and recognizing that because of the symmetry of $\underset{\sim}{\sigma}$ and the commutivity of δ with $\underset{\sim}{\nabla}$,

$$\underset{\sim}{\sigma} : \delta\underset{\sim}{\varepsilon} = \underset{\sim}{\sigma} : \delta\underline{\nabla u} = \underset{\sim}{\sigma} : \underline{\nabla\delta u} \tag{2.26}$$

and further that

$$\underset{\sim}{\nabla} \cdot [\underset{\sim}{\sigma} \cdot \delta\underset{\sim}{u}] = (\underset{\sim}{\nabla} \cdot \underset{\sim}{\sigma}) \cdot \delta\underset{\sim}{u} + \underset{\sim}{\sigma} : \nabla\delta\underset{\sim}{u} \tag{2.27}$$

then

$$\int_V \underset{\sim}{\sigma} : \delta\underset{\sim}{\epsilon} \; dv = - \int_V (\underset{\sim}{\nabla} \cdot \underset{\sim}{\delta}) \cdot \delta\underset{\sim}{u} \; dv + \int_{\delta v} \underset{\sim}{n} \cdot \underset{\sim}{\sigma} \cdot \delta\underset{\sim}{u} \; ds \quad (2.28)$$

If variations in the displacement field are required to satisfy the rigid (displacement) boundary conditions,

$$\delta W = \int_V [\underset{\sim}{\nabla} \cdot \underset{\sim}{\sigma} + \underset{\sim}{b}] \cdot \delta\underset{\sim}{u} \; dv - \int_{S_\tau} [\underset{\sim}{n} \cdot \underset{\sim}{\sigma} - \underset{\sim}{T}] \cdot \delta\underset{\sim}{u} \; ds$$

$$\delta T = \int_V \rho \; \dot{\underset{\sim}{u}} \cdot \delta\dot{\underset{\sim}{u}} \; dv \qquad (2.29)$$

Inserting (2.29) into (2.28) and integrating δT by parts,

$$\int_{t_1}^{t_2} \int_V [\underset{\sim}{\nabla} \cdot \underset{\sim}{\sigma} + b - \rho\ddot{u}] \cdot \delta\underset{\sim}{u} \; dv \; dt - \int_{t_1}^{t_2} \int_{S_\tau} [\underset{\sim}{n} \cdot \underset{\sim}{\sigma} - \underset{\sim}{T}]$$

$$\delta\underset{\sim}{u} \; ds \; dt + \left[\int_V \rho\dot{\underset{\sim}{u}} \cdot \delta\underset{\sim}{u} \; dv \right]_{t_1}^{t_2} = 0 \qquad (2.30)$$

Since $\delta\underset{\sim}{u}$ is arbitrary, the three terms must vanish independently. The first yields the equations of motion (2.14), the second the natural boundary conditions (2.16a), and the third the usual requirement of Hamilton's principle that the variations $\delta\underset{\sim}{u}$ vanish at the endpoints t_1 and t_2.

The principle says nothing about the initial conditions, which must be stated separately. When used as a direct variational principle

in space, it is unable to generate the initial conditions for the discretized coordinates. If the initial conditions are restricted to a rigid body motion, the discretized initial conditions can be sampled by inspection. However, this certainly is a defect in the general utility of the principle. A procedure to embed the initial conditions in Hamilton's principle in conjunction with a direct variational method in time was presented by Stuiver [31, 32] for a system of ordinary differential equations. However, it does not appear to resolve the spatial discretization of arbitrary initial conditions.

2. Leitman's Principle

An alternative to the integro-differential equation of motion (2.18) is the integral equation (2.21) which contains the initial conditions. It can be shown to be the Euler equation of the Gurtin type principle presented by Leitman [5], which in terms of displacement is

$$V\{\underset{\sim}{u}\} = \int_V [\tfrac{1}{2} \; \dot{g} * \underset{\sim}{C} \circledast \underset{\sim}{\varepsilon} * \underset{\sim}{\varepsilon} - \dot{g} * \underset{\sim}{C} \circledast \underset{\sim}{\theta} * \underset{\sim}{\varepsilon}$$

$$- \underset{\sim}{f} * \underset{\sim}{u} + \tfrac{1}{2} \rho \underset{\sim}{u} * \underset{\sim}{u}] \; dv$$

$$- \int_{S_\tau} g * \underset{\sim}{\overline{T}} * \underset{\sim}{u} \; ds \qquad (2.31)$$

An admissible thermomechanical state $\{\underset{\sim}{\sigma}, \underset{\sim}{\varepsilon}, \underset{\sim}{u}, \underset{\sim}{\theta}\}$ is one for which

(1) the symmetric stress tensor is determined by the constitutive equation (2.10);

(2)   the strains are obtained from the displacements by (2.15);

(3)   the displacement vector satisfies the rigid boundary conditions
      (2.16b) and the initial conditions (2.17);

(4)   the pseudo temperature θ is a prescribed function of position
      and time, associated with the solution of the heat conduction
      boundary value problem for the body. See, for example, Wilson
      & Nickell [43].

The principle states that among all admissible thermomechanical
states, that which satisfies the displacement equations of motion (2.21)
and stress boundary conditions (2.16a) is given by

$$\delta V = 0 \tag{2.32}$$

This can be seen by performing the variation

$$\delta V\{\underset{\sim}{u}\} = \int_V [\dot{g} * \underset{\sim}{C} \circledast (\underset{\sim}{\epsilon} - \underset{\sim}{\theta}) * \delta\underset{\sim}{\epsilon} - \underset{\sim}{f} * \delta\underset{\sim}{u}$$

$$+ \rho\underset{\sim}{\ddot{u}} * \delta\underset{\sim}{u}]dv - \int_{S_\tau} g * \underset{\sim}{\overline{T}} * \delta u ds \tag{2.33}$$

Noting that $\underset{\sim}{\epsilon} = \underset{\sim}{\epsilon}_0 + \dot{g} * \dot{\underset{\sim}{\epsilon}}$,   then

$$\dot{g} * \sigma = \dot{g} * \dot{g} * [\underset{\sim}{C}_0(\underset{\sim}{\epsilon} - \underset{\sim}{\theta}) + \dot{\underset{\sim}{C}} \circledast (\underset{\sim}{\epsilon} - \underset{\sim}{\theta})]$$

$$= \dot{g} * \dot{g} * [\underset{\sim}{C}(\underset{\sim}{\epsilon}_0 - \underset{\sim}{\theta}_0) + \underset{\sim}{C} \circledast (\dot{\underset{\sim}{\epsilon}} - \dot{\underset{\sim}{\theta}})]$$

$$= \dot{g} * \underset{\sim}{C} \circledast (\underset{\sim}{\epsilon} - \underset{\sim}{\theta}) \tag{2.34}$$

Now using the divergence theorem as before (2.25-2.28)

$$\delta V\{u\} = - \int_V [g * (\nabla \cdot \sigma) + f - \rho \ddot{u}] * \delta u \, dv$$

$$+ \int_{S_\tau} g * [n \cdot \sigma - \overleftrightarrow{T}] * \delta u \, ds = 0 \qquad (2.35)$$

Then invoking Gurtin's generalization of Lagrange's lemma, [4], i.e., that if for all ω

$$\int_V \upsilon * \omega \, dv = 0 \qquad (2.36)$$

then

$$\upsilon = 0, \qquad (2.37)$$

the first term yields the equations of motion (2.19) and the second the natural boundary conditions (2.16a).

It will be seen that Leitman's principle offers a means for the spatial discretization of the initial conditions, whereas Hamilton's principle does not.

D. Representation of the Relaxation Modulus

The integral formulation (2.8) of linear viscoelastic constitutive theory requires the experimental determination of the kernel C, which is a fourth rank tensor of relaxation moduli. Only isotropic characterization is considered here, where only two scalar relaxation functions determine the tensor. Often, the material is assumed to be either elastic in dilatation, or to have a constant Poisson ratio, necessitating only one relaxation test.

Analyses may be performed using tabulated experimental data, as for example formulated by Sackman & Kaya [33]. However, for computational accuracy it is desirable to smooth the data by fitting an analytical expression to it. To minimize computation and storage in step-by-step time integration methods, a degenerate form is assumed for a typical non-aging kernel function, say the shear modulus.

$$G(t) = G_0 + \sum_{i=1}^{I} G_i \exp\left(-\frac{t}{\lambda_i}\right) \qquad (2.38)$$

where λ_i are characteristic relaxation times. This form is equivalent to a generalized Maxwell model. Thus,

$$\dot{G} * \underset{\sim}{u} = -\sum_{i=1}^{I} \frac{G_i}{\lambda_i} \exp\left(-\frac{t}{\lambda_i}\right) \int_0^t \exp\left(\frac{\tau}{\lambda_i}\right) \underset{\sim}{u}(\tau)\, dz \qquad (2.39)$$

and the current value of t is extracted from the I history integral vectors which can be accumulated step by step as $\underset{\sim}{u}$ is determined. An alternative form which also possesses this same property is being investigated by Sackman [34], using trigonometric functions, say

$$G(t) = G_0 + \sum_{i=1}^{I} G_i \cos \alpha_i t \qquad (2.40)$$

$$\dot{G} * \underset{\sim}{u} = -\sum_{i=1}^{I} G_i \alpha_i \left[\sin \alpha_i t \int_0^t \underset{\sim}{u} \cos \alpha_i \tau\, d\tau \right.$$

$$\left. - \cos \alpha_i t \int_0^t \underset{\sim}{u} \sin \alpha_i \tau\, d\tau \right] \qquad (2.41)$$

which requires accumulation of 2I history integral vectors.

Since both of the above sets of functions are relatively complete, any degenerate kernel may be approximated arbitrarily well by a sufficiently large number of terms (see p. 115 of [9]). Computational

effort is proportional to I, which should be no larger than needed. Up to ten terms are being used in quasistatic analyses [29, 35], but since in impact problems early time response is most important, fewer terms should suffice. In any case, the finite representation selected should best approximate the kernel in the time range under study, and not be extrapolated much beyond. A poor oscillatory fit has been reported by Nickell [35] if the characteristic times are chosen more than a decade apart. Lanczos [36] discusses the difficulty obtaining a unique exponential fit. To this writer, though, it appears that his poor results are due to the near equal real time spacing of the characteristic times which could be remedied by logarithmic spacing.

An alternative differential characterization of the kernel has been developed by Distefano & Pister [37], which appears to be less sensitive to characterization. How this model would be used in stress analysis has not yet been indicated.

For wave propagation problems, the instantaneous modulus is critical, and can be determined from ultrasonic tests [38]. However, the early time character cannot be predicted from standard creep or relaxation tests, and must be determined from dynamic tests. Impact tests and data reduction procedures such as being developed by Sackman [33] which generate a creep or relaxation function directly, show more promise than sinusoidal tests generating a dynamic modulus.

3. SPATIAL DISCRETIZATION

A. Variational Principles as Direct Methods in Space

Finite element expansions provide efficient means to discretize Leitman's displacement variational principle for linear solids. Through the use of prescribed piecewise polynomial interpolation functions with minimal support, the displacement field is expressed in terms of N nodal point displacement time functions.

$$\underset{\sim}{u}_N(\underset{\sim}{x}, t) \;=\; \sum_{n=1}^{N} \underset{\sim}{\phi}_n(\underset{\sim}{x}) \; \underset{\sim}{r}_n(t) \;=\; \Phi(\underset{\sim}{x}) \; \underset{\sim}{r}(t) \tag{3.1}$$

Applying the strain-displacement relation (2.15), the engineering strain vector

$$< \epsilon_{11}, \; \epsilon_{22}, \; \epsilon_{33}, \; \gamma_{12}, \; \gamma_{13}, \; \gamma_{23} >^T \;=\; \psi(\underset{\sim}{x}) \; \underset{\sim}{r} \tag{3.2}$$

Thus the functional (2.31) becomes

$$V\{\underset{\sim}{u}_N\} \;=\; V_N\{\underset{\sim}{r}\} \;=\; \frac{1}{2} \, \dot{g} \star \underset{\sim}{r}^T \star K \circledast \underset{\sim}{r} \;-\; g \star \underset{\sim}{r}^T \star \underset{\sim}{P}$$

$$+\; \frac{1}{2} \, \underset{\sim}{r}^T \star M \, \underset{\sim}{r} \;-\; \underset{\sim}{r}^T \star M \, (\underset{\sim}{r}_0 + \dot{\underset{\sim}{r}}_0 \, t) \tag{3.3}$$

where

$$K(t - \tau) \;=\; \int_V \psi^T(\underset{\sim}{x}) \; C \, [\underset{\sim}{x}; \, t - \tau] \, \psi(\underset{\sim}{x}) \; dv \tag{3.4}$$

is the conventional stiffness matrix with the substitution of the (6 x 6) time dependent relaxation modulus matrix representation of the rank four tensor $\underset{\sim}{C}$,

$$M = \int_V \Phi^T(\underset{\sim}{x}) \; \Phi(\underset{\sim}{x}) \; \rho(\underset{\sim}{x}) \; dv \tag{3.5}$$

is the consistent mass matrix, and

$$\underset{\sim}{P}(t) = \int_V [\underset{\sim}{b}(\underset{\sim}{x}) + \psi^T(\underset{\sim}{x}) \; C \; [\underset{\sim}{x}, \; t - \tau] \circledast \underset{\sim}{\dot{\theta}}(\tau)] \; dv$$

$$+ \int_{S_\tau} \Phi^T(\underset{\sim}{x}) \; \bar{\underset{\sim}{T}}(\underset{=}{s}) \; d\underset{\sim}{s} \tag{3.6}$$

is the vector of nodal point forces, including the effective thermal loads. Extremization of the principle requires

$$\delta V = \delta \underset{\sim}{r}^T * [\underset{\sim}{\dot{g}} * K \circledast \underset{\sim}{r} - g * \underset{\sim}{P} + M(\underset{\sim}{r} - \underset{\sim}{r}_0 - \underset{\sim}{\dot{r}}_0 t)] = 0 \tag{3.7}$$

Since $\delta \underset{\sim}{r}$ is arbitrary,

$$M\underset{\sim}{r} + g * K \circledast \underset{\sim}{\dot{r}} = g * \underset{\sim}{P} + M(\underset{\sim}{r}_0 + \underset{\sim}{\dot{r}}_0 t) \tag{3.8}$$

which is the discrete integral equation of motion. The instantaneous stiffness can be separated by integrating by parts, and assuming the initial stress is zero,

$$M\underset{\sim}{r} + g * (K_0 \underset{\sim}{r} + \dot{K} \circledast \underset{\sim}{r}) = g * \underset{\sim}{P} + M(\underset{\sim}{r}_0 + \underset{\sim}{\dot{r}}_0 t) \tag{3.9}$$

where the instantaneous stiffness matrix K_0 is independent of time, and $\dot{K}$ is defined in the same way as $\dot{\underset{\sim}{C}}$ (see 2.12). For an elastic solid, $\dot{K} = 0$.

If Hamilton's principle had been used instead of Leitman's principle, the discretized Euler integro-differential equation would be

$$M\ddot{\underset{\sim}{r}} + K_o \dot{\underset{\sim}{r}} + K \circledast \underset{\sim}{r} = \underset{\sim}{P} \tag{3.10}$$

which is also obtained directly from (3.9) by differentiating twice with respect to time. The only difference is that the initial conditions for (3.10) are not obtainable from Hamilton's principle.

The question of approximation posed in this chapter is to what extent does the solution $\underset{\sim}{U}_N(x, t)$ obtained from (3.1) and (3.9) or (3.10) approximate the solution to (2.18).

B.   Spectrum of Original and Projection Operator

For an elastic solid, the equation of motion (3.10) permits a separation of the time variable, and thus a solution by eigenfunction expansion. Even though in most viscoelastic situations (multi-material or thermal induced time dependent inhomogeneities), separation is not possible, a study of the eigenvalue problem indicates the degree of approximation possible from the basis provided at a fixed time by a given spatial discretization. The separation can be accomplished by the substitution

$$\underset{\sim}{u}(x, t) = \underset{\sim}{\phi}(x) e^{i\omega t} \tag{3.11}$$

into either the equation of motion (2.18) or the variational principles (2.22) or (2.31), generating the governing eigenvalue problem. The errors in the approximate spectrum will be exhibited for a few examples, and then their significance in the forced response will be studied.

1. Simple Bar Theory

For a homogeneous isotropic elastic bar, under the kinematic assumption of plane sections remaining plane, and ignoring radial stress and inertia, the eigenproblem is governed by the ordinary differential equation,[*]

$$- \tilde{E} \frac{\partial^2 \phi}{\partial x^2} = \omega^2 \rho \phi \tag{3.12}$$

or the variational principle

$$\frac{1}{2} \int_0^L \left[\tilde{E} \frac{\partial \phi}{\partial x}^2 - \omega^2 \rho \phi^2 \right] dx = \min \tag{3.13}$$

supplemented by appropriate homogeneous boundary conditions. For the general solution,

$$\phi(x) = A \sin \frac{\lambda x}{L} + B \cos \frac{\lambda x}{L} \tag{3.14}$$

the governing equation requires $\omega = \lambda C_0 / L$, where $C_0^2 = \tilde{E}/\rho$. For a free-free or fixed-fixed bar, the existence of a non-trivial solution requires that $\lambda = n\pi$, while for a free-fixed or fixed-free bar, $\lambda = (2n - 1) \frac{\pi}{2}$, n a positive integer.

Consider a spatial discretization of (3.13) into N equal elements. Then, the algebraic eigenvalue problem resulting from the minimization of the principle is

$$K \hat{\phi} = \bar{\omega}^2 M \hat{\phi} \tag{3.15}$$

---

[*] $\tilde{E}$ will be used throughout for Young's modulus to distinguish it from the shifter operative.

where for the piecewise linear finite element expansion,

$$K = \sum_{n=1}^{N} a_n^T \ K_n \ a_n \ , \qquad K_n = \frac{\tilde{E}}{\Delta x} \left| \begin{array}{cc} 1 & -1 \\ -1 & 1 \end{array} \right|$$

(3.16)

$$M = \sum_{n=1}^{N} a_n^T \ M_n \ a_n \ , \qquad M_n = \frac{\rho \Delta x}{6} \left| \begin{array}{cc} 2 & 1 \\ 1 & 2 \end{array} \right|$$

and a_n is a Boolean element assembly matrix. Both K and M are symmetric banded matrices of size $N + 1$. This generalized eigenvalue problem may be regarded as a difference equation, for if a typical equation is extracted,

$$- \diamondsuit \ \hat{\phi}_k \ = \ \frac{\bar{\omega}^2 \ \Delta x^2}{c_o^2} \ (1 + \frac{1}{6} \ \diamondsuit \ ) \ \hat{\phi}_k$$

(3.17)

is obtained, where $\diamondsuit = \Delta \nabla$, $\Delta = E - 1$, $\nabla = 1 - E^{-1}$, and $E^k \ f_j = f_{j + k}$ are the second central difference, forward difference, backward difference and shifter operators, respectively [39] applied to node k. The general solution of the difference equation is

$$\hat{\phi}_k \ = \ \bar{A} \sin \bar{\lambda} \frac{k}{N} \ + \ \bar{B} \cos \bar{\lambda} \frac{k}{N}$$

(3.18)

The satisfaction of (3.17) requires that

$$\bar{\omega} \ = \ \frac{2 \ C_o}{\Delta x} \ \frac{\sin \frac{\bar{\lambda}}{2N}}{\sqrt{1 - \frac{2}{3} \sin^2 \frac{\bar{\lambda}}{2N}}}$$

(3.19)

where use has been made of the important property of even difference operators

$$\triangle \left\{ \begin{array}{c} \sin \bar{\lambda} \frac{k}{N} \\ \cos \bar{\lambda} \frac{k}{N} \end{array} \right\} = - 4 \sin^2 \frac{\bar{\lambda}}{2N} \left\{ \begin{array}{c} \sin \bar{\lambda} \frac{k}{N} \\ \cos \bar{\lambda} \frac{k}{N} \end{array} \right\} \qquad (3.19a)$$

Since the piecewise linear expansion satisfies the continuity requirement of the variational theorem, $\bar{\omega}$ is an upper bound to ω.

The difference equation (3.17) must be assigned boundary conditions. These must not only simulate the boundary conditions of the differential equation (3.12), but when combined with the governing difference equation (3.17) evaluated at 0 (or N) must be the same as the first (or last) equation of the matrix eigenproblem (3.15). For unmixed conditions of prescribed ϕ or its derivative, this simulation is the one of the ordinary finite difference method. The case of a mixed condition will be discussed later.

Using a central difference approximation for gradient boundary conditions, one obtains for the unmixed conditions considered above that $\bar{\lambda} = \lambda$, and thus the eigenvectors ϕ_k exactly sample the exact eigenfunctions $\phi(x)$ at the mesh points. However, the piecewise linear approximate eigenfunctions $\phi_N(x)$ defined from the ϕ_k by (3.1) are not equal in the functional norm (3.13). This raises the question of the significance of the value of the functional as a norm in judging approximations.

If the mass is lumped at the nodes, the mass matrix in (3.15) is diagonal, simplifying the algebraic eigenvalue problem. The difference equation (3.17) becomes

$$- \diamondsuit \, \hat{\phi}_k = \frac{\bar{\omega}^2 \, \Delta x^2}{c_o^2} \, \hat{\phi}_k \qquad (3.20)$$

and the same solution form (3.18) yields

$$\bar{\omega} = \frac{2 \, C_o}{\Delta x} \sin \frac{\bar{\lambda}}{2N} \qquad (3.21)$$

Note that the stiffness operator on the left of (3.17) and (3.20) is the same as that obtained from an elementary finite difference approximation of the differential operator on the left of (3.12). This is a rare case, and usually not true for two space variables.

Within the band width restriction of the finite element matrices, a higher order approximation is possible with no increase in computational effort. Utilizing a finite difference identity presented on page 152 of Hildebrand [39], that is

$$\diamondsuit \, \phi_k = \Delta x^2 \left(1 + \frac{1}{12} \diamondsuit + \text{h.o.t.}\right) \left(\frac{\partial^2 \phi}{\partial x^2}\right)_k \qquad (3.22)$$

inserting (3.12), and ignoring higher order terms,

$$- \diamondsuit \, \hat{\phi}_k = \frac{\bar{\omega}^2 \, \Delta x^2}{c_o^2} \left(1 + \frac{1}{12} \diamondsuit \right) \hat{\phi}_k \qquad (3.23)$$

which can be interpreted through (3.15) as representing the same stiffness matrix with a modified mass matrix. For this case,

$$\bar{\omega} = \frac{2 C_0}{\Delta x} \frac{\sin \frac{\bar{\lambda}}{2N}}{\sqrt{1 - \frac{1}{3} \sin^2 \frac{\lambda}{2N}}} \tag{3.24}$$

This leads to the speculation that in two dimensional problems one might be able to find higher order difference methods with no greater coupling than the finite element method.

For all three cases, noting that $\bar{\lambda} = \lambda$, the ratio of approximate to the exact frequency is

$$\frac{\bar{\omega}}{\omega} = \frac{2}{\eta\pi} \frac{\sin \eta \frac{\pi}{2}}{\sqrt{1 - 2\alpha \sin^2 \eta \frac{\pi}{2}}} \quad , \quad \eta = \frac{\lambda}{N\pi} \tag{3.25}$$

where for lumped mass $(\alpha = o)$, consistent mass $(\alpha = 1/3)$, and for the higher mass $(\alpha = 1/6)$. The parameter α also is the ratio of the off diagonal coefficient in the mass matrix to the row or column sum. For all four unmixed boundary conditions, $0 < \eta < 1$ is a rational number; either n/N or $(2n - 1)/2N$, n a positive integer. Both forms can be extended to the spectrum of rational numbers, permitting the approximation to the nth frequency by an N element model to be exhibited in a single curve, for all n and N. These curves are shown for the three models in Figure 1.

2. Mindlin-Herrmann Bar Theory

To offer a better understanding of the effect of spatial discretization on wave propagation phenomena and to give some expression
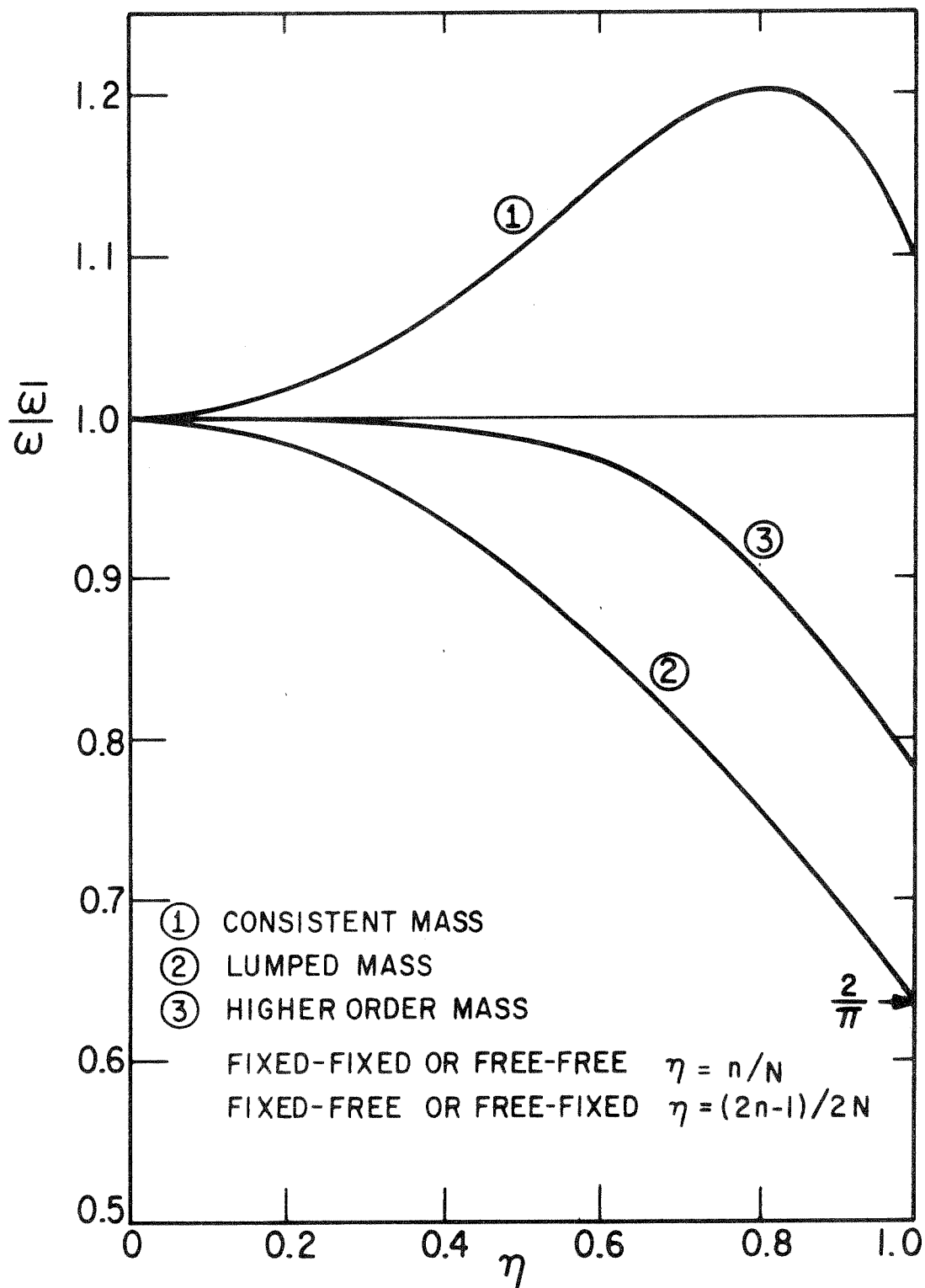
FIG. 3.1 ERROR IN DISCRETE SPECTRUM
OF SIMPLE BAR

to the effect of a second space variable, consider the two radial mode unmodified Mindlin-Herrmann theory for longitudinal motion of bars [24]. This theory is a truncation of a more general radial expansion presented by Mindlin-McNiven [25].

Applying Hamilton's principle to axisymmetric motions of a circular isotropic elastic elastic rod, with radius a,

$$2\pi \int_{t_1}^{t_2} [\ \delta T + \delta W\ ]\ dt\ = 0 \qquad (3.26)$$

where

$$T\ =\ \frac{1}{2} \int_0^L \int_0^a \rho\ [\ (\dot{u})^2 + (\dot{w})^2\ ]\ rdrdz$$

$$(3.27)$$

$$W\ =\ -\ \frac{1}{2} \int_0^L \int_0^a [\ \sigma_r\,\varepsilon_r + \sigma_\theta\,\varepsilon_\theta + \sigma_z\,\varepsilon_z + \tau_{rz}\,\gamma_{rz}\ ]\ rdrdz$$

The kinematic assumptions of the two mode theory are

$$u\ (r,\ z,\ t)\ =\ \frac{r}{a}\ \hat{u}\ (z,\ t)$$

$$(3.28)$$

$$w\ (r,\ z,\ t)\ =\ \hat{w}\ (z,\ t)$$

which lead to the strains

$$\varepsilon_r\ =\ \varepsilon_\theta\ =\ \frac{1}{a}\ \hat{u}$$

$$\varepsilon_z\ =\ \hat{w}'$$

$$(3.29)$$

$$\gamma_{rz}\ =\ \frac{r}{a}\ \hat{u}'$$

and stresses

$$\sigma_r = \sigma_\theta = 2(\lambda + \mu) \frac{1}{a} \hat{u} + \lambda \hat{w}'$$

$$\sigma_z = (\lambda + 2\mu) \hat{w}' + 2\lambda \frac{1}{a} \hat{u} \qquad (3.30)$$

$$\tau_{rz} = \mu \frac{r}{a} \hat{u}'$$

where λ, μ are Lame's constants for an isotropic elastic solid. Then

$$T = \frac{1}{2} \int_0^L \rho \frac{a^2}{2} [\frac{1}{2}(\dot{\hat{u}})^2 + (\dot{\hat{w}})^2] \, dz$$

$$W = -\frac{1}{2} \int_0^L \frac{a^2}{2} [4(\lambda + \mu) \frac{1}{a^2} (\hat{u})^2 + 4\lambda \frac{1}{a} \hat{w}' \hat{u} \qquad (3.31)$$

$$+ (\lambda + 2\mu)(\hat{w}')^2 + \frac{1}{2} \mu (\hat{u}')^2] \, dz$$

The Euler equations of the principle are

$$(\lambda + 2\mu) \hat{w}'' + 2\lambda \frac{1}{2} \hat{u}' = \rho \ddot{\hat{w}}$$

$$\frac{1}{a} \mu \hat{u}'' - 4(\lambda + \mu) \frac{1}{a^2} \hat{u} - 2\lambda \frac{1}{a} \hat{w}' = \frac{1}{2} \rho \ddot{\hat{u}} \qquad (3.32)$$

which are equation (20) of [24] with $\kappa = \kappa_1 = 1$. It is not of concern here how well this theory approximates three dimensional elasticity theory. The system (3.32) will be considered as given, and the effect of discretization of the remaining space variable will be studied.

To study the spectrum of the system, consider a sinusoidal pulse, for which

$$\hat{u} = U \exp [i \gamma (z - ct)]$$
$$\hat{w} = W \exp [i \gamma (z - ct)]$$

(3.33)

where c is the wave velocity, and the wave length $\Lambda = \frac{2\pi}{\gamma}$.
Then

$$\begin{bmatrix} (A_{11} - c^2) & A_{12} \\ A_{21} & (A_{22} - c^2) \end{bmatrix} \begin{bmatrix} U \\ W \end{bmatrix} = 0$$

(3.34)

where

$$A_{11} = \frac{\mu}{\rho} + \frac{8 (\lambda + \mu)}{\gamma^2 a^2 \rho}$$

$$A_{12} = \frac{4\lambda}{\gamma a \rho}$$

(3.35)

$$A_{21} = + \frac{2\lambda}{\gamma a \rho}$$

$$A_{22} = \frac{\lambda + 2\mu}{\rho}$$

The frequency equation is

$$c^4 - [A_{11} + A_{22}] c^2 + (A_{11} A_{22} - A_{12} A_{21}) = 0$$

(3.36)

Now consider an N element discretization of the axial direction. Let

$$\hat{u} (z, t) = \underset{\sim}{\phi}^T (z) \underset{\sim}{u}_0 (t)$$
$$\hat{w} (z, t) = \underset{\sim}{\phi}^T (z) \underset{\sim}{w}_0 (t)$$

(3.37)

where $\underset{\sim}{u}_o$, $\underset{\sim}{w}_o$ are the vectors of radial and axial displacements at $N + 1$ equally spaced sections along the length of the bar, and $\phi_k(z)$ is the piecewise linear interpolation function defined to be one at node k and zero at all others. Then

$$T = \frac{1}{2} [\dot{\underset{\sim}{u}}_o^T M_{11} \dot{\underset{\sim}{u}}_o + \dot{\underset{\sim}{w}}_o^T M_{22} \dot{\underset{\sim}{w}}_o]$$

$$W = - \frac{1}{2} [\underset{\sim}{u}_o^T K_{11} \underset{\sim}{u}_o + 2 \underset{\sim}{u}_o^T K_{12} \underset{\sim}{w}_o + \underset{\sim}{w}_o^T K_{22} \underset{\sim}{w}_o]$$

(3.38)

where

$$M_{11} = \frac{1}{2} M_{22} = \frac{1}{4} \rho a^2 A$$

$$K_{11} = \frac{1}{4} \mu a^2 B + 2 (\lambda + \mu) A$$

$$K_{12} = 2\lambda a C$$

$$K_{22} = \frac{a^2}{2} (\lambda + 2\mu) B$$

(3.39)

$$A = \int_0^L \underset{\sim}{\phi}\, \underset{\sim}{\phi}^T\, dz = \sum_{n=1}^N a_n^T A_n a_n, \quad A_n = \frac{\Delta z}{6} \begin{vmatrix} 2 & 1 \\ 1 & 2 \end{vmatrix}$$

$$B = \int_0^L (\underset{\sim}{\phi}')(\underset{\sim}{\phi}')^T\, dz = \sum_{n=1}^N a_n^T B_n a_n, \quad B_n = \frac{1}{\Delta z} \begin{vmatrix} 1 & -1 \\ -1 & 1 \end{vmatrix}$$

(3.40)

$$C = \int_0^L (\underset{\sim}{\phi})(\underset{\sim}{\phi}')^T\, dz = \sum_{n=1}^N a_n^T C_n a_n, \quad C_n = \frac{1}{2} \begin{vmatrix} 1 & 1 \\ -1 & -1 \end{vmatrix}$$

and a_n is the Boolean assembly matrix for element n. The discretized equations of motion are then

$$M_{11}\; \ddot{u}_{\sim 0} + K_{11}\; u_{\sim 0} + K_{12}\; w_{\sim 0} = 0$$

$$M_{22}\; \ddot{w}_{\sim 0} + K_{12}^T\; u_{\sim 0} + K_{22}\; w_{\sim 0} = 0$$

(3.41)

Extracting the k th pair of equations,

$$\frac{\Delta z}{4}\; \rho a^2\; (1 + \frac{1}{6} \square)\; \ddot{u}_0^k + [- \frac{1}{4} \mu\; \frac{a^2}{\Delta z} \square$$

$$+ 2\; (\lambda + \mu)(1 + \frac{1}{6} \square)\Delta z]\; u_0^k + 2\lambda a\; \frac{1}{2}\; (E - E^{-1})\; w_0^k = 0$$

(3.42)

$$\frac{\Delta z}{2}\; \rho a^2\; (1 + \frac{1}{6} \square)\; \ddot{w}_0^k - 2\lambda a\; \frac{1}{2}\; (E - E^{-1})\; u_0^k$$

$$+ [- \frac{a^2}{2\Delta z}\; (\lambda + 2\mu) \square]\; w_0^k = 0$$

Again considering a sinusoidal pulse, let

$$u_0^k = \bar{U}\; \exp [\; i\, \gamma\, (k\Delta z - ct)\;]$$

$$w_0^k = \bar{W}\; i\, \exp [\; i\, \gamma\, (k\Delta z - ct)\;]$$

(3.43)

Then

$$\begin{bmatrix} (\bar{A}_{11} - \bar{B}_{11}\; \bar{C}^2) & \bar{A}_{12} \\[2ex] \bar{A}_{21} & (\bar{A}_{22} - \bar{B}_{22}\; \bar{C}^2) \end{bmatrix} \begin{bmatrix} \bar{U} \\[2ex] \bar{W} \end{bmatrix} = 0$$

(3.44)

where

$$\overline{A}_{11} = \frac{\mu}{\rho} \left(\frac{a}{\Delta z}\right)^2 \sin^2 \frac{\gamma \Delta z}{2} + 2 \frac{(\lambda + \mu)}{\rho} \left(1 - \frac{2}{3} \sin^2 \frac{\gamma \Delta z}{2}\right)$$

$$\overline{A}_{12} = -\frac{2\lambda}{\rho} \left(\frac{a}{\Delta z}\right) \sin \gamma \Delta z = \overline{A}_{21}$$

(3.45)

$$\overline{A}_{22} = 2 \left(\frac{a}{\Delta z}\right)^2 \left(\frac{\lambda + 2\mu}{\rho}\right) \sin^2 \frac{\gamma \Delta z}{2}$$

$$\overline{B}_{11} = \frac{1}{4} (\gamma a)^2 \left(1 - \frac{2}{3} \sin^2 \frac{\gamma \Delta z}{2}\right) = \frac{1}{2} \overline{B}_{22}$$

The frequency equation is then

$$\overline{B}_{11} \overline{B}_{22} \overline{c}^4 - (\overline{A}_{11} \overline{B}_{22} + \overline{A}_{22} \overline{B}_{11}) \overline{c}^2 + (\overline{A}_{11} \overline{A}_{22} - \overline{A}_{12} \overline{A}_{21}) = 0$$

(3.46)

The exact phase velocity from (3.36) and the approximate values for different discretization ratios $m = \frac{a}{\Delta z}$ are evaluated as a function of $(\frac{a}{\Lambda})$ and shown in Figure 2, for $\nu = 1/4$. For a lumped mass model, $B_{11} = \frac{1}{4} (\gamma a)^2$.

3. Membrane

The spectral approximation of the clamped rectangular membrane of length a and width b can be studied in the same manner as the simple bar. Here the eigenvalue problem is governed by

$$\nabla^2 \phi + \frac{\omega^2}{c^2} \phi = 0$$

(3.47)

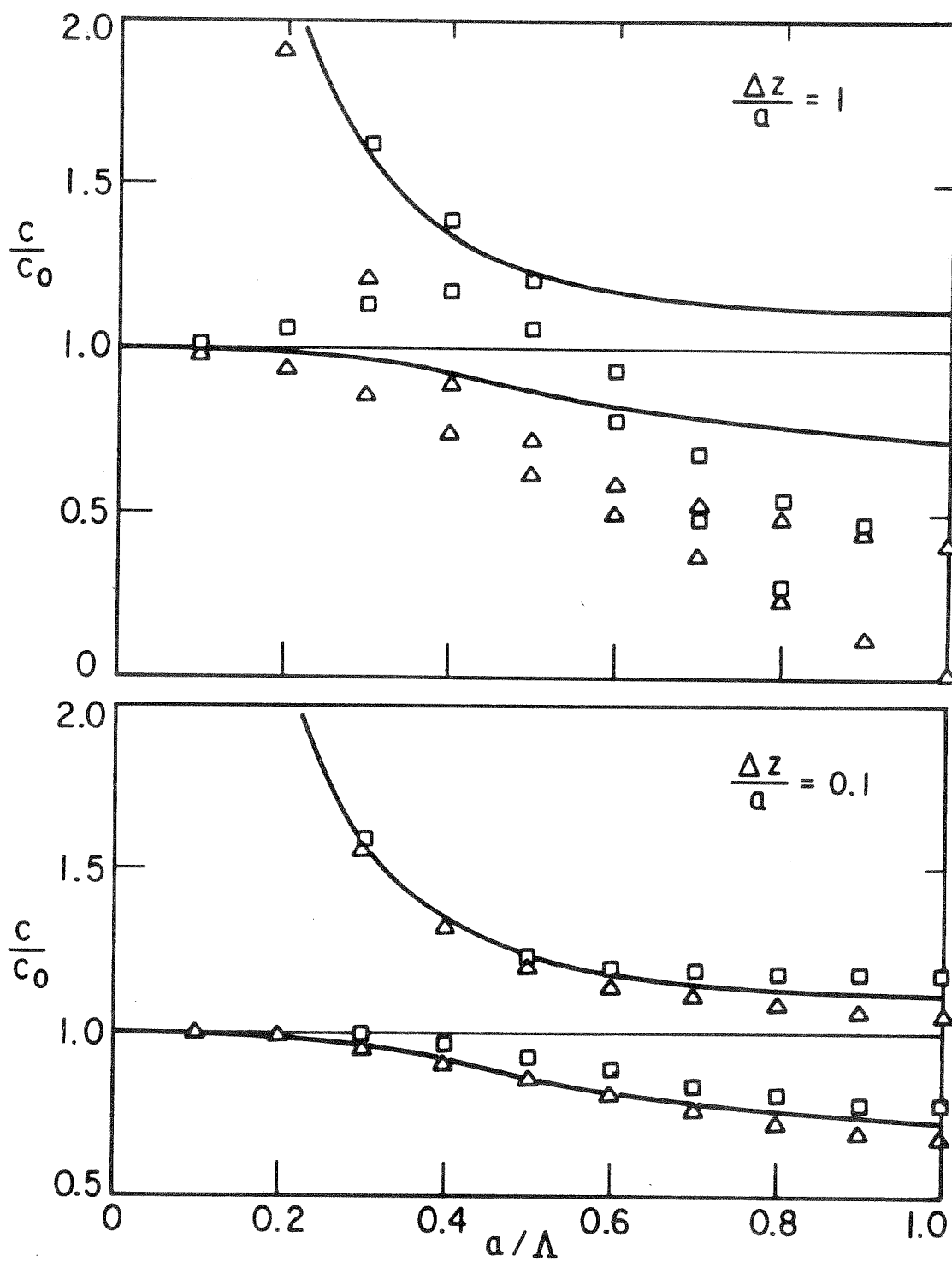$$\phi (x, 0) = \phi (x, b) = \phi (0, y) = \phi (a, y) = 0$$

FIG. 3.2 SPECTRAL APPROXIMATION OF UNMODIFIED
MINDLIN – HERRMANN BAR THEORY
△ LUMPED MASS, ▢ CONSISTENT MASS, — EXACT

or by the equivalent variational problem

$$\frac{1}{2} \int_0^a \int_0^b [(\frac{\partial \phi}{\partial x})^2 + (\frac{\partial \phi}{\partial y})^2 - \frac{\omega^2}{c^2} \phi^2] \, dx \, dy = min \qquad (3.48)$$

This eigenvalue problem also governs the transient analysis of a wide range of problems (e.g. heat conduction and flow through porous media). Assuming a solution of the form

$$\phi (x, y) = sin \frac{m\pi x}{a} sin \frac{n\pi y}{b} \qquad (3.49)$$

which satisfies the boundary conditions, (3.47) requires

$$\omega^2 = \frac{4c^2}{\Delta x^2} [(\frac{m\pi}{2M})^2 + (\frac{\Delta x}{\Delta y})^2 (\frac{n\pi}{2N})^2] \qquad (3.50)$$

where $a = M\Delta x$ and $b = N\Delta y$.

If the differential equation (3.47) is approximated by the ordinary five point Laplacian finite difference operator, applied to an M x N rectangular mesh,

$$[\triangledown_i + (\frac{\Delta x}{\Delta y})^2 \triangledown_j + \frac{\bar{\omega}^2}{c^2} \Delta x^2] \Phi_{ij} = 0 \qquad (3.51)$$

$$i = 1, 2, .. M - 1, \quad j = 1, 2, ... N - 1$$

with

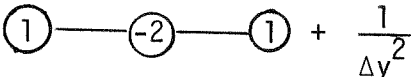$$\Phi_{oj} = \Phi_{Mj} = \Phi_{io} = \Phi_{in} = 0 \qquad (3.52)$$

where Φ_{ij} is the approximate value of ϕ at the mesh points and $\triangledown_i$ is the second central difference operator with respect to i defined previously. Assuming

$$\Phi_{ij} = \sin \frac{m\pi i}{M} \sin \frac{n\pi j}{N} \tag{3.53}$$

requires

$$\bar{\omega}^2 = \frac{4c^2}{\Delta x^2} \left[\sin^2 \left(\frac{m\pi}{2M} \right) + \left(\frac{\Delta x}{\Delta y} \right)^2 \sin^2 \left(\frac{n\pi}{2N} \right) \right] \tag{3.54}$$

The associated stencil to (3.51) is

stiffness $\quad \dfrac{1}{\Delta x^2}$ ①——②——① $+ \dfrac{1}{\Delta y^2}$

$$\begin{array}{c} ① \\ ② \\ ① \end{array}$$

$$\tag{3.55}$$

mass $\qquad\qquad\qquad\qquad\qquad ①$

Consider now the bilinear quadrilateral expansion over the same $M \times N$ rectangular mesh.

$$\phi (x, y) = \underset{\sim}{\psi}^T (x, y) \underset{\sim}{\phi}_0 \tag{3.56}$$

where $\underset{\sim}{\phi}_0$ is the vector of nodal point values, and $\psi_k (x, y)$ is the bilinear interpolation function defined to be one at node k (or i, j), zero at all others, and bilinear in the elements adjacent to node k.

The details of the formation will be omitted. Substitution of (3.56) into (3.48) gives

$$\frac{1}{2} \underset{\sim}{\phi}_0^T \left(K - \frac{\omega^2}{c^2} M \right) \underset{\sim}{\phi}_0 = min \tag{3.57}$$

where

$$K = \sum_{i=1}^{M} \sum_{j=1}^{N} a_{ij}^T K_{ij} a_{ij}$$

$$M = \sum_{i=1}^{M} \sum_{j=1}^{N} a_{ij}^T M_{ij} a_{ij}$$

(3.58)

a_{ij} is the Boolean element assembly matrix, and K_{ij} and M_{ij} are the element stiffness and consistent mass matrices.

$$K_{ij} = \frac{\Delta y}{6\Delta x} \begin{vmatrix} 2 & -2 & 1 & -1 \\ & 2 & -1 & 1 \\ & & 2 & -2 \\ \text{sym} & & & 2 \end{vmatrix} + \frac{\Delta x}{6\Delta y} \begin{vmatrix} 2 & 1 & -2 & -1 \\ & 2 & -1 & -2 \\ & & 2 & 1 \\ \text{sym} & & & 2 \end{vmatrix}$$

(3.59)

$$M_{ij} = \frac{\Delta x \Delta y}{36} \begin{vmatrix} 4 & 2 & 2 & 1 \\ & 4 & 1 & 2 \\ & & 4 & 2 \\ \text{sym} & & & 4 \end{vmatrix}$$
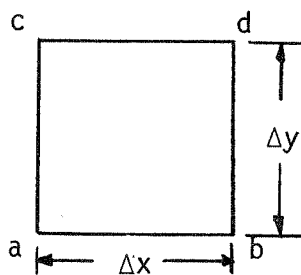
The minimization of the principle yields

$$\left[K - \frac{\bar{\omega}^2}{c^2} M \right] \phi_0 = 0$$

(3.60)

Extracting the equation at node (i, j) and dividing by $\Delta x \Delta y$.

$$\left[\frac{1}{\Delta x^2} \left(1 + \frac{1}{6}\,\square_j\right)\square_i + \frac{1}{\Delta y^2}\left(1 + \frac{1}{6}\,\square_i\right)\square_j \right.$$

$$\left. + \frac{\bar{\omega}^2}{c^2}\left(1 + \frac{1}{6}\,\square_i\right)\left(1 + \frac{1}{6}\,\square_j\right) \right] \Phi_{ij} = 0 \qquad (3.61)$$

which corresponds to the stencil

$$\frac{1}{\Delta x^2}\frac{1}{6}\begin{bmatrix}1 & -2 & 1\\ 4 & -8 & 4\\ 1 & -2 & 1\end{bmatrix} + \frac{1}{\Delta y^2}\frac{1}{6}\begin{bmatrix}1 & 4 & 1\\ -2 & -8 & -2\\ 1 & 4 & 1\end{bmatrix} + \frac{\bar{\omega}^2}{c^2}\frac{1}{36}\begin{bmatrix}1 & 4 & 1\\ 4 & 16 & 4\\ 1 & 4 & 1\end{bmatrix} \qquad (3.62)$$

which is seen to be a generalization of the ordinary finite difference stencil (3.55). Note that if $\Phi_{ij} = \Phi_i$, $\square_j\,\Phi_i = 0$, reducing (3.61) to

$$\left[\square_i + \frac{\bar{\omega}^2}{c^2}\left(1 + \frac{1}{6}\,\square_i\right) \right] \Phi_i = 0 \qquad (3.61a)$$

which is the same as (3.17) for the simple bar (or string).

Again using solution for (3.53), the frequency condition becomes

$$\bar{\omega}^2 = \frac{4c^2}{\Delta x^2}\left[\sin^2\frac{m\pi}{2M}\left(1 - \frac{2}{3}\sin^2\frac{n\pi}{2N}\right)\right.$$

$$\left. + \frac{\Delta x^2}{\Delta y^2}\sin^2\frac{n\pi}{2N}\left(1 - \frac{2}{3}\sin^2\frac{m\pi}{2M}\right)\right]/CM \qquad (3.63)$$

where

$$CM = (1 - \frac{2}{3} \sin^2 \frac{m\pi}{2M}) (1 - \frac{2}{3} \sin^2 \frac{n\pi}{2N})$$

If the mass is lumped in conjunction with the finite element stiffness matrix, CM = 1.

As in the case of the bar, the errors in the eigenvalues can be displayed for all $\frac{m}{M}$ and $\frac{n}{N}$. The full range of $\frac{n}{N}$ is shown for $\frac{m}{M}$ of 1/8, 1/2, and 7/8 in Figure 3. Simple finite difference, finite element with consistent mass, and finite element with lumped mass models are compared.

Bounds for the eigenvalues of membranes with irregular boundaries are investigated by Weinberger [40,41] for various finite difference methods.

4. Beam

The use of the polynomial solution of the homogeneous static beam as interpolation functions for a finite element vibration study appears to have been developed independently by Archer [20] and Leckie and Lindberg [23]. Their results were presented numerically for several discretizations. Here the approximation is displayed in analytic form, and static condensation of rotational degrees of freedom when that inertia is ignored, is investigated.

The eigenproblem for a beam according to Euler-Bernoulli theory is

$$\tilde{E}I \frac{\partial^4 \phi}{\partial x^4} - \omega^2 \mu \phi = 0 \tag{3.64}$$
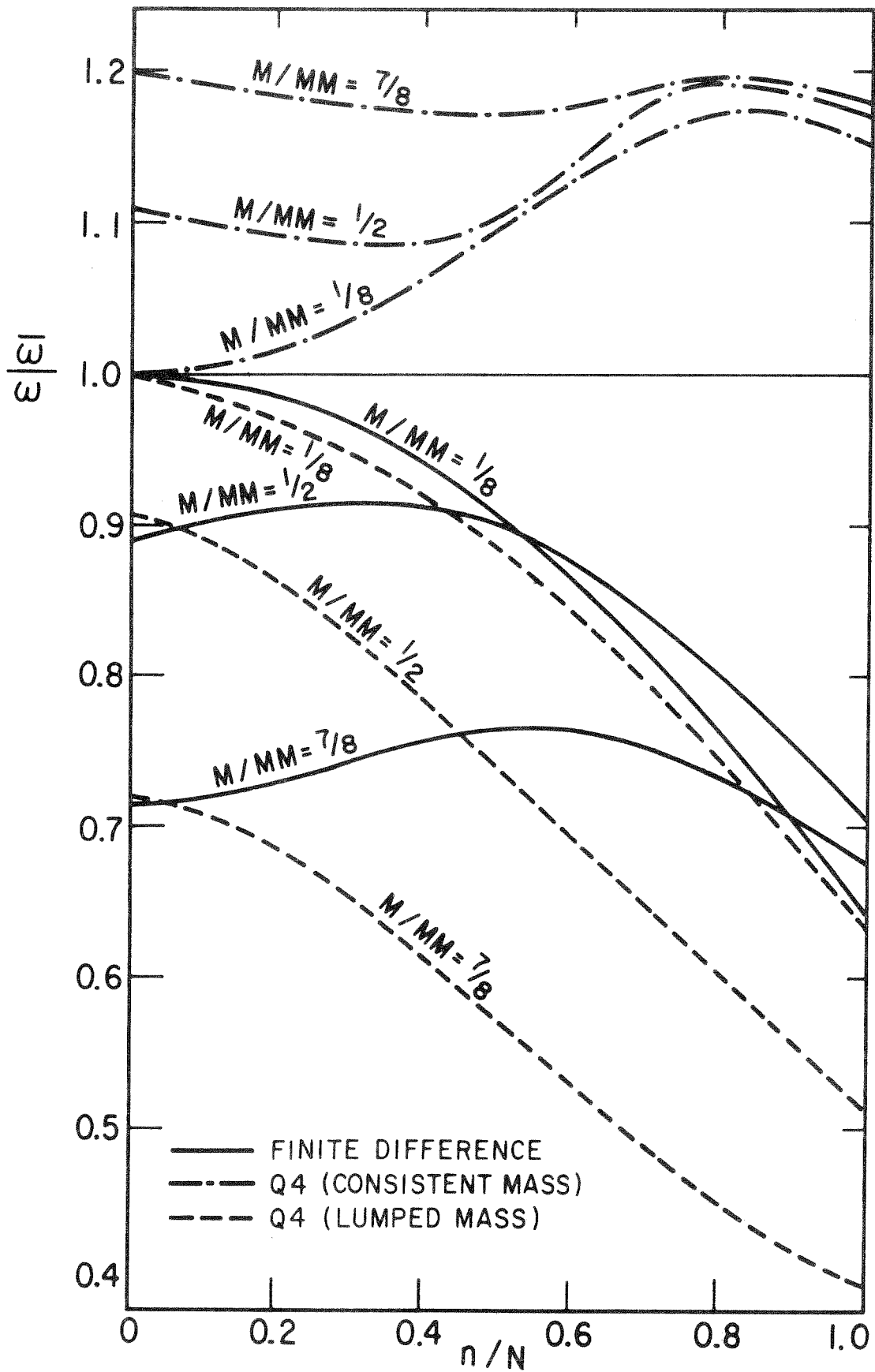
FIG. 3.3 ERRORS IN EIGENVALUES OF VIBRATING MEMBRANE

subject to appropriate homogeneous boundary conditions, or the variational statement

$$\frac{1}{2} \int_0^L [\ \widetilde{EI}\ (\frac{\partial^2 \phi}{\partial x^2})^2\ -\ \omega^2 \mu \phi^2\ ]\ dx\ =\ min \tag{3.65}$$

The exact solution of (3.64) is

$$\phi(x) = A \sin \lambda \frac{x}{L} + B \cos \lambda \frac{x}{L} + C \sinh \lambda \frac{x}{L} + D \cosh \lambda \frac{x}{L} \tag{3.66}$$

where

$$\omega^2\ =\ c^2\ (\frac{\lambda}{L})^4\ ,\quad c^2\ =\ \frac{\widetilde{EI}}{\mu}$$

and λ is determined from the boundary conditions.

Replacing (3.64) by the simplest finite difference operator,

$$[\ \triangle/^2\ -\ \frac{\bar{\omega}^2 \Delta x^4}{c^2}\ ]\ \Phi_i\ =\ 0 \tag{3.67}$$

The solution to this difference equation is the same as (3.66). In this case, x is restricted to $\frac{i}{N}$ and

$$\Phi_i = A \sin \bar{\lambda}\ \frac{i}{N} + B \cos \bar{\lambda}\ \frac{i}{N} + C \sinh \bar{\lambda}\ \frac{i}{N} + D \cosh \bar{\lambda}\ \frac{i}{N} \tag{3.68}$$

where

$$\bar{\omega}^2\ =\ \frac{c^2}{\Delta x^4}\ 16\ \sin^4\ \frac{\bar{\lambda}}{2N}$$

Since, for fixed $\bar{\lambda}$, $N \to \infty$ implies $\sin \frac{\bar{\lambda}}{2N} \to \frac{\bar{\lambda}}{2N}$, $\lim\limits_{N \to \infty}$
$\bar{\omega}^2 = \frac{c^2 \lambda^4}{\Delta x^4 N^4} = \omega^2$ and the approximation is convergent.

For the finite element model, nodal rotations $\underset{\sim}{\theta}_0$ as well as transverse displacements $\underset{\sim}{\phi}_0$ are global variables. Letting

$$\phi(x) = \underset{\sim}{\psi}^T(x) \underset{\sim}{\phi}_0 + \underset{\sim}{\Lambda}^T(x) \underset{\sim}{\theta}_0 \tag{3.69}$$

where $\psi_k(x)$ is the piecewise cubic interpolation function defined to be one at node k, zero at all others, and zero slope at all nodes; $\Lambda_k(x)$ is zero at all nodes with unit slope at node k and zero slope at all others. The eigenproblem then becomes

$$\begin{vmatrix} K_{11} & K_{12} \\ K_{12}^T & K_{22} \end{vmatrix} \left\{ \begin{array}{c} \underset{\sim}{\phi}_0 \\ \underset{\sim}{\theta}_0 \Delta x \end{array} \right\} = \frac{\bar{\omega}^2}{c^2} \begin{vmatrix} M_{11} & M_{12} \\ M_{12}^T & M_{22} \end{vmatrix} \left\{ \begin{array}{c} \underset{\sim}{\phi}_0 \\ \underset{\sim}{\theta}_0 \Delta x \end{array} \right\} \tag{3.70}$$

$$K_{11} = \int_0^L (\underset{\sim}{\psi}'')(\underset{\sim}{\psi}'')^T \, dx = \sum_{n=1}^N a_n^T K_{11}^n a_n, \quad K_{11}^n = \frac{2}{\Delta x^3} \begin{vmatrix} 6 & -6 \\ -6 & 6 \end{vmatrix}$$

$$K_{22} = \int_0^L (\underset{\sim}{\Lambda}'')(\underset{\sim}{\Lambda}'')^T \, dx = \sum_{n=1}^N a_n^T K_{22}^n a_n, \quad K_{22}^n = \frac{2}{\Delta x^3} \begin{vmatrix} 2 & 1 \\ 1 & 2 \end{vmatrix}$$

$$\tag{3.71}$$

$$K_{12} = \int_0^L (\underset{\sim}{\psi}'')(\underset{\sim}{\Lambda}'')^T \, dx = \sum_{n=1}^N a_n^T K_{12}^n a_n, \quad K_{12}^n = \frac{2}{\Delta x^3} \begin{vmatrix} 3 & 3 \\ -3 & -3 \end{vmatrix}$$

$$M_{11} = \int_0^L (\underset{\sim}{\psi})(\underset{\sim}{\psi})^T \, dx = \sum_{n=1}^N a_n^T M_{11}^n a_n, \quad M_{11}^n = \frac{\Delta x}{420} \begin{vmatrix} 156 & 54 \\ 54 & 156 \end{vmatrix}$$

$$M_{22} = \int_0^L (\underset{\sim}{\Lambda})(\underset{\sim}{\Lambda})^T \, dx = \sum_{n=1}^N a_n^T \, M_{22}^n \, a_n, \quad M_{22}^n = \frac{\Delta x}{420} \begin{vmatrix} 4 & -3 \\ -3 & 4 \end{vmatrix}$$

$$M_{12} = \int_0^L (\underset{\sim}{\psi})(\underset{\sim}{\Lambda})^T \, dx = \sum_{n=1}^N a_n^T \, M_{12}^n \, a_n, \quad M_{12}^n = \frac{\Delta x}{420} \begin{vmatrix} 22 & -13 \\ 13 & -22 \end{vmatrix}$$

Extracting the k th equation, and letting $\gamma = \dfrac{\bar{\omega}^2 \Delta x^4}{840 c^2}$,

$$\begin{vmatrix} (A_{11} - \gamma B_{11}) & (A_{12} - \gamma B_{12}) \\ -(A_{12} - \gamma B_{12}) & (A_{22} - \gamma B_{22}) \end{vmatrix} \begin{Bmatrix} \phi_k \\ \theta_k \Delta x \end{Bmatrix} = 0 \qquad (3.72)$$

where

$$A_{11} = -6 \ \square \qquad\qquad B_{11} = 6 (70 + 9 \ \square)$$

$$A_{12} = 3 (E - E^{-1}) \qquad\qquad B_{12} = -13 (E - E^{-1}) \qquad (3.73)$$

$$A_{22} = 6 + \square \qquad\qquad B_{22} = -2 - 3 \ \square$$

are difference operators.

The general solution of (3.72) can be found to be of the same form as (3.68) for ϕ_k and with

$$\theta_k = \frac{1}{2} (E - E^{-1}) \ \phi_k \qquad (3.74)$$

Noting that $A_{\alpha\alpha} \phi_k = \hat{A}_{\alpha\alpha} \phi_k$, $B_{\alpha\alpha} \theta_k = \hat{B}_{\alpha\alpha} \theta_k$, $A_{12} \theta_k \Delta x = \hat{A}_{12} \phi_k$, and $B_{12} \theta_k \Delta x = \hat{B}_{12} \phi_k$, where $\hat{A}_{\alpha\beta}$, $\hat{B}_{\alpha\beta}$ are constants, then the frequency condition becomes

$$A \gamma^2 - B \gamma + C = 0 \qquad (3.75)$$

where

$$A = \hat{B}_{11} \hat{B}_{22} - \hat{B}_{12}^2$$

$$B = \hat{B}_{11} \hat{A}_{22} + \hat{B}_{22} \hat{A}_{11} - 2 \hat{A}_{12} \hat{B}_{12} \qquad (3.76)$$

$$C = \hat{A}_{11} \hat{A}_{22} - \hat{A}_{12}^2$$

and

$$\hat{A}_{11} = 24 \sin^2 \frac{\overline{\lambda}}{2N} \qquad\qquad \hat{B}_{11} = 12 (35 - 18 \sin^2 \frac{\overline{\lambda}}{2N})$$

$$\hat{A}_{12} = - 6 \sin \frac{\overline{\lambda}}{N} \qquad\qquad \hat{B}_{12} = 26 \sin \frac{\overline{\lambda}}{N} \qquad (3.77)$$

$$\hat{A}_{22} = 4 (1 - \frac{2}{3} \sin^2 \frac{\overline{\lambda}}{N}) \qquad \hat{B}_{22} = 2 (1 + 6 \sin^2 \frac{\overline{\lambda}}{2N})$$

Now

$$\frac{\overline{\omega}^2}{\omega^2} = 840 (\frac{N}{\lambda})^4 \gamma \qquad (3.78)$$

where

$$\gamma = \gamma (\frac{\overline{\lambda}}{N}).$$

Consider all the unmixed zero boundary conditions for a beam; e.g. a) simply supported at both ends, b) fixed-fixed, c) free-free, d) clamped-free. The various frequencies will not be determined, the only concern being whether $\overline{\lambda}$ differs from λ. Since the discrete form (3.68) simulates the exact form (3.66), $\phi = 0$ conditions are identical. Consider

$$\theta_k = \frac{1}{2} (E-E^{-1}) \phi_k = 0 \quad \text{at} \quad k = 0 \text{ or } N \qquad (3.79)$$

Noting that

$$
\frac{1}{2} \left(E - E^{-1} \right)
\left\{
\begin{array}{c}
\sin \bar{\lambda} \frac{k}{N} \\[6pt]
\cos \bar{\lambda} \frac{k}{N} \\[6pt]
\sinh \bar{\lambda} \frac{k}{N} \\[6pt]
\cosh \bar{\lambda} \frac{k}{N}
\end{array}
\right\}
= \sin \frac{\bar{\lambda}}{N}
\left\{
\begin{array}{c}
\cos \bar{\lambda} \frac{k}{N} \\[6pt]
-\sin \bar{\lambda} \frac{k}{N} \\[6pt]
\cosh \bar{\lambda} \frac{k}{N} \\[6pt]
\sinh \bar{\lambda} \frac{k}{N}
\end{array}
\right\}
\tag{3.80}
$$

except for the factor, which drops out in a zero condition, (3.79) exactly simulates the zero slope condition at either end. A zero moment, implying $\phi'' = 0$, is simulated by $\square\!\!\!\!\diagdown\, \phi_k = 0$. Noting that

$$
\square\!\!\!\!\diagdown
\left\{
\begin{array}{c}
\sin \bar{\lambda} \frac{k}{N} \\[6pt]
\cos \bar{\lambda} \frac{k}{N} \\[6pt]
\sinh \bar{\lambda} \frac{k}{N} \\[6pt]
\cosh \bar{\lambda} \frac{k}{N}
\end{array}
\right\}
= 4 \sin^2 \frac{\bar{\lambda}}{2N}
\left\{
\begin{array}{c}
-\sin \bar{\lambda} \frac{k}{N} \\[6pt]
-\cos \bar{\lambda} \frac{k}{N} \\[6pt]
\sinh \bar{\lambda} \frac{k}{N} \\[6pt]
\cosh \bar{\lambda} \frac{k}{N}
\end{array}
\right\}
\tag{3.81}
$$

again, except for the factor, the simulation does not alter the eigen-condition. Finally, zero shear, implying $\phi''' = 0$, is simulated by $\frac{1}{2} \left(E - E^{-1} \right) \square\!\!\!\!\diagdown\, \phi_k = 0$, and the combination of the above identities indicates the correct simulation of the eigencondition. Thus for all the unmixed boundary conditions, the eigenvectors exactly sample the true eigenfunctions and $\bar{\lambda} = \lambda$. This permits a parametric display of approximate frequency as a function of $\frac{\lambda}{N} = \eta\pi$. For the hinged-hinged beam $\eta = \frac{n}{N}$, n an integer denoting the mode. For other boundary condition see page 203 of [16], where λ is given.
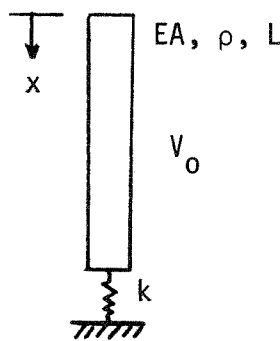
Since the cubic displacement functions satisfy the continuity requirement of the variational problem (3.65), the above method yields an upper bound to the eigenvalues. If only the lower modes are deemed important, a reduction of the eigenvalue problem to translational degrees of freedom only can be accomplished by neglecting the rotational inertias and statically condensing out the rotations. Usually then, the translational inertia is lumped, as done for the beam by Archer [20], and for the plate by Clough and Felippa [19]. In the above analytic form, $\hat{B}_{12} = \hat{B}_{22} = 0$, $\hat{B}_{11} = 420$, and

$$\gamma = \frac{1}{420} (\hat{A}_{11} - \hat{A}_{12}^2 / \hat{A}_{22}) \tag{3.82}$$

The first branch of the spectrum for the full finite element model is compared with the translational coordinate model and the finite difference model in Figure 4.

C. Impact of Elastic Bar on Elastic Spring

Consider the longitudinal impact of an elastic bar on an elastic spring. The governing equation is

$$\frac{\partial^2 u}{\partial x^2} = \frac{1}{c^2} \frac{\partial^2 u}{\partial t^2} , \quad c^2 = \frac{\tilde{E}}{\rho} \tag{3.83}$$

subjected to the boundary conditions

$$\tilde{E}A \frac{\partial u}{\partial x} (o, t) = o$$

$$\tilde{E}A \frac{\partial u}{\partial x} (L, t) + k u (L, t) = o \tag{3.84}$$

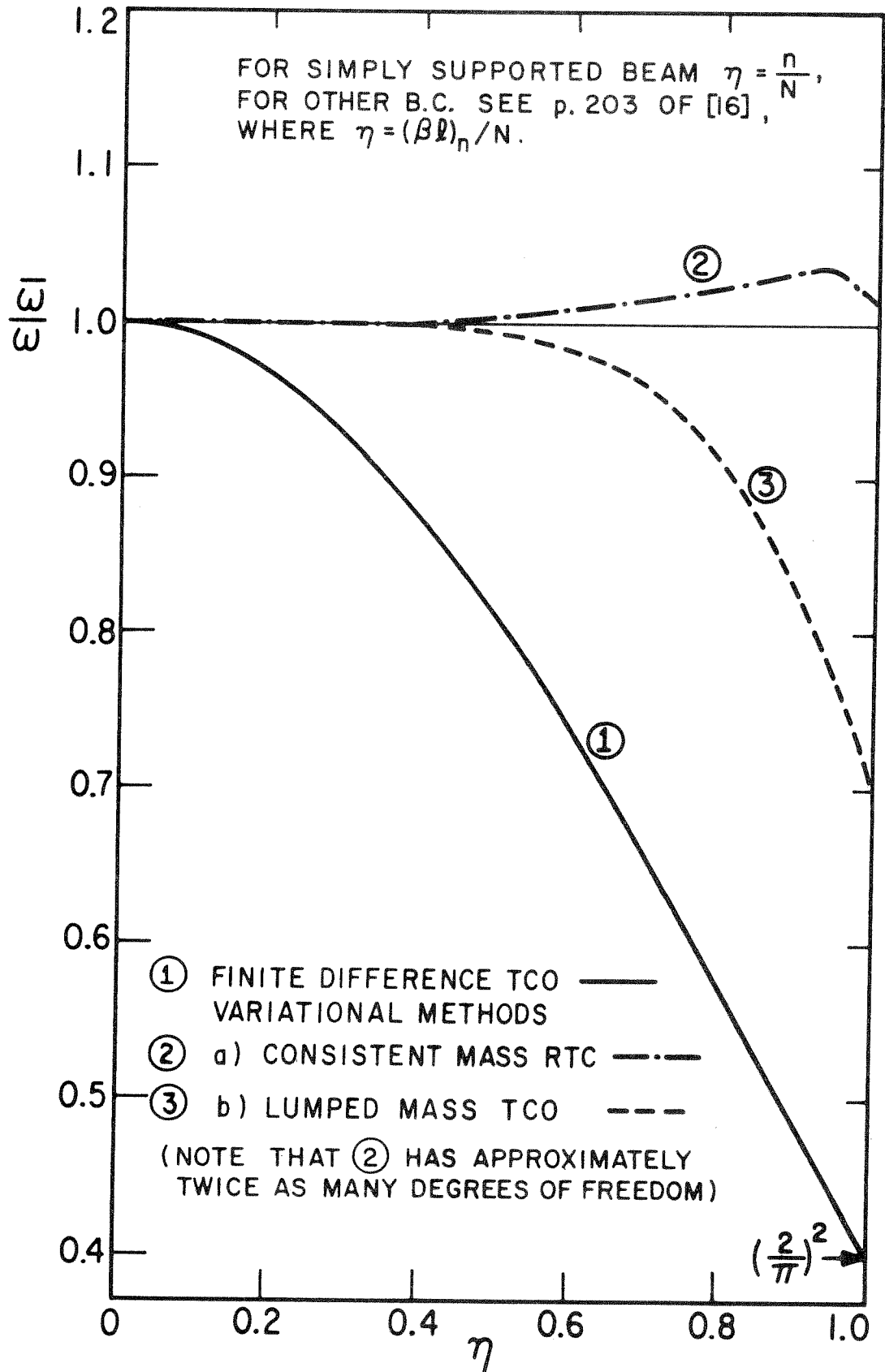EA, ρ, L

x

V_o

k

FIG. 3.4 ERRORS IN EIGENVALUES OF BEAM

and initial conditions

$$u(x, 0) = 0, \quad \dot{u}(x, 0) = \frac{\partial u}{\partial t}(x, 0) = V_0 \qquad (3.85)$$

The exact solution is

$$u(x, t) = V_0 t + f(x + ct) + g(x - ct) \qquad (3.86)$$

where the particular solution $V_0 t$ has been separated out so that the unknown functions f and g satisfy zero initial conditions and will be determined from the boundary conditions. For $t < 2L/c$, (3.86) has the form

$$u(x, t) = V_0 t + f\left(t + \frac{x}{c} - \frac{L}{c}\right) H\left(t + \frac{x}{c} - \frac{L}{c}\right)$$
$$+ g\left(t - \frac{x}{c} - \frac{L}{c}\right) H\left(t - \frac{x}{c} - \frac{L}{c}\right) \qquad (3.87)$$

where $H(\theta)$ is the Heaviside step function, zero for $\theta < 0$ and one for $\theta \geq 0$. The first arbitrary function represents the initial wave front emanating from the bottom at impact. The second function represents the reflected wave from the free boundary at the top.

Applying the boundary condition at $x = 0$

$$\frac{\partial u}{\partial x}(0, t) = \frac{1}{c}\left[f'\left(t - \frac{L}{c}\right) - g'\left(t - \frac{L}{c}\right) \right] H\left(t - \frac{L}{c}\right) = 0 \qquad (3.88)$$

where $f' \equiv \frac{df}{d\theta}(\theta)$. Thus, $g'(\theta) = f'(\theta)$ and g differs from f by no more than a constant. Then for $t < L/c$, and $\bar{t} \equiv t + \frac{x - L}{c}$,

$$u_0 \ (x, \ t) \ = \ V_0 t \ + \ f \ (\overline{t}) \ H \ (\overline{t})$$

(3.89)

$$\frac{\partial u_0}{\partial x} \ (x, \ t) \ = \ \frac{1}{c} \ f' \ (\overline{t}) \ H \ (\overline{t})$$

and for $\frac{L}{c} < t < \frac{2L}{c}$, $\overline{\overline{t}} \equiv t - \frac{x+L}{c}$, and $\overline{t}$ as above,

$$u_1 \ (x, \ t) \ = \ u_0 \ (x, \ t) \ + \ f \ (\overline{\overline{t}}) \ H \ (\overline{\overline{t}})$$

(3.90)

$$\frac{\partial u_1}{\partial x} \ (x, \ t) \ = \ \frac{\partial u_0}{\partial x} \ (x, \ t) \ - \ \frac{1}{c} \ f' \ (\overline{\overline{t}}) \ H \ (\overline{\overline{t}})$$

Applying the boundary condition at $x = L$,

$$\frac{EA}{c} \ f' \ (t) \ + \ k \ f(t) \ = \ - \ k \ V_0 t$$

(3.91)

with $f(0) \ = \ 0$. Thus, letting $\beta \ = \ \frac{kc}{EA}$,

$$f' \ (\theta) \ + \ \beta \ f \ (\theta) \ = \ - \ \beta \ V_0 \ \theta$$

(3.92)

for which

$$f \ (\theta) \ = \ V_0 \ [\ (\ 1 \ - \ e^{-\beta\theta} \ ) \ \frac{1}{\beta} \ - \ \theta \ ]$$

(3.93)

$$\frac{\partial f}{\partial \theta} \ (\theta) \ = \ - \ V_0 \ (\ 1 \ - \ e^{-\beta\theta} \ )$$

Now (3.83) may also be solved by separation of variables. That elementary exercise leads to

$$u(x,t) \ = \ \sum_{n=0}^{\infty} \ [A_n \ \cos \omega_n t + B_n \ \sin \omega_n t][C_n \ \cos \frac{\lambda_n x}{L} + D_n \ \sin \frac{\lambda_n x}{L}] \quad (3.94)$$

where $\omega_n = \dfrac{\lambda_n c}{L}$. The gradient boundary condition at $x = o$ implies that $D_n = 0$, permitting $C_n = 1$, while the mixed boundary condition at $x = L$ leads to the eigencondition

$$- \lambda \ \sin \lambda \ + \ r \cos \lambda \ = o, \quad r = \frac{kL}{EA} \tag{3.95}$$

By trigonometric identity, (3.94) may be cast in the form

$$u \ (x, t) \ = \ \sum_{n=o}^{\infty} \ [\ A_n \cos \frac{\lambda_n}{L} (x + ct) \ + \ B_n \ \sin \frac{\lambda_n}{L} (\ x + ct)]$$

$$\tag{3.96}$$

$$+ \ \sum_{n=o}^{\infty} \ [\ C_n \cos \frac{\lambda_n}{L} (x - ct) \ + \ D_n \ \sin \frac{\lambda_n}{L} (x - ct)]$$

The first series clearly represents an arbitrary function $f \ (x + ct)$ and the second series an arbitrary function $g \ (x - ct)$. In the limit, then, (3.96) is equivalent to (3.86).

Letting $\phi_n \ (x) = \cos \dfrac{\lambda_n x}{L}$ denote the eigenfunction, then

$$u \ (x, t) \ = \ \sum_{n=o}^{\infty} \ [\ A_n \cos \omega_n t \ + \ B_n \ \sin \omega_n t \ ] \ \phi_n \ (x) \tag{3.97}$$

Applying the initial conditions, $A_n = o$ and

$$\dot{u} \ (x, o) \ = \ \sum_{n=o}^{\infty} \ B_n \ \omega_n \ \phi_n \ (x) \ = \ V_o \tag{3.98}$$

Thus $B_n \omega_n$ are the coefficients in the eigenfunction expansion of the constant initial velocity V_0. Using the orthogonality of the eigenfunctions over the interval (o, L),

$$B_n = \frac{2 V_0}{\omega_n \lambda_n} \frac{\sin \lambda_n}{(1 + \frac{1}{r} \sin^2 \lambda_n)} \tag{3.99}$$

The difference equations for the finite element, ordinary finite difference, and higher order difference models of the simple bar eigenproblem have already been given in equations (3.17), 3.20), and (3.23). They are all represented by

$$- \diagdown\!\!\!\!\diagup \hat{\phi}_k = \gamma (1 + \frac{\alpha}{2} \diagdown\!\!\!\!\diagup) \hat{\phi}_k \tag{3.100}$$

where $\gamma = \frac{\omega^2 \Delta x^2}{c^2}$, and $\alpha = 1/3, 0, 1/6$ respectively. The general solution is given by (3.18) where $\bar{\omega}$ and $\bar{\lambda}$ are related by

$$\bar{\omega} = \frac{2c_0}{\Delta x} \frac{\sin \frac{\bar{\lambda}}{2N}}{\sqrt{1 - 2\alpha \sin^2 \frac{\bar{\lambda}}{2N}}} \tag{3.101}$$

The gradient boundary condition at $x = o$ requires $\bar{A} = o$, and thus

$$\hat{\phi}_k = \bar{B} \cos \bar{\lambda} \frac{k}{N} \tag{3.102}$$

Applying the mixed condition at $x = L$, with a central difference approximation of the derivatives, the following simulation results,

$$\frac{\tilde{EA}}{2\Delta x} (E - E^{-1}) \hat{\phi}_n + k \hat{\phi}_n = 0 \tag{3.103}$$

Inserting (3.102) and identity (3.80) leads to the eigencondition

$$- N \, \sin \, \frac{\overline{\lambda}}{N} \, \sin \, \overline{\lambda} \, + \, r \, \cos \, \overline{\lambda} \, = \, 0 \qquad\qquad (3.104)$$

which simulates (3.95) and converges to it as $N \to \infty$. Note that $\overline{\lambda}$ and thus the eigenvectors (3.102) are independent of α, though different frequencies $\overline{\omega}$ result from (3.101).

Although the above is the natural finite difference simulation of the boundary condition, it is not consistent with the matrix eigenproblem derived by the finite element method. Consider the last equation of the finite element matrix system (3.15) with the spring at node N, expressed in its difference operator form,

$$(\, \nabla \, + \, \frac{r}{N} \,) \, \hat{\phi}_N \, = \, \frac{\gamma}{2} \, (\, 1 \, - \, \alpha \, \nabla \,) \, \hat{\phi}_N \qquad\qquad (3.105)$$

The left side comes from the stiffness matrix and the right from the mass matrix. That difference simulation to the boundary condition (3.84b) is now sought which, when combined with the general difference equation (3.100) so as to eliminate the phantom node $N + 1$ and symmetrize the set, yields (3.105). Multiplying (3.105) by two and subtracting (3.100) yields

$$(\, 2\nabla \, + \, \diagdown \!\!\!\!\diagup \, + \, \frac{2r}{N} \,) \, \hat{\phi}_N \, = \, - \, \frac{1}{2} \, \gamma \, \alpha \, (\, 2\nabla \, + \, \diagdown \!\!\!\!\diagup \,) \, \hat{\phi}_N \qquad\qquad (3.106)$$

Noting the identity that

$$2\nabla \, + \, \diagdown \!\!\!\!\diagup \, = \, \Delta \, + \, \nabla \, = \, E - E^{-1} \, , \qquad\qquad (3.107)$$

then

$$\left(1 + \frac{1}{2} \gamma \alpha \right) \frac{N}{2} \left(E - E^{-1} \right) \hat{\phi}_N + r \hat{\phi}_N = 0 \qquad (3.108)$$

must be the boundary condition satisfied, which is different from (3.104) and makes $\bar{\lambda}$ depend on α. For lumped mass ($\alpha = o$), and (3.108) is the same as (3.103). Further, since

$$\lim_{N \to \infty} \gamma = \lim_{N \to \infty} \frac{4 \sin^2 \frac{\bar{\lambda}}{2N}}{\left(1 - 2 \alpha \sin^2 \frac{\bar{\lambda}}{2N} \right)} = 0 \qquad (3.109)$$

then (3.108) converges to (3.84) for all α. The insertion of (3.102) into (3.108) yields the eigencondition properly associated with the variational formulations,

$$- \left(1 + \frac{1}{2} \gamma \alpha \right) N \sin \frac{\bar{\lambda}}{N} \sin \bar{\lambda} + r \cos \bar{\lambda} = 0 \qquad (3.110)$$

which, although different from (3.104), still converges to the exact eigencondition (3.95).

Although (3.104) or (3.110) will generate an infinite sequence of roots of (3.95), the formula (3.101) will yield only a finite number of $\bar{\omega}$ because it is a periodic function of $\bar{\lambda}$. This is expected for a finite degree of freedom system. The algebraic eigenvalue problem represented by (3.100) has $N + 1$ eigenvalues, unless $r \to \infty$, in which case there are N. Further, as $r \to o$, $\bar{\omega}_o \to o$, a rigid body mode. However, the difference condition (3.110) with (3.101) yields only N eigenvalues if only real $\bar{\lambda}$ are admitted. The eigenvector of the highest mode is not of the cosine form (3.102), has no obvious inter-pretation, and is a poor approximation to the $N + 1$ true eigenfunction, which is a cosine function.

Let $\hat{\phi}^n$ denote the n th eigenvector, with components

$$\hat{\phi}_k^n = \cos \lambda_n \frac{k}{N} \tag{3.111}$$

These vectors satisfy the matrix eigenvalue equation

$$K \hat{\phi}^n = \bar{\omega}_n^2 M \hat{\phi}^n \tag{3.112}$$

and the orthogonality condition

$$(\hat{\phi}^m)^T K \hat{\phi}^n = (\hat{\phi}^m)^T M \hat{\phi}^n = 0 , (m \neq n) \tag{3.113}$$

Now, the discrete field solution

$$\hat{u}_k (t) = \sum_{n=0}^{N} [\bar{A}_n \cos \bar{\omega}_{nt} + \bar{B}_n \sin \bar{\omega}_{nt}] \phi_k^n \tag{3.114}$$

in view of the initial conditions, yields $A_n = 0$ and

$$\dot{\hat{u}}_k (o) = \sum_{n=0}^{N} \bar{B}_n \bar{\omega}_n \hat{\phi}_k^n = V_o \tag{3.115}$$

Thus $\bar{B}_n \bar{\omega}_n$ are the coefficients in the eigenvector expansion of the constant initial velocity V_o. Thus

$$B_n = \frac{1}{\bar{\omega}_n} \frac{(\hat{\phi}^n)^T M V_o}{(\hat{\phi}^n)^T M \hat{\phi}^n} \tag{3.116}$$

Numerical results from the difference eigenproblem (3.110) and (3.101) agreed exactly with those from the algebraic problem (3.112) obtained from the eigenvalue routine HQRW for the N cosine modes. The difference

scheme failed to capture the N + 1 mode, since only the cosine eigenvector form (3.102) was admitted. The complex roots were not investigated, where the last mode would be found.

The mode superposition results for the three finite degree of freedom models are compared with the exact solution of the continuum problem and the exact eigenexpansion truncated to an equal number of terms, in Figures 3.5-3.9. Twenty element models are compared for foundation stiffness ratios of twenty and forty, showing the trend from acceleration to shock waves. Spatial distributions of bar stress are shown at the time the initial wave has traveled half way down the bar, and at the time the reflection from the free end has traveled half way back. The exact eigenexpansion results are excellent. The finite element model produces a dip of opposite sign ahead of the wave, affecting the reflected wave also. The lumped mass model exhibits a decaying precursor ahead of the wave front, with oscillations behind it. The higher order model responds as the average of the other two, and gives the best results of the three. It is judged that the consistent mass results are qualitatively the most unsatisfactory of the three. They indicate for wave propagation problems a phenomenon similar to that discussed by Washizu [22] for the heat conduction problem. The results are not worth the extra effort of the banded rather than diagonal mass matrix. Only the higher order mass model justifies the effort of the banded mass matrix, but it should be pointed out that there is no quarantee that a higher order mass operator may be found for arbitrary two and three dimensional problems.
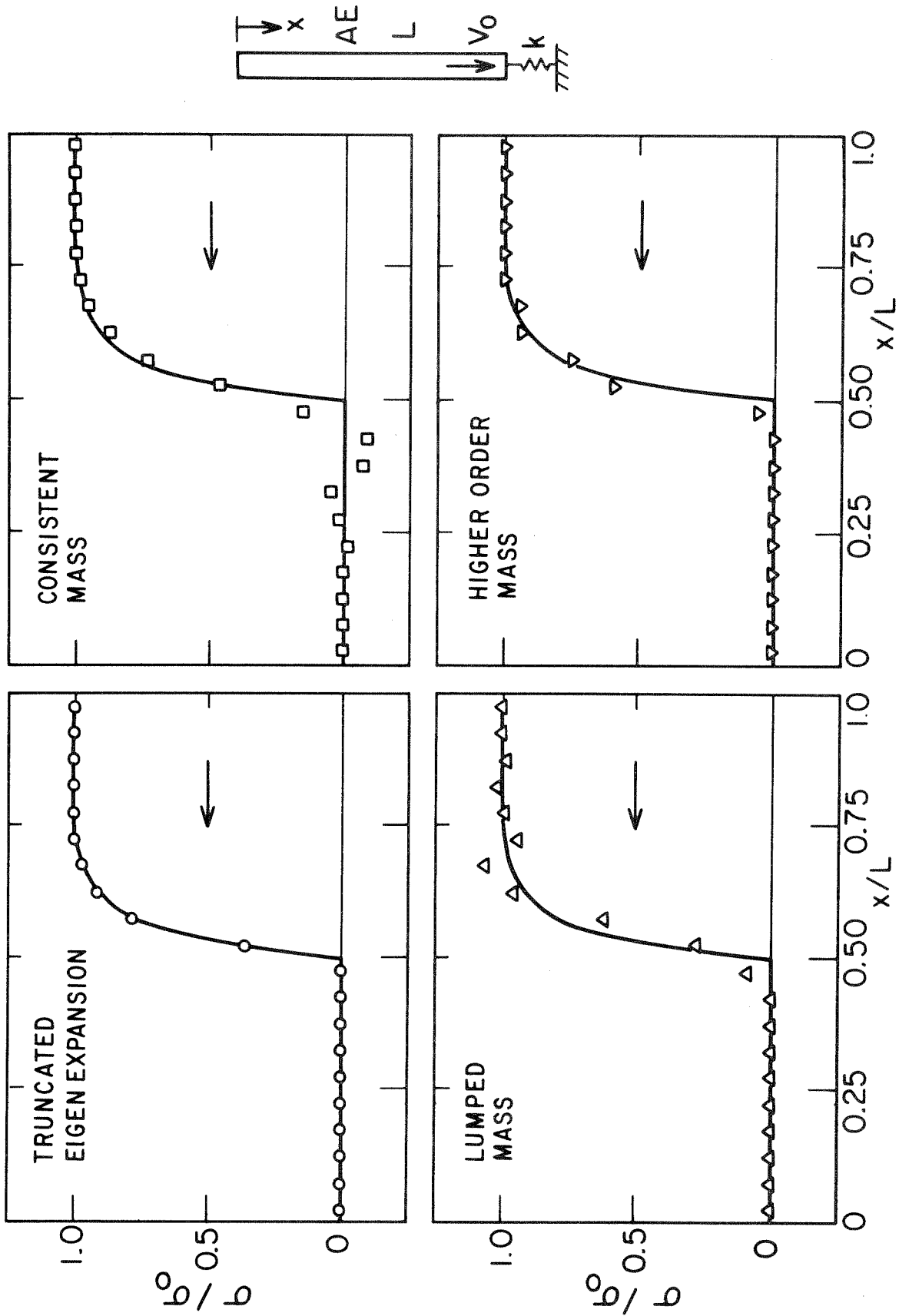
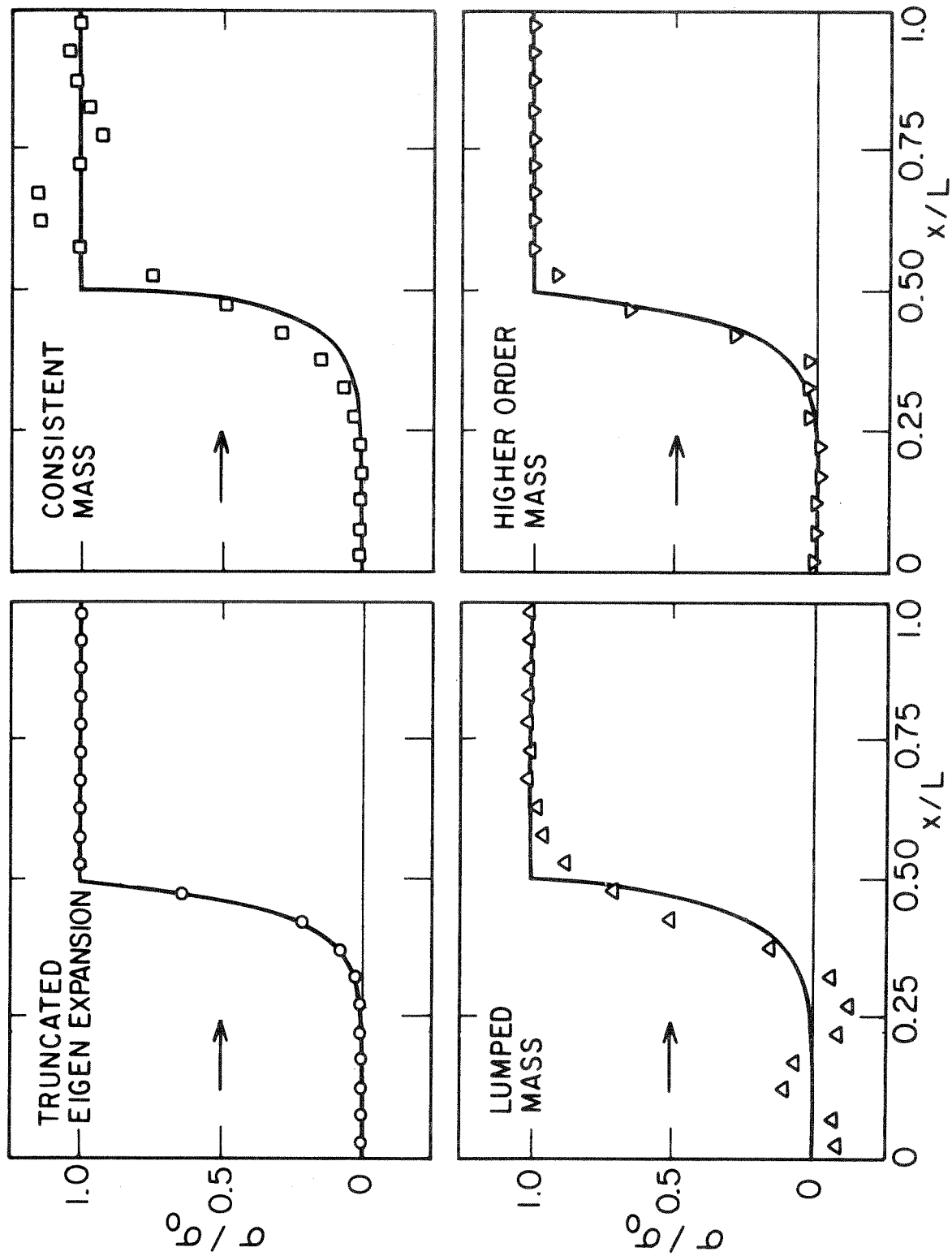FIG. 3.5 AXIAL STRESS AT $t = 0.5$ L/C ($R = kL/AE = 20$, $L/\Delta x = 20$)

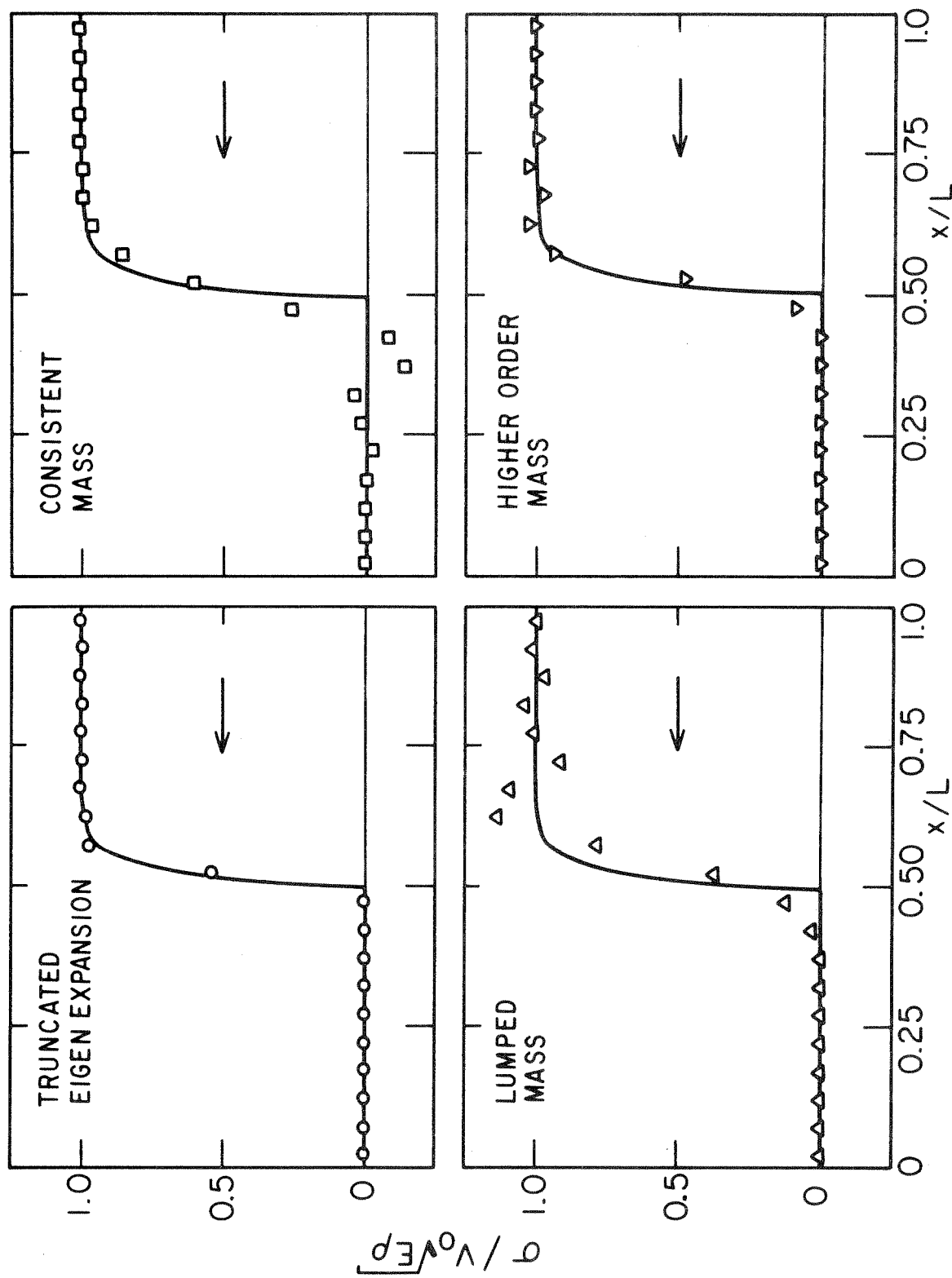FIG. 3.6 AXIAL STRESS AT t = 1.5 L/C ($R = kL/AE = 20$, $L/\Delta x = 20$)

FIG. 3.7 AXIAL STRESS AT $t = 0.5\ L/C$ $(R = kL/AE = 40,\quad L/\Delta x = 20)$

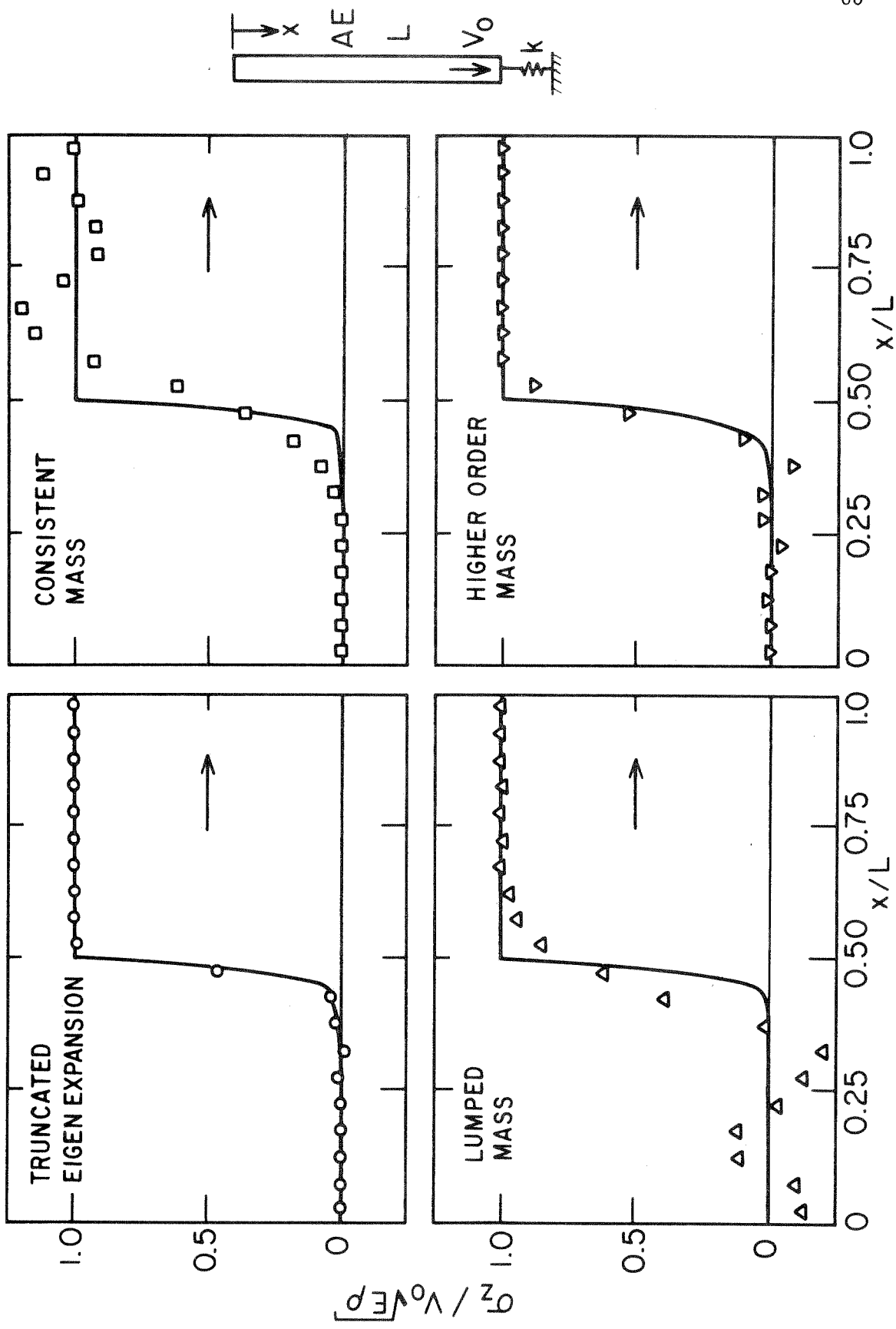FIG. 3.8 AXIAL STRESS AT t = 1.5 L/C   (R = kL/AE = 40, L/Δx = 20)

D. Step Stress on Viscoelastic Half Space

Consider the one dimensional problem of an initially quiessant, isothermal, viscoelastic half space subjected to a uniform step pressure. The equation of motion is

$$\frac{\partial \sigma_x}{\partial x} = \rho \frac{\partial^2 u}{\partial t^2} \tag{3.117}$$

and the linear constitutive equation is

$$\sigma_x(t) = C_D(o) \frac{\partial u}{\partial x}(t) + \int_0^t \dot{C}_D(t - \tau) \frac{\partial u}{\partial x} dt \tag{3.118}$$

where $C_D \equiv k + \frac{4}{3} G$ is the dilational relaxation modulus. These lead to the integro-differential equation of motion

$$\frac{\partial^2 u}{\partial x^2} + \dot{\bar{C}}_D * \frac{\partial^2 u}{\partial x^2} = \frac{1}{c^2} \frac{\partial^2 u}{\partial t^2} \tag{3.119}$$

where $c = \sqrt{C_D(o)/\rho}$ is the dilatational velocity, and $\bar{C}_D = C_D/C_D(o)$.

The problem is also described by the variational statement $\delta V = 0$. Leitman's principle takes the form

$$V\{u\} = \lim_{L \to \infty} \int_0^L \frac{1}{2} \left[\dot{g} * C_D * \frac{\partial u}{\partial x} * \frac{\partial u}{\partial x} + \rho u * u \right] dx$$

$$\tag{3.120}$$

$$+ g * \bar{\sigma}_0 * u(o)$$

An N element finite element approximation to the semi-infinite domain leads to the discrete principle $\delta \ V_N \ \{\hat{u}\} = 0$, where (3.3) becomes

$$V_N \ \{\hat{u}\} = \frac{1}{2} \ \dot{g} * \hat{u}^T * K * \underset{\sim}{u} - g * \hat{u}^T * \underset{\sim}{P}$$

$$+ \frac{1}{2} \ \hat{\underset{\sim}{u}}^T * M \ \hat{\underset{\sim}{u}} \tag{3.121}$$

and $L = N\Delta x$ is chosen large enough so that the near field solution is insensitive to the boundary condition at L. The Euler equation is

$$\dot{g} * K * \hat{\underset{\sim}{u}} + M \ \hat{\underset{\sim}{u}} = g * \underset{\sim}{P} \tag{3.122}$$

or in view of (2.34)

$$g * K_0 \hat{\underset{\sim}{u}} + g * \dot{K} * \hat{\underset{\sim}{u}} + M \hat{\underset{\sim}{u}} = g * \underset{\sim}{P} \tag{3.123}$$

where the matrix $K = \overline{C}_D \ K_0$ is proportional to the instantaneous elastic stiffness.

For this problem with zero initial conditions, Hamilton's extended principle could equally be used, where

$$\delta V \ \{u\} = - \int_{t_1}^{t_2} \lim_{L \to \infty} \int_0^L [\ C_D(o) \frac{\partial u}{\partial x} + C_D * \frac{\partial u}{\partial x}] \frac{\partial}{\partial x} (\delta u) - \rho u \ \delta \ u \ ] \ dt$$

$$- \int_{t_1}^{t_2} \overline{\sigma}_0 \ \delta u \ (o) \ dt = 0 \tag{3.124}$$

The same finite element discretization yields Lagrange's equations,

$$K_0 \hat{\underset{\sim}{u}} + \dot{\hat{K}} * \hat{\underset{\sim}{u}} + M \ddot{\hat{\underset{\sim}{u}}} = \underset{\sim}{P} \tag{3.125}$$

which is equivalent to (3.123) which can be obtained from (3.125) by convolving it with time and invoking the initial conditions.

The proportionality of K to K_0 permits solution by separation of variables. Letting

$$\hat{\underset{\sim}{u}}(t) = \hat{\underset{\sim}{\phi}} \, \psi(t) \tag{3.126}$$

and substituting into (3.125) leads to

$$(\psi + \dot{\bar{C}}_D * \psi) K_0 \hat{\underset{\sim}{\phi}} + M \hat{\underset{\sim}{\phi}} \ddot{\psi} = 0 \tag{3.127}$$

or

$$K_0 \hat{\underset{\sim}{\phi}} + \frac{\ddot{\psi}}{\psi + \dot{\bar{C}}_D * \psi} M \hat{\underset{\sim}{\phi}} = 0 \tag{3.128}$$

The first vector is independent of time. For the second to also be, the ratio of time functions must be constant , or

$$K_0 \hat{\underset{\sim}{\phi}} - \omega^2 M \hat{\underset{\sim}{\phi}} = 0 \tag{3.129}$$

and

$$\frac{1}{\omega^2} \ddot{\psi} + \psi + \dot{\bar{C}}_D * \psi = 0$$

The first is the same as for the elastic bar, indicating the spectral analysis to be governed by the instantaneous modulus. The time equation is no longer simply harmonic, but rather an ordinary integro-differential equation for each mode, incorporating the viscoelastic dissipation.

The concern of this Chapter is with the approximation afforded by a finite degree of freedom system. Thus, it is the exact solution of (3.122), (3.123), (3.125) or (3.129) which is desired (all equivalent). Since all formulations would require some approximate time integration scheme, consider the limit, then, of those solutions as $\Delta t \rightarrow o$.

As an example consider the problem presented by Nickell [42], where the material is assumed to have an elastic bulk modulus, and a standard solid shear relaxation modulus of the form

$$G(t) = G_g + (G_g - G_r)(1 - \exp(-t/\lambda)) \qquad (3.130)$$

where G_g is called the glassy (or instantaneous) modulus, G_r is called the rubbery (or equilibrium) modulus, and λ the characteristic relaxation time. The example has the folowing properties;

$$
\begin{aligned}
\rho &= 1.80 \text{ dyne} - \sec^2/cm^2 \\
K &= 2.35 \times 10^{10} \text{ dyne}/cm^2 \\
G_g &= 1.275 \times 10^{10} \text{ dyne}/cm^2 \\
G_r &= 0.125 \times 10^{10} \text{ dyne}/cm^2 \\
\lambda &= 10^{-6} \sec = 1 \mu \sec
\end{aligned}
\qquad (3.131)
$$

which result is a dilatational velocity $c = 1.5 \times 10^5$ cm/μ sec. Nickell presents an accurate numerical inversion of the Laplace transform

of the solution which may be regarded as the "exact" solution. His finite element results will be discussed later, in the context of time integration schemes.

The response of the half space to a step pressure at several different times is shown in Figures 3.9, 4.0. Results are compared for the lumped mass, consistent mass, and higher order mass discretizations. Oscillations for the lumped and consistent mass models are similar to the elastic case. The higher order mass results show no significant improvement.
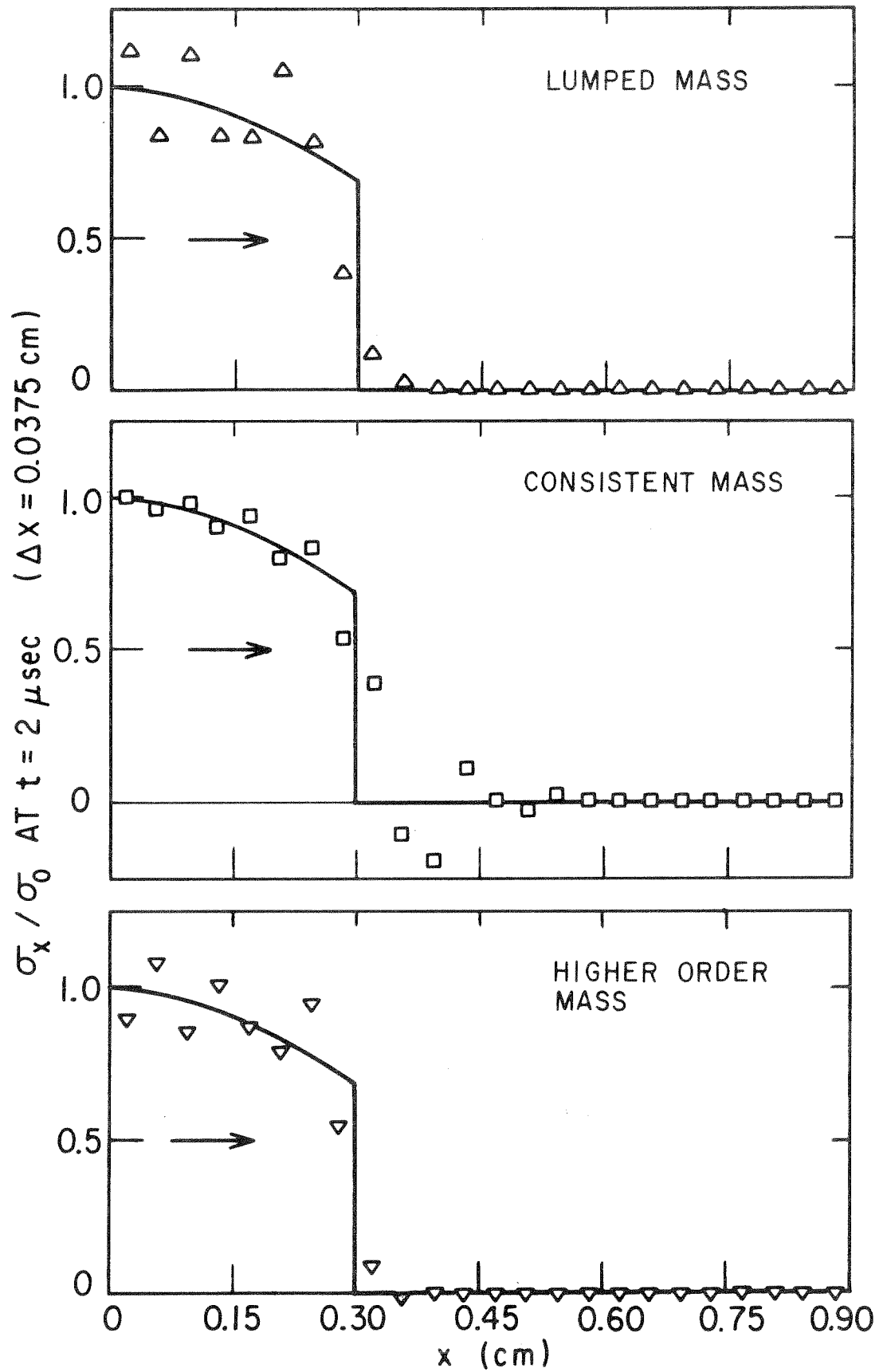
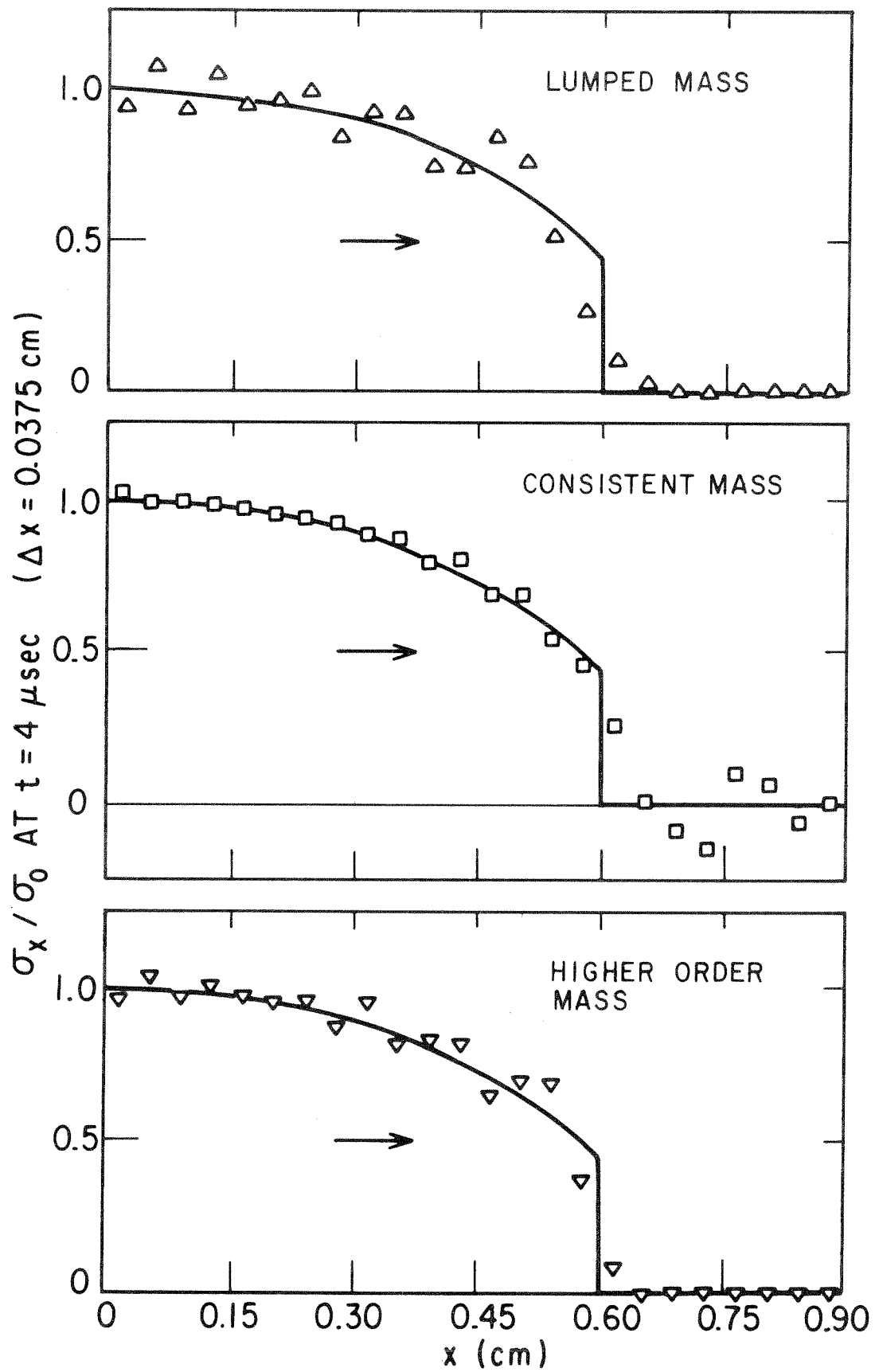FIG. 3.9   STEP STRESS ON VISCOELASTIC HALF SPACE

FIG. 3.10 STEP STRESS ON VISCOELASTIC HALF SPACE

4. TIME INTEGRATION OF DISCRETE SYSTEM

A. Mode Superposition vs Direct Integration

In previous Chapters the spatial discretization of the dynamic problem of a viscoelastic solid has led to a system of ordinary integro-differential equations,

$$M\ddot{r} + K_0 r + \dot{K} \circledast r = P \tag{4.1}$$

or a fully equivalent system of integral equations

$$Mr + g * K_0 r + g * \dot{K} \circledast r = g * P + M (r_0 + \dot{r}_0 t) \tag{4.2}$$

The previous Chapter dealt primarily with the special elastic case where $\dot{K} = 0$, or where separation of variables is possible for the viscoelastic problem. In these special cases, step-by-step integration of the coupled equations (4.1) or (4.2) is not necessary, in that a modal analysis is possible.

This writer has not seriously studied the relative efficiency of the modal method, because of greater interest in the more general problem with time dependent coefficients where modal analysis is not possible. For elastic systems on the order of one hundred degrees of freedom, modal analysis is probably more efficient. The computer program HQRW developed by Felippa [44] offers an efficient tool for implementing such an analysis. He employs a Householder transformation to perform a direct tridiagonalization of the matrix, followed by a modified Q-R algorithm for the iterative determination of the eigenvalues. Only as many eigenvectors as desired are computed by inverse iteration using the

Wilkenson shift.   For large systems having a diagonal mass matrix, transformation of the eigenvalue problem to canonical form retains both the symmetry and banded structure of the problem. Here, another Felippa code, BANEIG[*], employs a method of Rutishauser for successive deflation of the eigenproblem, retaining the banded structure lost be the HQRW routine.

In a vibration problem, where the time of interest is after multiple reflections, only a small number of modes need by computed, and the modal method is more efficient.

In impact problems, (essentially a short time response before multiple reflections) the solution is rich in all modes of the discrete spectrum. Here spurious oscillations near discontinuity surfaces arise, as discussed in the previous Chapter. Since the higher modes of the discrete spectrum are in error, one may ignore them, or weight them proportionately less by some smoothing process such as sigma smoothing [36]. These options of modal superposition are depicted in Figure 4.1 and 4.2 for the case previously studied, impact of an elastic bar on an elastic spring, to indicate a possible criterion for evaluating step-by-step methods. The details of modal smoothing techniques will not be treated here.

B. Step-by-Step Methods

For both the elastic initial boundary value problem and its spatially discrete initial value representation the time solution can be considered determined by the initial data at some time; similarly the
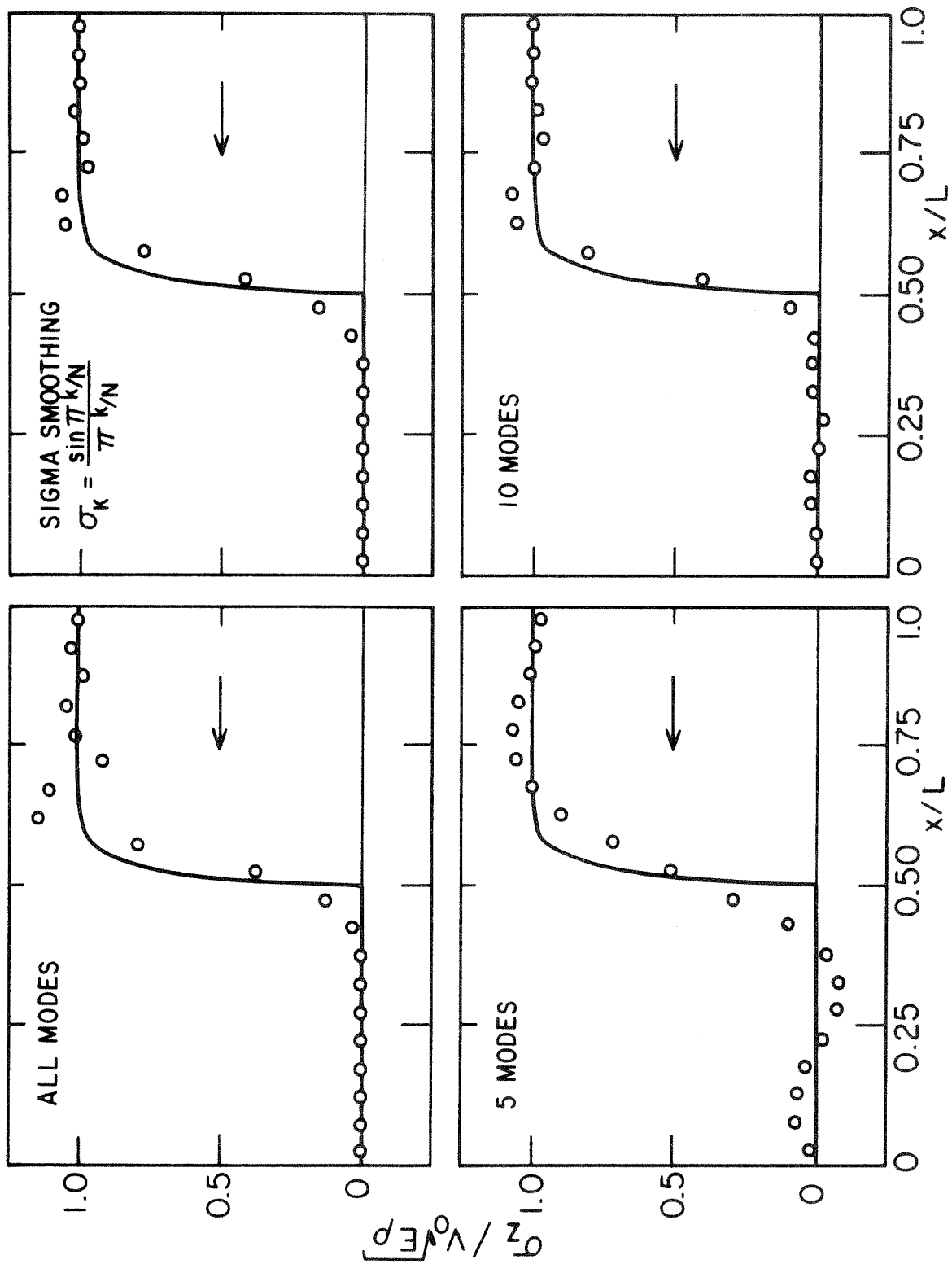
---

* See reference [45,46].

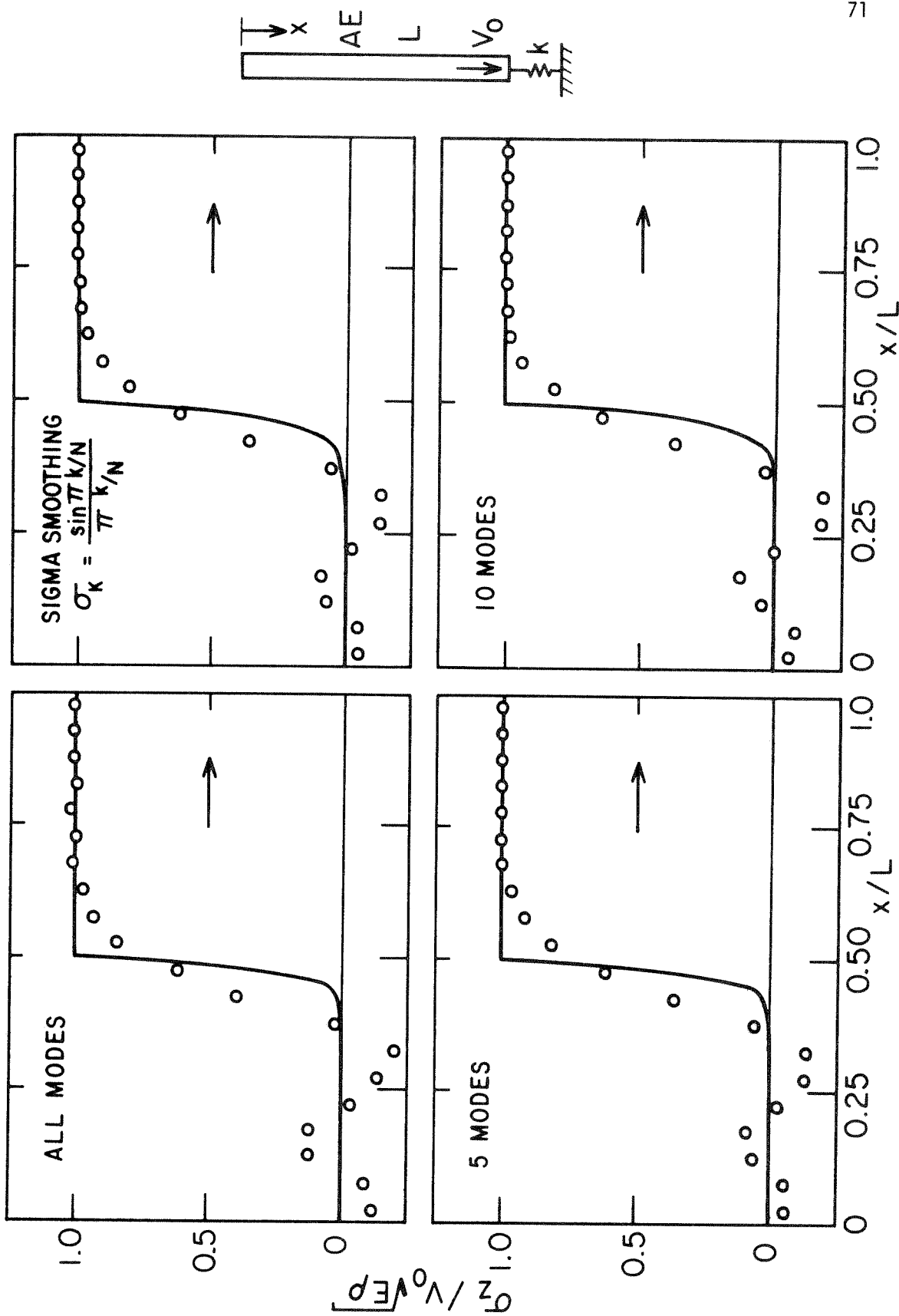FIG. 4.1 AXIAL STRESS AT t = 0.5 L/C (R=kL/AE=40 , L/Δx =20, LUMPED MASS)

70

71

FIG. 4.2 AXIAL STRESS AT t = 1.5 L/C   (R = kL/AE = 40, L/Δx = 20, LUMPED MASS)

approximate time solution at the end of a time interval Δt can be considered determined from the displacements and velocities at the beginning of the interval.[*]

1. Newmark's Family of Methods

Newmark discussed a family of one step methods for non-linear structural dynamics problems in 1959 [47]. The solution at the end of a time step is expressed by a Taylor series, with the remainder approximated by a quadrature formula,

$$
\underset{\sim}{r}_{k+1} = \underset{\sim}{r}_k + \Delta t \, \dot{\underset{\sim}{r}}_k + \int_0^{\Delta t} (\Delta t - \tau) \, \ddot{\underset{\sim}{r}} \, d\tau
$$
(4.3)
$$
\simeq \underset{\sim}{r}_k + \Delta t \, \dot{\underset{\sim}{r}}_k + (\frac{1}{2} - \beta) \Delta t^2 \, \ddot{\underset{\sim}{r}}_k + \beta \Delta t^2 \, \ddot{\underset{\sim}{r}}_{k+1}
$$

$$
\dot{\underset{\sim}{r}}_{k+1} = \dot{\underset{\sim}{r}}_k + \int_0^{\Delta t} \ddot{\underset{\sim}{r}} \, d\tau
$$
(4.4)
$$
\simeq \dot{\underset{\sim}{r}}_k + (1 - \gamma) \Delta t \, \ddot{\underset{\sim}{r}}_k + \gamma \Delta t \, \ddot{\underset{\sim}{r}}_{k+1}
$$

where β and γ are free parameters of the quadrature, and the accelerations are determined from the differential equation. Specialization of these constants leads to a variety of well known methods, which will be indicated later. If $\beta = 0$ and the mass matrix is diagonal, the method

---

[*]That the solution for a viscoelastic problem also depends upon an initial history in a special way is recognized, but ignored here to address an important aspect of the elastic response.

is explicit, whereas for any $\beta > 0$, the method is implicit, requiring the solution of a system of linear algebraic equations to advance the solution. Here, the technique will be applied to the linear viscoelastic system defined by (4.1). For automation of this process, let

$$\underset{\sim}{A} = \underset{\sim}{r}_k + \Delta t \, \dot{\underset{\sim}{r}}_k + (\frac{1}{2} - \beta) \, \Delta t^2 \, \ddot{\underset{\sim}{r}}_k \tag{4.5}$$

$$[K_0 + \frac{1}{\beta \, \Delta t^2} M] \, \underset{\sim}{r}_{k+1} = \underset{\sim}{P}_{k+1} + \frac{1}{\beta \, \Delta t^2} M \, \underset{\sim}{A} - (\dot{K} \circledast \underset{\sim}{r})_{k+1} \tag{4.6}$$

$$\ddot{\underset{\sim}{r}}_{k+1} = [\underset{\sim}{r}_{k+1} - \underset{\sim}{A}] \, \frac{1}{\beta \, \Delta t^2} \tag{4.7}$$

$$\dot{\underset{\sim}{r}}_{k+1} = \dot{\underset{\sim}{r}}_k + (1 - \gamma) \, \Delta t \, \ddot{\underset{\sim}{r}}_k + \gamma \, \Delta t \, \ddot{\underset{\sim}{r}}_{k+1} \tag{4.8}$$

where the convolution of $\dot{K}$ goes back to the zero (stress free) time. Its discretization will be deferred until later. The initial acceleration is given by

$$\ddot{\underset{\sim}{r}}_0 = M^{-1} \{ \underset{\sim}{P}_0 - K_0 \, \underset{\sim}{r}_0 \} \tag{4.9}$$

If $\dot{K} = 0$, or the discretization of the hereditary integral is not made to depend on $\underset{\sim}{r}_{k+1}$, the left hand coefficient matrix of (4.6) need be factored only when Δt changes, greatly reducing the computational effort.

2. Integral Formulation

If one applies the integral equation of motion (4.2) step-by-step, its use as a recursive algorithm requires appropriate quadrature formulas for the three integrals. Noting the similarity in the structure of the three convolutions with (4.3), let

$$\int_0^{\Delta t} (\Delta t - \tau) K_0 \, \underset{\sim}{r} \, d\tau \cong (\tfrac{1}{2} - \beta) \Delta t^2 K_0 \, \underset{\sim}{r}_k + \beta \Delta t^2 K_0 \, \underset{\sim}{r}_{k+1}$$

$$\int_0^{\Delta t} (\Delta t - \tau) \underset{\sim}{P} \, d\tau \cong (\tfrac{1}{2} - \beta) \Delta t^2 \underset{\sim}{P}_k + \beta \Delta t^2 \underset{\sim}{P}_{k+1} \qquad (4.10)$$

$$\int_0^{\Delta t} (\Delta t - \tau) \dot{k} \circledast \underset{\sim}{r} \, d\tau \cong (\tfrac{1}{2} - \beta) \Delta t^2 (\dot{k} \circledast \underset{\sim}{r})_k + \beta \Delta t^2 (\dot{k} \circledast \underset{\sim}{r})_{k+1}$$

If the function $\underset{\sim}{P}(t)$ is known analytically, then the second integral could be computed exactly, a property not shared by the Newmark approach of the previous section. Again deferring discretization of the interior hereditary integral, insert (4.10) into (4.2), and divide by $\beta \Delta t^2$,

$$[K_0 + \frac{1}{\beta \Delta t^2} M] \, \underset{\sim}{r}_{k+1} = \underset{\sim}{P}_{k+1} + \frac{1}{\beta \Delta t^2} \{ (\tfrac{1}{2} - \beta) \Delta t^2 [\underset{\sim}{P}_k - K_0 \, \underset{\sim}{r}_k$$

$$(4.11)$$

$$- (\dot{k} \circledast \underset{\sim}{r})_k] + M (\underset{\sim}{r}_k + \dot{\underset{\sim}{r}}_k \Delta t) \} - (\dot{k} \circledast \underset{\sim}{r})_{k+1}$$

If one defines

$$M \, \ddot{\underset{\sim}{r}}_k = \underset{\sim}{P}_k - K_0 \, \underset{\sim}{r}_k - (\dot{k} \circledast \underset{\sim}{r})_k \qquad (4.12)$$

and uses the previous definition of $\underset{\sim}{A}$, one gets (4.6), the same formula as the Taylor series method. To apply this to the next step, one needs a rule for advancing the velocities. Differentiating (4.2)

$$M\dot{\underset{\sim}{r}} + h * K_0 \underset{\sim}{r} + h * \dot{K} \circledast \underset{\sim}{r} = h * \underset{\sim}{P} + M \dot{\underset{\sim}{r}}_0 \tag{4.13}$$

where $h(t)$ is the Heaviside step function. Applying it step-by-step, and noting the similarity in the structure of the integral with the second of the previous section, let

$$\int_0^{\Delta t} K_0 \underset{\sim}{r}\, d\tau \cong (1 - \gamma) \Delta t\, K_0 \underset{\sim}{r}_k + \gamma \Delta t\, K_0 \underset{\sim}{r}_{k+1}$$

$$\int_0^{\Delta t} \underset{\sim}{P}\, d\tau \cong (1 - \gamma) \Delta t\, \underset{\sim}{P}_k + \gamma \Delta t\, \underset{\sim}{P}_{k+1} \tag{4.14}$$

$$\int_0^{\Delta t} \dot{K} \circledast \underset{\sim}{r}\, d\tau \cong (1 - \gamma) \Delta t\, (\dot{K} \circledast \underset{\sim}{r})_k + \gamma \Delta t\, (\dot{K} \circledast \underset{\sim}{r})_{k+1}$$

Substituting into (4.13)

$$M \dot{\underset{\sim}{r}}_{k+1} = (1 - \gamma) \Delta t\, [\underset{\sim}{P}_k - K_0 \underset{\sim}{r}_k - (\dot{K} \circledast \underset{\sim}{r})_k]$$
$$+ \gamma \Delta t\, [\underset{\sim}{P}_{k+1} - K_0 \underset{\sim}{r}_{k+1} - (\dot{K} \circledast \underset{\sim}{r})_{k+1}] + M \dot{\underset{\sim}{r}}_k \tag{4.15}$$

and using the definition of $\ddot{\underset{\sim}{r}}$, one gets (4.8). Thus, the step-by-step application of the integral method is essentially equivalent to Newmark's method, with the one advantage of defining a generalized load rather than

discretely sampling it. If one substitutes the differential equation (4.1) into the Taylor series remainder in (4.3) before using the quadrature formula, one gets the integral formulation, including the generalized loads.

C. Error and Stability Analysis of Discrete Elastic Systems

An error analysis of (4.1) with $\dot{K} = 0$ accomplished by studying a single degree of freedom. If the transformation

$$\underset{\sim}{r} = \Phi \underset{\sim}{z} \tag{4.16}$$

modally decomposes (4.1) into

$$\underset{\sim}{\ddot{z}} + \Lambda \underset{\sim}{z} = \underset{\sim}{P^*} \tag{4.17}$$

where

$$K \Phi = M \Phi \Lambda$$

$$\Phi^{-1} M \Phi = 1 \tag{4.18}$$

$$\underset{\sim}{P^*} = \Phi^{-1} \underset{\sim}{P}$$

and Λ is the diagonal matrix of eigenvalues ω_i^2, with the columns ϕ^i of Φ the corresponding eigenvectors, then the same transformation

$$\underset{\sim}{r}_k = \Phi \underset{\sim}{z}_k \tag{4.19}$$

uncouples the numerical integration of the system (4.6). In effect, the same time step is applied to each mode, even though Λ and Φ are not computed.

Considering the single equation

$$\ddot{z} + \omega^2 z = P^*$$ (4.20)

the application of the algorithm defined by (4.5) to (4.8) to successive time steps and the elimination of the velocity and acceleration leads to the following second order difference equation in terms of displacement only:

$$\mathcal{L}(\beta, \gamma) = [(1 + \beta \theta^2) \diagup\!\!\!\!\diagdown + \theta^2] \bar{z}_k + (\gamma - \tfrac{1}{2}) \theta^2 \nabla \bar{z}_k$$

$$= [1 + \beta \diagup\!\!\!\!\diagdown + (\gamma - \tfrac{1}{2}) \nabla] \Delta t^2 - P_k^*$$ (4.21)

where $\theta^2 = \omega^2 \Delta t^2$, and $\diagup\!\!\!\!\diagdown$, ∇ are the second central and backward difference operators introduced in the previous Chapter.

Introducing the notation $\alpha^2 = \theta^2/(1 + \beta \theta^2)$ and $\delta = \gamma - \tfrac{1}{2}$, one gets

$$(\diagup\!\!\!\!\diagdown + \alpha^2) \bar{z}_k + \delta \alpha^2 \nabla \bar{z}_k = 0$$ (4.22)

for the homogeneous case. Seeking a solution of the form

$$\bar{z}_k = \lambda^k$$ (4.23)

leads to the characteristic equation

$$\lambda^2 - (2 - \alpha^2 - \delta \alpha^2) \lambda + (1 - \delta \alpha^2) = 0$$ (4.24)

for which

$$\lambda = R \exp (\pm i a) \tag{4.25}$$

where

$$R = \sqrt{1 - \alpha^2 \delta} \tag{4.26}$$

and

$$a = \tan^{-1} \frac{\alpha \sqrt{1 - \frac{\alpha^2}{4}(1 + \delta)^2}}{1 - \frac{\alpha^2}{2}(1 + \delta)} \tag{4.27}$$

If $\gamma < 1/2$, a negative damping is introduced by the algorithm, leading ultimately to an unbounded response, even if oscillatory. For $\gamma > 1/2$, a positive damping is introduced, ultimately annihilating the transient response. For this reason, Newmark, Nickell [48] restricted further discussion to the case $\gamma = 1/2$. For naturally discrete systems this seems reasonable. However, the generality of this damping parameter will be retained here, as a potential throttle on the spurious osscilations of the discrete system (4.1) itself, in its approximation to discontinuities in the exact continuum solution.

To ensure an oscillatory response, a must be real. For a to be real

$$1 - \frac{1}{4}\alpha^2 (1 + \delta)^2 \geq 0 \tag{4.28}$$

Thus, a stability limit is imposed on Δt such that

$$\theta \leq [\ \tfrac{1}{4}\ (1 + \delta)^2 - \beta\ ]^{-\,1/2} \tag{4.29}$$

For the algorithm to be unconditionally stable,

$$\beta \geq \tfrac{1}{4}\ (1 + \delta)^2 \tag{4.30}$$

which includes the special value of $\beta = 1/4$, $\delta = 0$ given by Newmark. Positive δ decreases the stability limit, or increases the β needed for unconditional stability.

The undamped case $(\delta = 0)$ has been discussed by Newmark [47] and by Nickell [48]. For this case

$$a = \tan^{-1} \frac{\alpha \sqrt{1 - \tfrac{1}{4}\alpha^2}}{1 - \tfrac{1}{2}\alpha^2} = 2 \sin^{-1} (\tfrac{\alpha}{2}) \tag{4.31}$$

For the particular loading

$$P_k^* = P_0 + \dot{P}_0\ k\ \Delta t \tag{4.32}$$

the difference equation (4.22) has the solution

$$\bar{z}_k = A \cos ka + B \sin ka + \frac{P_0}{\omega^2} + \frac{\dot{P}_0\ \Delta t}{\omega^2}\ k \tag{4.33}$$

Imposing the initial conditions, then

$$z_0 = A + \frac{P_0}{\omega^2} \tag{4.34}$$

$$\dot{z}_0 \simeq \frac{z_1 - z_{-1}}{2\,\Delta t} = \frac{2\,B\,\sin a + 2\,\frac{1}{\omega^2}\,\dot{P}_0\,\Delta t}{2\,\Delta t} \tag{4.35}$$

and thus,

$$\bar{z}_k = z_0 \cos ka + \dot{z}_0\,\Delta t\,\frac{\sin ka}{\sin a} + \frac{P_0}{\omega^2}\,(1 - \cos ka)$$

$$+ \frac{\dot{P}_0\,\Delta t}{\omega^2}\,\left(k - \frac{\sin ka}{\sin a}\right) \tag{4.36}$$

which simulates the exact solution of (4.20), for that particular loading, of

$$z_k = z_0 \cos k\theta + \frac{\dot{z}_0\,\Delta t}{\theta}\,\sin k\theta + \frac{P_0}{\omega^2}\,(1 - \cos k\theta)$$

$$\tag{4.37}$$

$$+ \frac{\dot{P}_0\,\Delta t}{\omega^2}\,\left(k - \frac{\sin k\theta}{\theta}\right)$$

Although the forms of the solution are similar, the approximate period is in error in the ratio

$$\frac{\bar{T}}{T} = \frac{\theta}{a} \tag{4.38}$$

This ratio, as a function of $\Delta t/T$, is plotted in Figure 4.3. Although $\beta = 1/4$ is the threshold of unconditional stability, one sees that as $\Delta t >> T$, (i.e., $\theta \to \infty$), the approximate period tends toward twice the time step, a meaningless oscillating result of finite amplitude. Thus, unconditional stability should not be pushed too far.
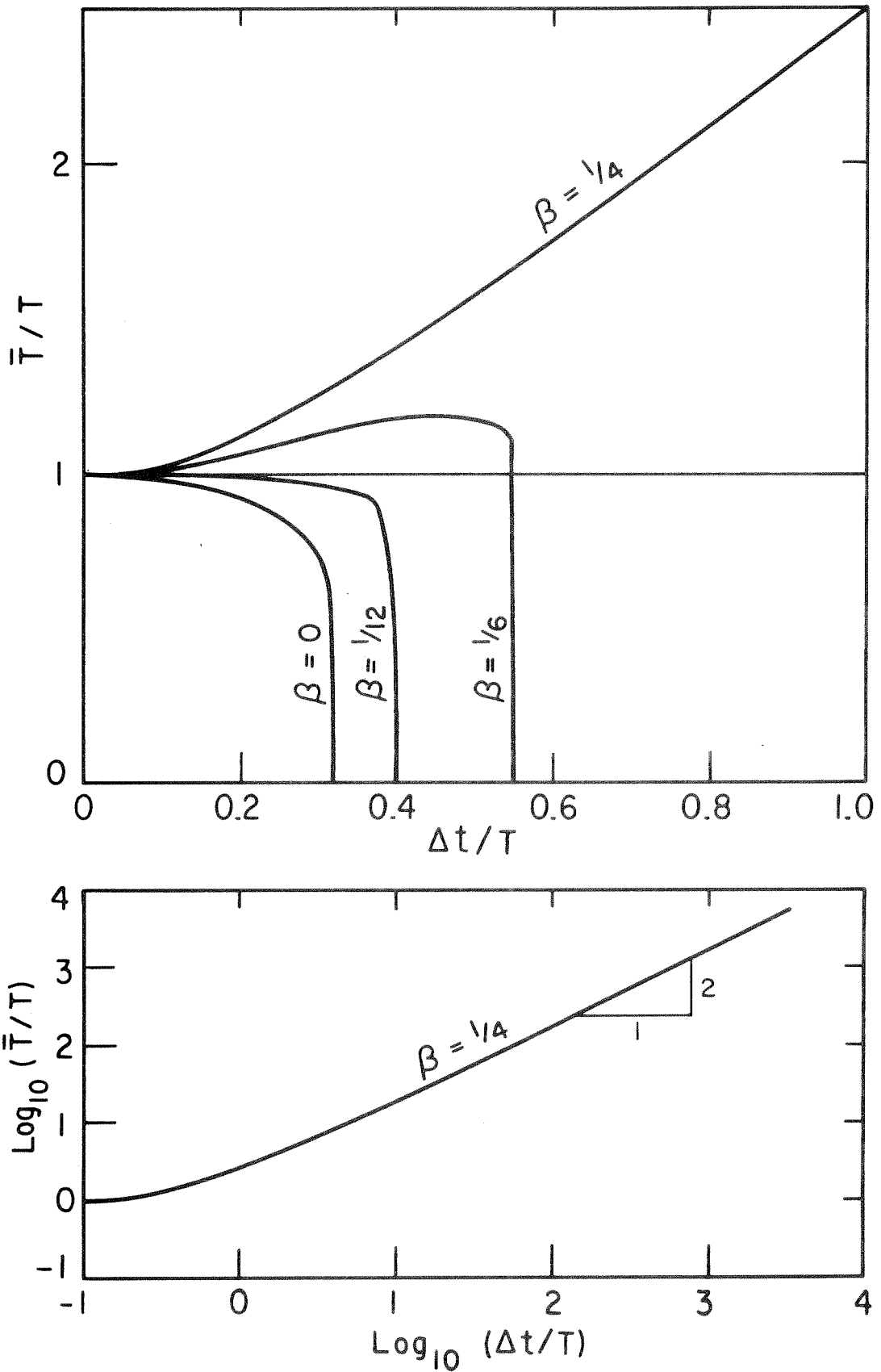
FIG. 4.3 PERIOD RATIO OF β METHODS $(\gamma = 1/2)$

The peak responses to an initial displacement, and to the step load, are correct, but those due to initial velocity, and a linear load are in error. Newmark claimed [47] that the average acceleration method (β = 1/4) produced the correct peak response to an initial velocity and accordingly advocated that method as most suitable for step-by-step integration of dynamic problem. However, he incorrectly imposed the initial velocity condition (4.35) and his equation (23) as well as his table (2.6) are incorrect. Comparing (4.36) with (4.37) the error in peak response to an initial velocity is actually given by

$$\frac{\theta}{\sin a} = \frac{1 + \beta \theta^2}{\sqrt{1 + (\beta - \frac{1}{4}) \theta^2}} \qquad (4.39)$$

which for β = 1/4 increases quadratically with Δt. Thus for large time steps, large amplitudes compound the erroneous periods of the higher modes of the system. Although these errors do not grow in time, they can seriously perturb the total solution even though the Fourier component of the mode is small.

Newmark's family of β methods with γ = 1/2 (δ = 0), includes the following well known methods:

1. (β = 0) This explicit method is equivalent to that obtained by the usual second central difference

approximation to the second time derivative of (4.1) or (4.20). It is unstable for $\Delta t > 0.318$ T.

2. (β = 1/12) This implicit method of Fox and Goodwin [ ], has the optimum β for convergence as $\Delta t \to 0$. It is unstable for $\Delta t > 0.389$ T.

3. (β = 1/6) "Linear acceleration" method. Unstable for
   Δt > 0.551 T.

4. (β = 1/4) "Average acceleration" method. Unconditionally
   stable.

Can an optimum β be recommended? For an individual equation, figure (4.3) shows that for any Δt there is a β (or conversely, for any β there is a Δt) that yields the exact period, but this offers no help for the system of equations (4.1).

For an accurate integration of the system of equations (4.1) with the largest possible time step, the higher order method of Fox and Goodwin (β = 1/12) offers a tempting possibility. If the highest frequency of the system can be estimated then the time step required to ensure stability can be calculated. This presumes that the higher frequencies are important in the solution. For most vibration problems this is not so, and the small time step required to ensure stability of the higher modes results in unnecessary computation. In shock problems, even though higher modes are important, the higher modes of the discrete system are significantly in error, and it is hardly worth integrating them accurately. Finally, in continuum problems with large variations in mesh size, or with large relative stiffnesses between two materials, the highest frequency may be orders of magnitude greater than the effective frequencies of the solution in the range of interest. Thus, an unconditionally stable algorithm seems imperative for the more complicated dynamic problems.

For simplicity, once one has selected the degree of damping desired, β can be computed from (4.30) to guarantee unconditional

stability. However, if one can obtain an upper bound for the highest frequency of the system, then applying (4.29) one need only have

$$\beta \geq \frac{1}{4} (1 + \delta)^2 - \frac{1}{\theta^2_{max}} \tag{4.40}$$

In other words, β need not be as great as indicated by (4.30), and thus the method could be made more accurate if one is willing to computationally estimate the highest frequency. Figure 4.3 shows the considerable improvement that can be made in reducing β from 1/4 down toward 1/12.

D. Suppression of Higher Modes

1. Wilson's Method

The first effort of which this writer is aware to compensate in linear structural dynamics analysis for the spurious oscillations inherent in discrete approximations to continuum problems was Wilson [50]. He started with the linear acceleration method commonly in use at the time for step-by-step dynamics analyses of structures. This method which is a member of the Newmark family ($\beta = 1/6$ and $\gamma = 1/2$) was popular because of its derivation from the intuitively pleasing notion of continuity in time of displacement, velocity, and acceleration, the latter two fields being derivable from the first. Wilson's modification of the method, motivated by the desire to minimize unwanted oscillations, clouded the notion of continuity of the fields in time, but succeeded in generating an unconditionally stable algorithm with sufficient inherent damping to suppress the oscillations of the higher modes. The full derivation of his method will not be given here [50]. The basic motivation is that the acceleration field of the linear acceleration

method ought to be most accurate at the midpoint of the time interval. Thus, if one wants to advance Δt, one applies the linear acceleration method to an interval of 2 Δt and then evaluates the result at Δt, and then proceeds step-by-step.

Considering (4.21) for the linear acceleration method, one may define the following difference operation

$$\mathcal{L}_{(1/6\,,\,1/2)}\,\bar{z}_k = [(1 + \tfrac{1}{6}\theta^2)]\,\bar{z}_k$$
$$- [1 + \tfrac{1}{6}\,\boxed{\diagup}]\,P_k^*\,\Delta t^2 \tag{4.41}$$

Then, the Wilson method leads to the governing equation[*]

$$(\nabla + 1)\,\mathcal{L}_{(1/6)}\,\bar{z}_k + \theta^2\,\boxed{\diagup}\,\bar{z}_k = 0 \tag{4.42}$$

Letting

$$\bar{z}_k = \lambda^k \tag{4.43}$$

leads to the characteristic equation

$$(2 + \alpha^2)\,\lambda^3 - 5\lambda^2 + 4\lambda - 1 = 0 \tag{4.44}$$

for which all three roots remain within the unit circle for all $\theta = \omega\Delta t$, where $\alpha^2 = \theta^2/(1 + \tfrac{1}{6}\theta^2)$. This unconditional stability has already

---

[*] It should be noted form (4.42), that Wilson's method results in a third order difference equation approximating the second order differential equation (4.20), and should be investigated for the possibility of an unstable root.

been shown by Nickell [48]. The method, however, has considerable damping, more than is needed to control the spurious oscillations of the discrete approximation. The mid point idea has been generalized to an optimal point method by Farhoomand [51].

2. Nickell's Method

Another effort in a similar direction was presented by Nickell [52, 42, 48]. His spatial discretization was obtained from Gurtin type variational principles, resulting in the discrete set of integral equations (4.2). His basic time integration schemes result from introducing a one step quadrature formula into the convolution and solving to advance the displacements. The quadrature formula is obtained by introducing the interpolation field

$$\underset{\sim}{r}(t) = \phi_1(t) \, \underset{\sim}{r}_{k-1} + \phi_2(t) \, \dot{\underset{\sim}{r}}_{k-1} + \phi_3(t) \, \underset{\sim}{r}_k \qquad (4.45)$$

where ϕ_1, ϕ_2, and ϕ_3 are quadratic interpolation functions. It turns out that this is the highest order one step quadrature possible, and corresponds to the Fox-Goodwin method $(\beta = 1/12)$. However, the notion of continuity led Nickell to advance his velocity by differentiating his displacement field (4.45) to obtain a velocity field

$$\dot{\underset{\sim}{r}}(t) = \dot{\phi}_1(t) \, \underset{\sim}{r}_{k-1} + \dot{\phi}_2(t) \, \dot{\underset{\sim}{r}}_{k-1} + \dot{\phi}_3(t) \, \underset{\sim}{r}_k \qquad (4.46)$$

from which $\dot{\underset{\sim}{r}}_k$ is evaluated, rather than the consistent order approximation implied by (4.13) and (4.14) in the previous discussion of the integral method. Nickell's velocity formula becomes

$$\dot{\underset{\sim}{r}}_k = -\frac{2}{\Delta t} \, \underset{\sim}{r}_{k-1} - \dot{\underset{\sim}{r}}_{k-1} + \frac{2}{\Delta t} \, \underset{\sim}{r}_k \qquad (4.47)$$

But, from (4.2) and (4.45), together with the previous definition of $\ddot{\underset{\sim}{r}}_k$,

$$\underset{\sim}{r}_k = \underset{\sim}{r}_{k-1} + \Delta t\ \dot{\underset{\sim}{r}}_{k-1} + \frac{5}{12}\ \Delta t^2\ \ddot{\underset{\sim}{r}}_{k-1} + \frac{1}{12}\ \Delta t^2\ \ddot{\underset{\sim}{r}}_k \qquad (4.48)$$

and

$$\dot{\underset{\sim}{r}}_k = \dot{\underset{\sim}{r}}_{k-1} + \frac{5}{6}\ \Delta t\ \ddot{\underset{\sim}{r}}_{k-1} + \frac{1}{6}\ \Delta t\ \ddot{\underset{\sim}{r}}_k \qquad (4.49)$$

Thus, Nickell's basic method is seen to fall within the framework of the Newmark family with $\beta = 1/12$ and $\gamma = 1/6$. Since $\gamma < 1/2$ the method produces a negative damping (i.e., unconditionally unstable), a result indicated in his latest paper [48], and explains his earlier difficulty encountered in trying to do elastic wave propagation with his basic method. Guided by Wilson's experience, Nickell used a similar technique of evaluating his solution at the middle of a time step, then restarting the procedure from there. The details of his method are contained in [48], the pertinent result being that it is also unconditionally stable, and possesses inherent damping, though not as great as Wilson's method.

3. Newmark δ Control

Wilson's and Nickell's methods convert conditionally stable or unstable algorithms into unconditionally stable algorithms which smooth out high frequency oscillations through their inherent damping. The disadvantage of the damping is that it may destroy more of the solution than is desirable. Since both methods are convergent as $\Delta t \rightarrow o$, a smaller time step can revive desired oscillations at the cost of extra computational effort. In other words, all stable time integration

schemes will converge to the exact solution of the spatially discrete system, with attendant spurious high frequency oscillations in continuum impact problems.

The use of δ damping with the Newmark family of β methods permits a controlled degree of damping for any desired time step. The amount desired might be gauged from the amplitude decay equation (4.26), but more likely must be judged from experience. The use of this damping ought to be considered as a data smoothing technique. At present, it is a black art, similar to the artificial viscosity used for years to accomplish a similar purpose in hydrodynamic shock analyses [54].

E. Examples

1. Triangular Pulse in Elastic Slab

The effect of approximate time integration schemes in conjunction with a lumped mass spatial discretization is best illustrated by the one dimensional wave operator which governs the transmission of a plane wave through an elastic free-free slab. This operator (the same as the simple bar operator treated in the previour Chapters) is non-dispersive in character, so that a triangular stress pulse impacting one face of the slab travels undistorted through the slab, and back again, alternating from a compression to a tensile pulse due to the stress free boundary conditions. The lumped mass spatial discretization imposes its own inherent dispersion on the solution, as illustrated in the impact problem of the previous Chapter and further indicated in this example by the upper left portions of Figures 4.4 - 4.6. The notation $\Delta t \to 0$ implies the converged (or exact) time solution to the spatially
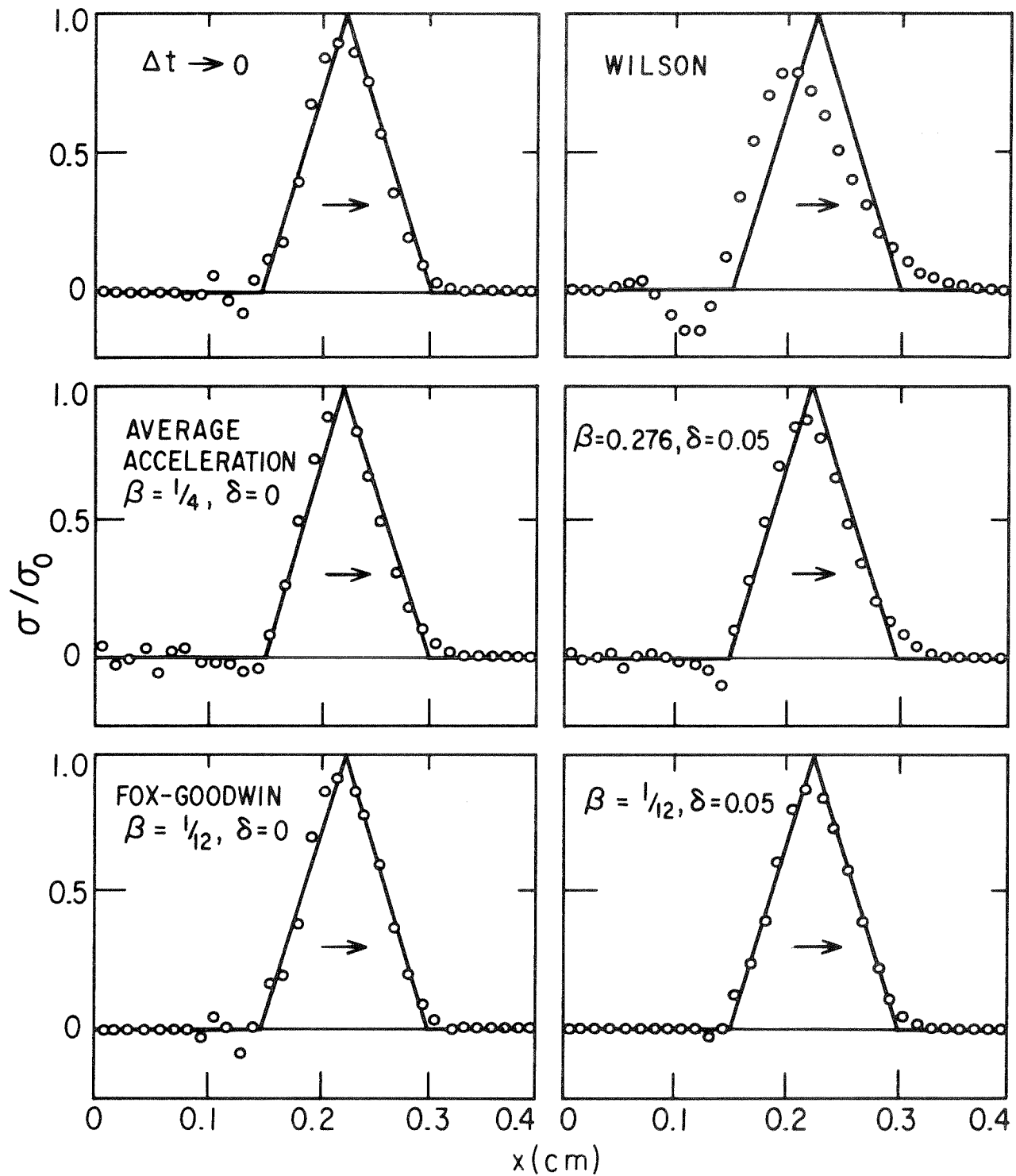
FIG. 4.4   TRIANGULAR PULSE THROUGH ELASTIC SLAB

$$t = 2\,\mu sec \;, \quad \Delta t = \frac{\Delta x}{C} = \frac{1}{12}\,\mu sec$$
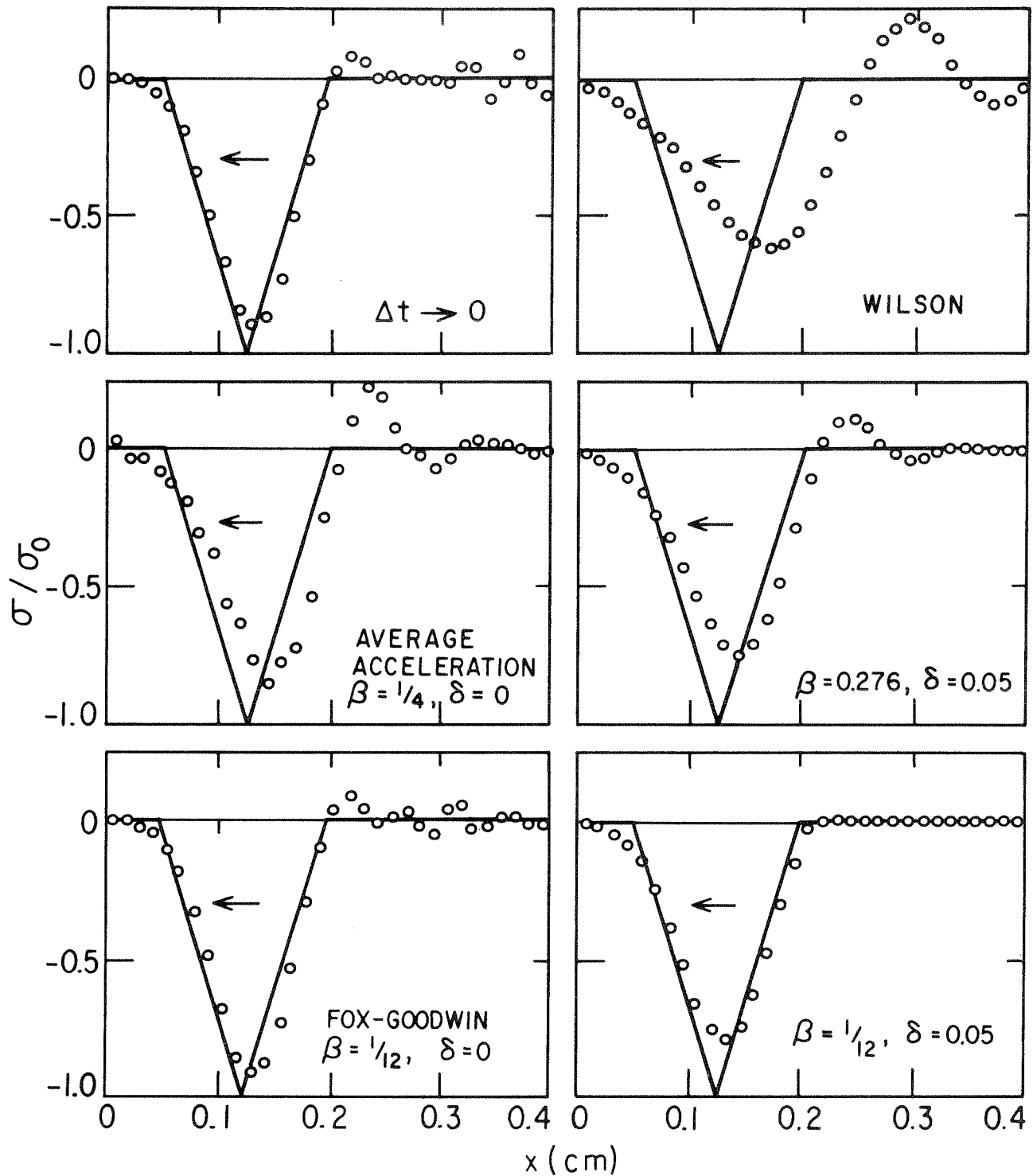
FIG. 4.5   TRIANGULAR PULSE THROUGH ELASTIC SLAB

$t = 5\mu sec$, $\Delta t = \dfrac{\Delta x}{c} = \dfrac{1}{12}\mu sec$
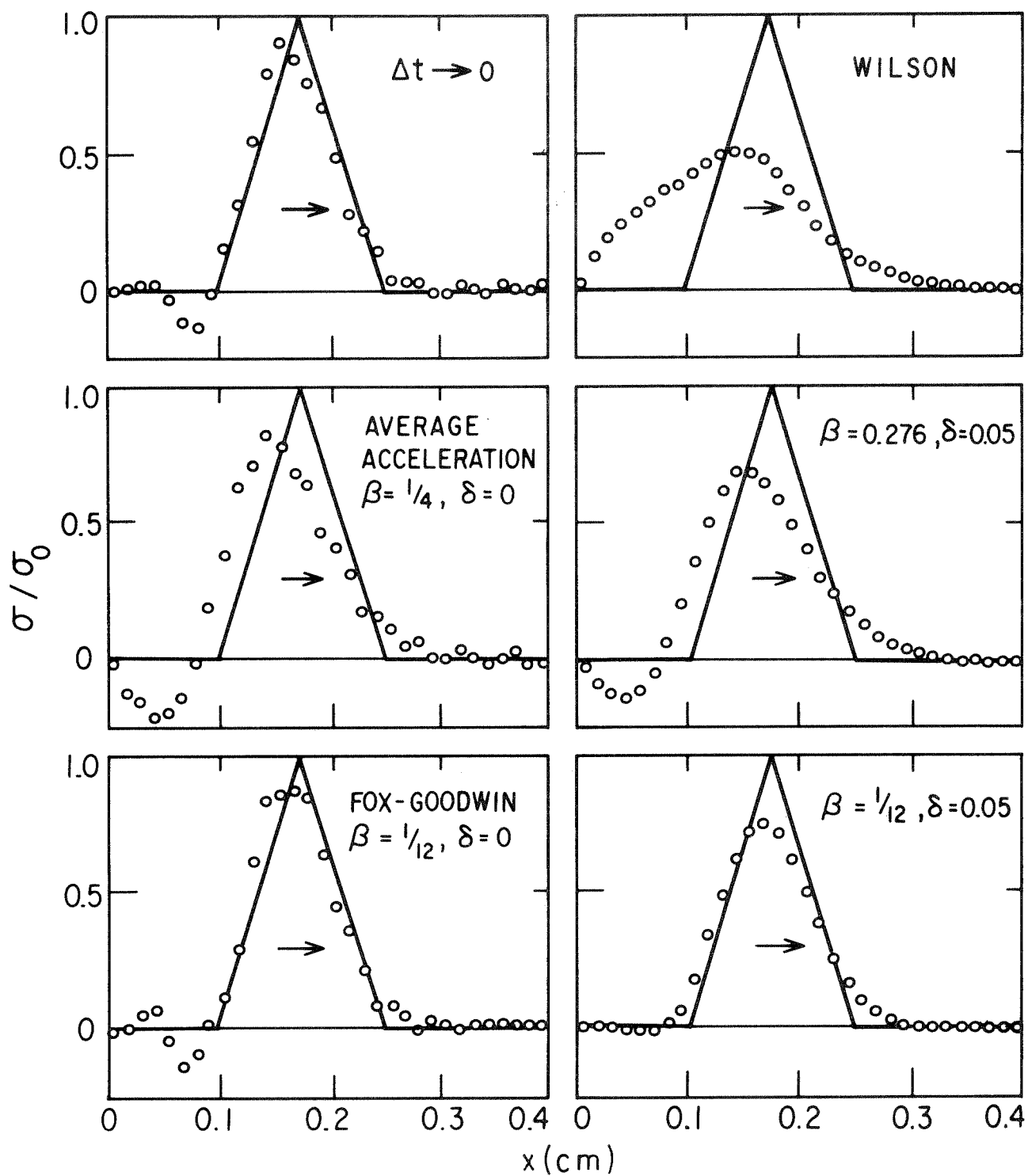
FIG. 4.6   TRIANGULAR PULSE THROUGH ELASTIC SLAB
$t = 7\,\mu\text{sec}\,, \quad \Delta t = \frac{\Delta x}{C} = \frac{1}{12}\,\mu\text{sec}$

discretized problem. As before high frequency oscillations emanate from
the discontinuity points of the solution. To achieve this converged time
result a time step of one fifth to one tenth of the characteristic time
of the material ($\Delta x/c$) was required.

For comparison the unconditionally stable "average acceleration"
method ($\beta = 1/4$), and the optimal β method of Fox and Goodwin
($\beta = 1/2$) are shown in the other left hand portions of the series of
figures. Both are shown for the characteristic time step of $\Delta x/c$,
with no artificial damping ($\delta = 0$). The average acceleration method
exhibits a noticable dispersion as time advances in addition to the high
frequency oscillations. The Fox-Goodwin method is remarkable similar to
the converged result.   Applying the frequency analysis of the previous
Chapter, namely Eq. (3.21) with $\lambda = n\pi$,

$$T_{min} = \frac{2\pi}{\omega_{max}} \geq \pi \frac{\Delta x}{c} \tag{4.50}$$

Now entering Figure 4.3, $\Delta t/T \leq .318$ for all modes, and for $\beta = 1/12$,
the frequencies of the discrete spectrum are accurate to five percent.
It is the high frequency oscillations which required five times more
computation to achieve pointwise convergences.

A small amount of δ damping was used in each case to
successfully smooth the high frequency oscillations. The β of .276
was computed from (4.30) to guarantee unconditional stability, though
all β values are stable at the time step considered. For comparison,
the Wilson algorithm is shown for the same time step. It involves about
ten percent more computation and leads to considerable damping as time
progresses.

The considerable success of the small artificial damping in conjunction with the low β leads to the recommendation to use the smallest β consistent with the stability requirement imposed by the time step desired. For any β (even the explicit $\beta = 0$), a small enough time step can be found to ensure stability. If that time step is considerably smaller than the characteristic time of the wave it would appear preferable to accept a larger β to ensure stability at the desired time step. This stresses the need to obtain an upper bound (or accurate estimate) of the highest frequency to enable one to compute the minimum acceptable β from equation (4.40).

For vibration problem the desired time step may even be orders of magnitude greater than the characteristic one. In such a problem the important low modes of the continuum are accurately approximated and the higher inaccurate but unimportant ones can be damped out with a suitable δ. Thus, the unconditionally stable average acceleration method (with suitable δ) is the simplest choice and should suffice.

2. Rigid Impact of Higher Order Bar

Although the evaluation of algorithms for general two and three dimensional wave propagation problems was an objective of this study, only simple problems amenable to exact solution (or economical empirical convergence) have been investigated. The simplest treatment of a second space variable is the thickness of a plate or the radius of a rod. The latter suited a pending related application and so a higher order bar theory was constructed. The problem considered is spatially discretized by the bilinear quadralateral finite element with one element through the radius. For the solid bar this allows three degrees of

freedom at each station along the bar and can be considered to define a three mode bar theory. The rigid impact of an isotropic elastic bar with $\nu = .4$ and a length of five times the radius was investigated. For the elastic bar the initial shock wave discontinuity is equal to that of the one dimensional strain wave, travels at the dilational velocity, and does not decay. The three mode theory (defined by the limit as $\Delta z \to 0$ and $\Delta t \to 0$ for one radial element) trails oscillations behind the mentioned discontinuity, ultimately followed by the group velocity phenomenon idealized at long times as the simple bar wave. For the short length of bar and time considered, the dilatational and simple bar phenomena remain highly coupled. The progress and reflection of the wave at the free end of the bar are depicted by the solid line in Figures 4.7 - 4.9. The dashed line represents the simple bar theory. The simple bar velocity c_0 and dilatational velocity c_1 are related by

$$\frac{c_0}{c_1} = \sqrt{\frac{(1 + \nu)(1 - 2\nu)}{(1 - \nu)}} \qquad (4.51)$$

and the simple bar theory stress amplitude is that same percentage of the dilatational jump. As time progresses, the dilatational spike narrows, and although in Figure 4.9 it is quite narrow, its train of oscillations still significantly affects the solution. This so-called "exact" solution of the one radial element theory was obtained as a converged result of the characteristic type algorithm discussed in the next Chapter. It provides a suitable basis for evaluating the general algorithms discussed in this Chapter.
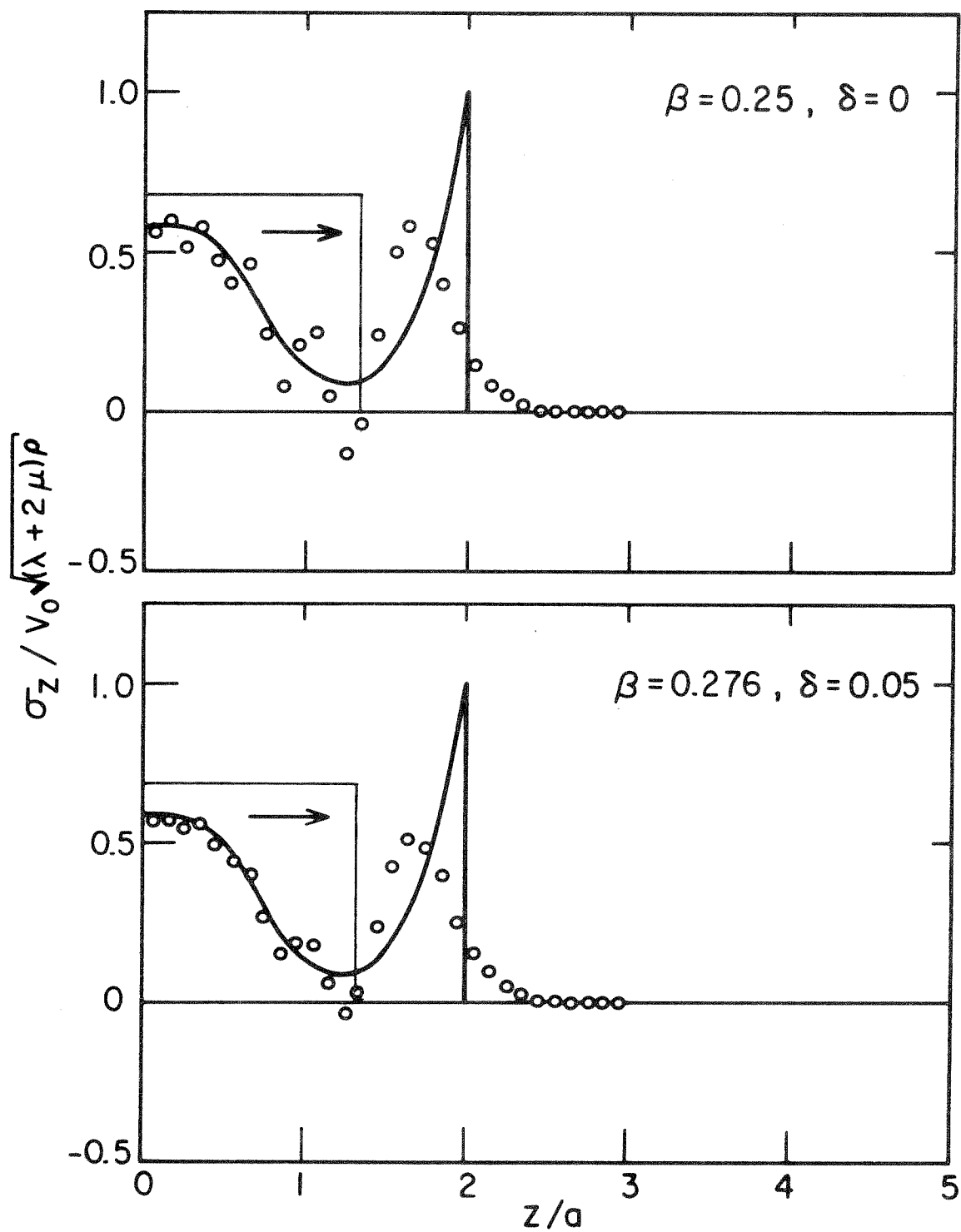
FIG. 4.7   RIGID IMPACT OF HIGHER ORDER BAR $(\nu = 0.4)$
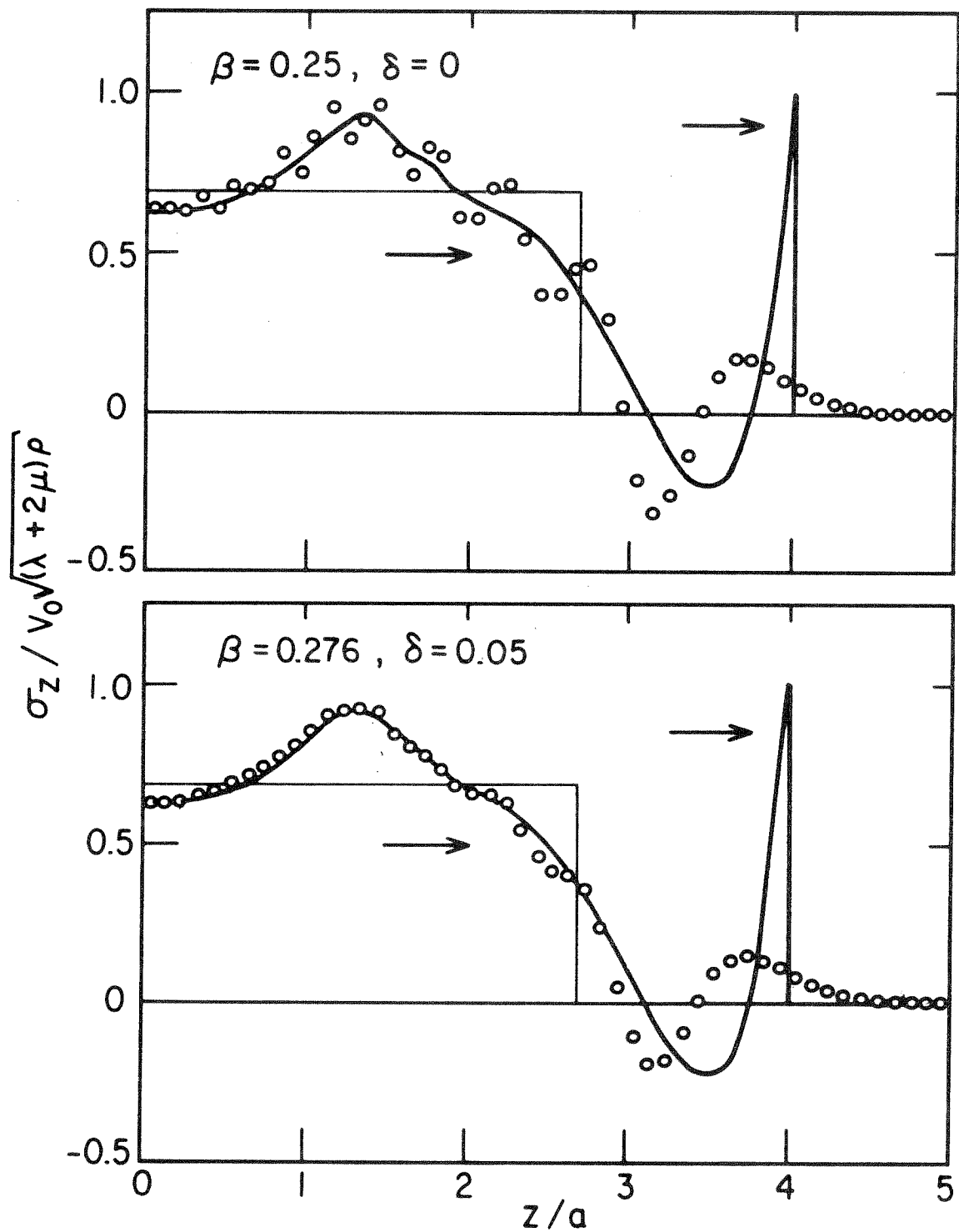$C_1 t/a = 2, \quad C_1 \Delta t/a = 0.1 \quad, \quad C_0/C_1 = 0.68$

FIG. 4.8 RIGID IMPACT OF HIGHER ORDER BAR $(\nu = 0.4)$
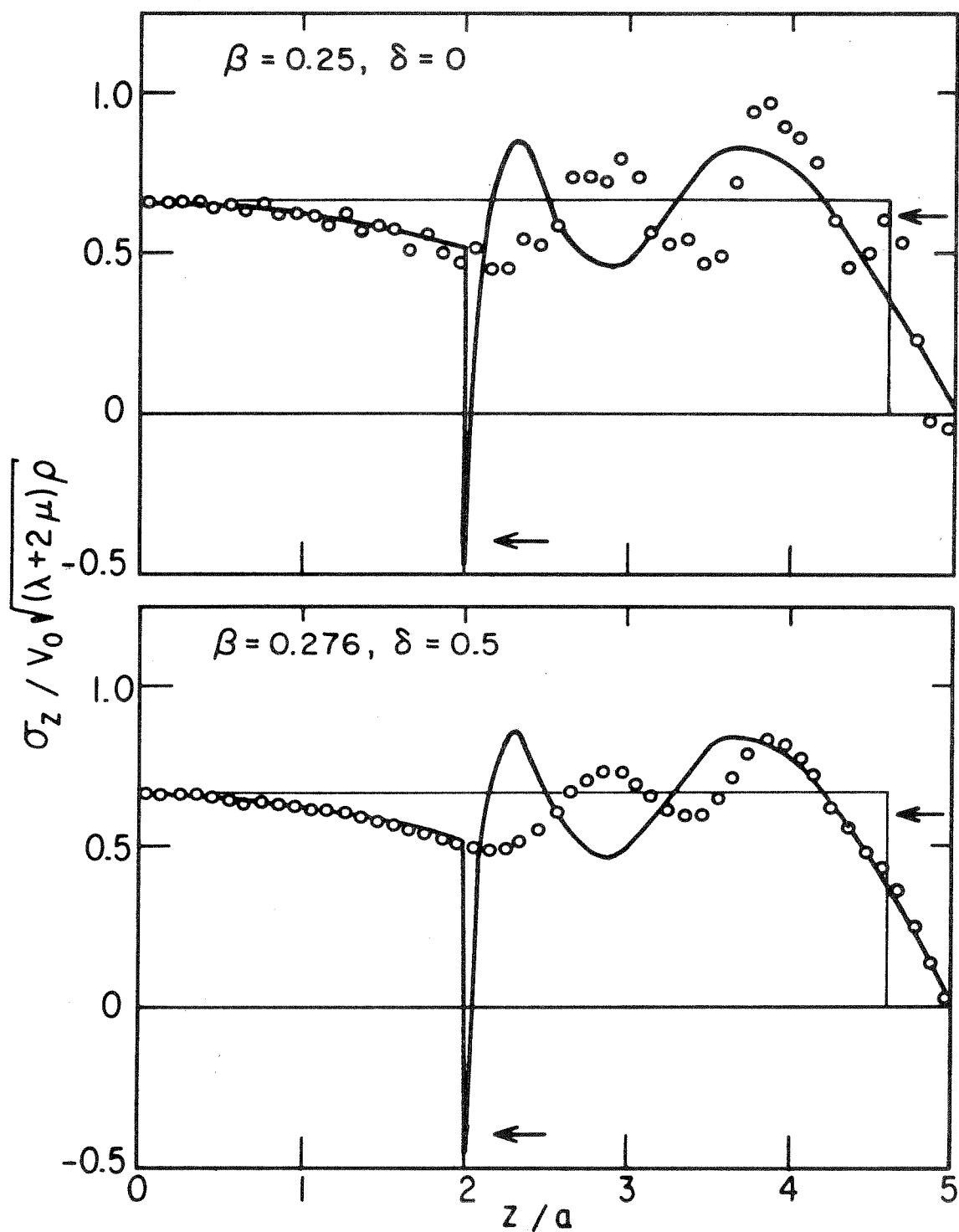$C_1 t/a = 4$, $C_1 \Delta t/a = 0.1$, $C_0/C_1 = 0.68$

FIG. 4.9 RIGID IMPACT OF HIGHER ORDER BAR ($\nu = 0.4$)
$C_l t/a = 8$, $C_l \Delta t/a = 0.01$, $C_0/C_l = 0.68$

The basic algorithm considered here is the unconditionally stable average acceleration method. Its two striking properties are 1) the smearing of the dilatational spike and 2) the high frequency oscillations emanating from the discontinuity and perturbing the solution for a considerable distance. The mesh used uas fifty elements (a total of 153 degrees of freedom). The lower figures show the successful smoothing of the high frequency oscillations with a small δ. There still remains a significant dispersion of the solution in the vicinity of the front. Many hundreds of elements would be required to even approach the height of the spike. This loss may have to be tolerated, but some understanding of the nature of the error seems necessary.

F. Approximation of Viscoelastic Integral

The extension of the Newmark family to viscoelastic problems requires only the time discretization of the hereditary integral at the end of equation (4.6). Its discussion has been deferred to this point because no error analysis has been attempted, nor does more than computational experiment seem feasible. However, the same idea is advocated that was presented by Taylor, Pister, and Goudreau [29] in the quasi-static case; that is, that rather than approximate the integral by a general quadrature formula, one ought to discretize the unknown displacement field by some appropriate interpolation function and then exactly integrate the kernel.* Taking advantage of known structure in this way has proved superior to global quadrature.

_____

*For temperature dependent kernels, an additional approximation must be introduced into the integration.

Let the displacement field be approximated piecewise, Then

$$(\dot{K} \circledast \underset{\sim}{r})_{k+1} = \sum_{i=1}^{k+1} \int_{t_i-1}^{t_i} \phi \, [T \, (t')] \, \dot{K} \, (\xi - \xi') \, \underset{\sim}{r} \, (t') \, dt' \qquad (4.52)$$

Integrating by parts, and noting that $\dot{K}$ does not contain the instantaneous modulus matrix, (i.e., $K = K_0 + K_1 \, (t)$),

$$(\dot{K} \circledast \underset{\sim}{r})_{k+1} = K_1 \, (\xi_{k+1}) \, r_0 + \sum_{i=1}^{k+1} \int_{t_i-1}^{t_i} K_1 \, (\xi - \xi') \, \underset{\sim}{\dot{r}} \, dt' \qquad (4.53)$$

Assuming $\underset{\sim}{r}$ to be piecewise linear, then

$$(\dot{K} \circledast \underset{\sim}{r})_{k+1} = K_1 \, (\xi_{k+1}) \, \underset{\sim}{r}_0 + \sum_{i=1}^{k+1} \Delta \, \underset{\sim}{r}_i \, I_i^{k+1} \qquad (4.54)$$

where

$$I_i^{k+1} = \frac{1}{\Delta t_i} \int_{t_i-1}^{t_i} K_i \, (\xi_{k+1} - \xi') \, dt' \qquad (4.55)$$

For the special structure of a kernel represented by an exponential series, the recurrence relation of [29] may be used.

Inserting (4.54) and (4.55) into (4.6) and moving the implicit part to the left hand side,

$$[K_0 + I^{k+1} + \frac{1}{\beta \Delta t^2} \, M] \, \underset{\sim}{r}_{k+1} = \underset{\sim}{P}_{k+1} + \frac{1}{\beta \Delta t^2} \, M\underset{\sim}{A} - \underset{\sim}{S}_{k+1}$$

where

$$\underset{\sim}{S}_{k+1} = K_1 (\xi_{k+1}) \underset{\sim}{r}_0 + \sum_{i=1}^{k} \Delta \underset{\sim}{r}_i I_i^{k+1} - I_{k+1}^{k+1} \underset{\sim}{r}_k$$

and $\underset{\sim}{A}$ is given by (4.5) and I_i^{k+1} by (4.55). For the isothermal case, I_{k+1}^{k+1} depends only on Δt and the coefficient matrix meed be factored only when Δt changes. For the general non-isothermal case it must be factored every time step. Although this is the procedure currently used in quasi-static thermo-viscoelastic analysis, the representation of the history integral by a less accurate explicit representation might be better in that many more time steps could be integrated with a single factored matrix. If radical changes in inhomogeneity result in time, periodic use of the implicit form might suffice. The numerical solution of thermo-viscoelastic problems in more than one space variable still needs much study, especially explicit methods or the alternating direction methods which minimize implicit computation.

5. EXPLICIT ALGORITHM AND CHARACTERISTICS

A. Special Property of the One Dimensional Wave Operator

The one dimensional wave operator

$$\frac{\partial^2 u}{\partial x^2} = \frac{1}{c^2}\frac{\partial^2 u}{\partial t^2} \tag{5.1}$$

possesses an important property which will prove useful in the approximation of a class of wave propagation solutions. The equation (5.1) may be transformed by the change of variables

$$\xi = x + c t$$
$$\eta = x - c t \tag{5.2}$$

into the equation

$$\frac{\partial^2 u}{\partial \xi \partial \eta} = 0 \tag{5.3}$$

whose solution

$$u(\xi,\eta) = f(\xi) + g(\eta) \tag{5.4}$$

for arbitrary f and g was already introduced in Chapter 3. If equation (5.3) is integrated over the diamond defined by lines of constant ξ and η in Figure 5.1, one obtains the exact relation

$$u_A = u_B + u_C - u_D \tag{5.5}$$

Thus, if u is known along the characteristic line ODB and the vertical axis, equation (5.5) exactly propagates the solution over the space-time grid.
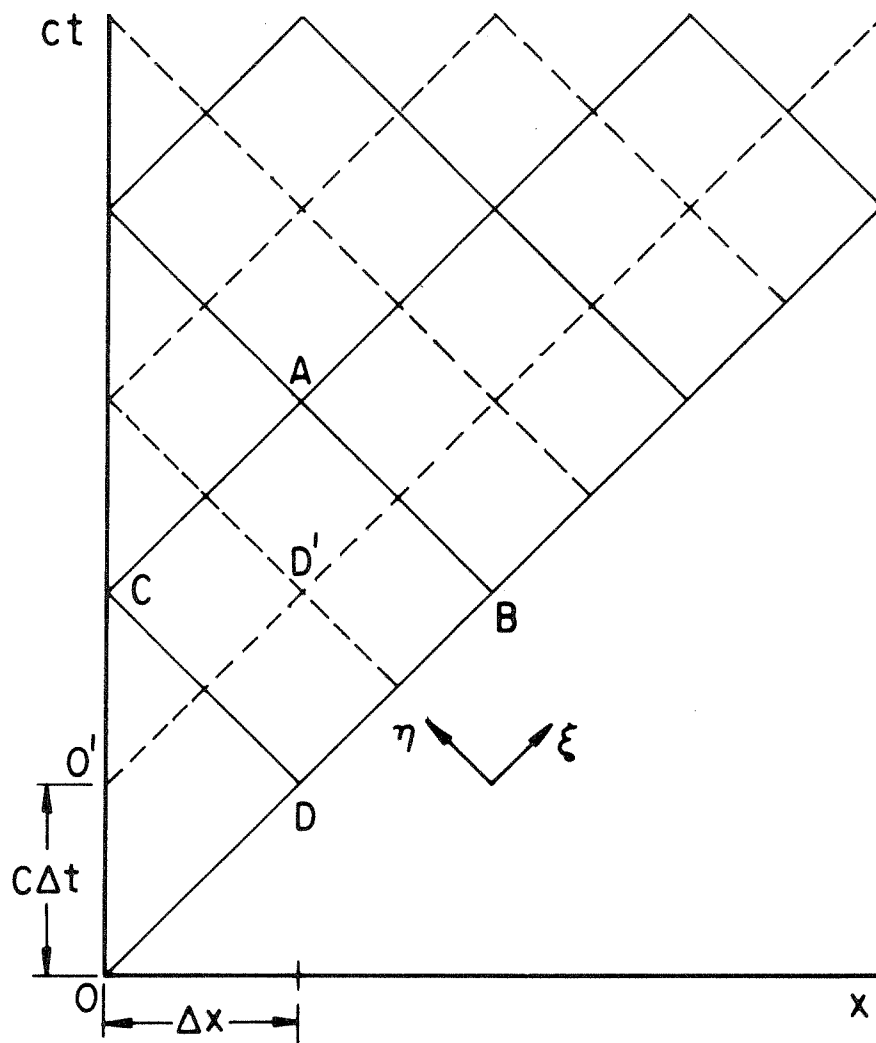
FIG. 5.1 CHARACTERISTIC GRID

Alternatively, if the displacements and velocities are known along some line of constant t, say the initial axis, where

$$u(x,0) = u_0(x)$$
$$\dot{u}(x,0) = \dot{u}_0(x)$$

(5.6)

one may use the exact relation given by Courant [2]

$$u(x,t) = \frac{1}{2}[u_0(x+ct) + u_0(x-ct)]$$

$$+ \frac{1}{2}\frac{1}{c}\int_{x-ct}^{x+ct} \dot{u}_0(\alpha)\,d\alpha$$

(5.7)

Applying this form to the line CD'B,

$$u_A = \frac{1}{2}[u_B + u_C] + \frac{1}{2}\frac{1}{c}\int_{CD'B} \dot{u}\,dx$$

(5.8)

The simplest discrete representation of (5.1) is obtained by approximating the second derivatives by the second central differences of the displacement. Applied at point D' of Figure 5.1,

$$\frac{u_B - 2u_{D'} + u_C}{\Delta x^2} = \frac{u_A - 2u_{D'} + u_D}{c^2 \Delta t^2}$$

(5.9)

which results in the following explicit algorithm for u_A:

$$u_A = \left(\frac{c\,\Delta t}{\Delta x}\right)^2 [u_B + u_C - 2u_{D'}] + 2u_{D'} - u_D$$

(5.10)

If the time step is chosen equal to the characteristic value (c Δt = Δx) the discrete propagation formula reduces to the exact one (5.5). This

was pointed out but not developed by Salvadori and Baron, p. 267 of [53].

If one introduces a central difference representation of the velocity,

$$\dot{u}_{D'} = \frac{u_A - u_D}{2 \Delta t} \tag{5.11}$$

and combines it with (5.5) to eliminate u_D,

$$u_A = \frac{1}{2} (u_B + u_C) + \dot{u}_{D'} \, \Delta t \tag{5.12}$$

The exact form (5.8) reduces to (5.12) if the velocity is constant over the interval CD'B, and $\Delta x = c \Delta t$. Thus one may propagate exactly a piecewise constant initial velocity field by the algorithm.

B. Explicit Algorithm as Characteristic Type

Consider now the more general hyperbolic equation

$$\frac{\partial^2 u}{\partial x^2} = \frac{1}{c^2} \frac{\partial^2 u}{\partial t^2} + \mathcal{L} (u) \tag{5.13}$$

where the linear operator $\mathcal{L}$ implies either the lower order differential operators contained in the wave equations governing cylindrical, spherical, or radial shear waves, or the linear integral operator of the simple viscoelastic bar discussed in Chapter 3. Integrating this equation over the diamond of Figure 5.1 and using (5.5)

$$u_A = u_B + u_C - u_D - \int_{ABDC} \mathcal{L} (u) \, da \tag{5.14}$$

The integral may now be approximated by an appropriate quadrature formula in terms of the four nodal displacements. The power of such an algorithm which exactly captures the discontinuity property of the solution will be

demonstrated in the examples to follow.

If the quadrature is made to depend on u_A, the method is locally implicit in that a division is required to determine u_A. It is not implicit in the sense of Chapter 4 in that u_A is not coupled to the other values of u along that line of constant t. Only the fully explicit form has been considered by this writer, but the other locally implicit forms probably have better stability properties and should be investigated.

The wave character of an operator such as (5.13) is disguised by the spatially discretized equation

$$M \ddot{\underset{\sim}{r}} + K_0 \underset{\sim}{r} + K \circledast \dot{\underset{\sim}{r}} = \underset{\sim}{P} \tag{4.1}$$

However, if the matrix K_0 does contain in part the discretization of a second space derivative, then the explicit $\beta = 0$ method using the characteristic time step contains the property of (5.14) with respect to that space variable.[*] If the operator $\mathcal{L}$ also contains second space derivatives with respect to additional space variables, important stability restrictions arise which limit the usefullness of the method.

In using $\beta = 0$ and $\gamma = 1/2$ with the characteristic time step in the algorithm of (4.B.1), an explicit time discretization of an applied boundary stress is implied. For the one dimensional wave operator this leads to the exact solution for displacements and stresses only if the applied stress is piecewise constant in time. The algorithm can be modified to yield exact results for piecewise linear applied

---

[*] In Chapter 3 it was shown that a piecewise linear expansion in the variational method was equivalent to the central difference approximation to the second spatial derivative.

stress if one uses the integral form contained in (4.B.2). In (4.10) a higher order quadrature may be used for the load vector integral than the $\beta = 0$ required in the stiffness integrals to generate the explicit method. A choice of $\beta = 1/4$ in the load integral then happens to ensure exact results for displacements and stresses for the one dimensional wave operator subjected to piecewise linear applied stress.

The method presented here is essentially the "discontinuous step" or "direct" method of Mehta and Davids [55] and Koenig and Davids [59]. They apply global balance laws to a discrete space-time element and write the discrete equations without ever considering the differential operator of the problem. The time step in their space-time element is chosen as the characteristic one, and so the same algorithm ensues as basically considered here. However, because the partial differential equations are never considered, they have no basis to assess the nature of the approximation and in particular the stability of the algorithm. They make claims for stability which are not supported by the examples to follow.

Another important method of solution for this family of generalized one dimensional problems is the classical method of characteristics. First the system is reduced to a system of first order partial differential equations. They are transformed into canonical form along the characteristic lines and then finite differences are used. An advantage of this method is that in the transformation to canonical form an ordinary differential equation results governing the intensities of discontinuities propagating through the medium. This equation yields values for the variables and their derivatives along the characteristic line ODB in Figure 5.1. Such jumps in the derivatives are only approxi-

mated by the explicit method presented here. The disadvantages of the method of characteristics is the retention of the space and time derivatives as additional primary variables, and the lack of an automated procedure for the spatial discretization of the subspace normal to the direction of propagation. That remains an open challenge for the full utilization of this otherwise powerful method.

C. One Dimensional Examples

1. Step Stress on a Viscoelastic Half Space

The problem of a step stress on a viscoelastic half space was formulated in Chapter 3, where the results of the converged numerical Laplace transform inversion obtained by Nickell [42] were presented. Figure 5.2 shows the approximation afforded by the explicit algorithm when the characteristic time step is used. Even a coarse mesh shows superior results to those of the finite degree of freedom model of Chapter 3 where a finer mesh was used. Since the elastic part of the operator is captured exactly by the algorithm, the oscillations about the exact solution are due to the approximation of the hereditary integral. The algorithm captures the exact location of the discontinuity, but only approximates the magnitude of it.

2. Triangular Pulse Through a Viscoelastic Slab

A second example, also taken from the work of Nickell [42], is that of a triangular stress pulse through a viscoelastic slab. The operator is the same as for the previous example, except that the stress free second surface of the slab defines a finite one dimensional domain. The triangular stress pulse is dispersed and decayed by the viscosity of the medium as it is reflected back and forth. The results of the explicit characteristic algorithm are presented in Figures 5.3 to 5.6 and compared
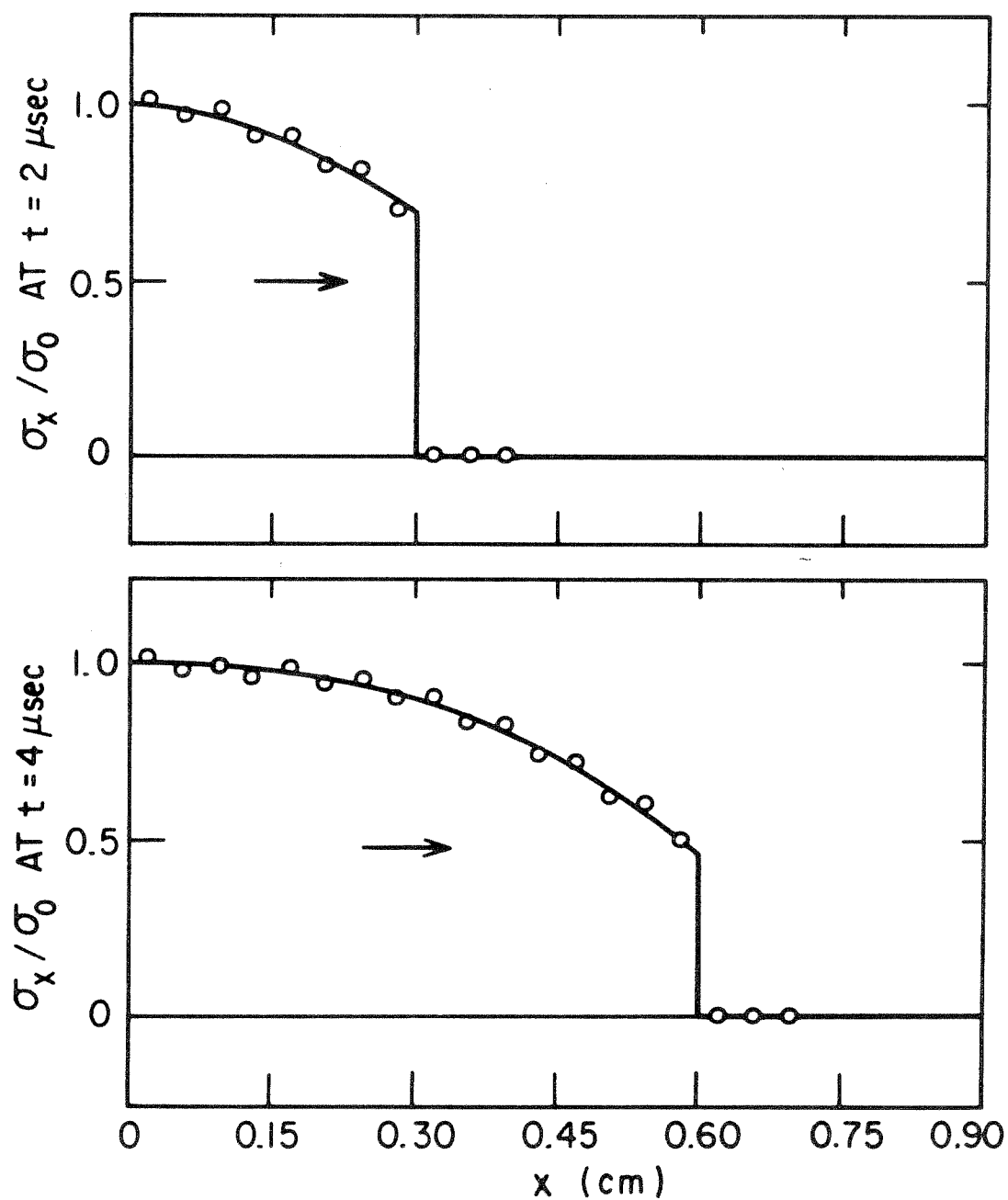
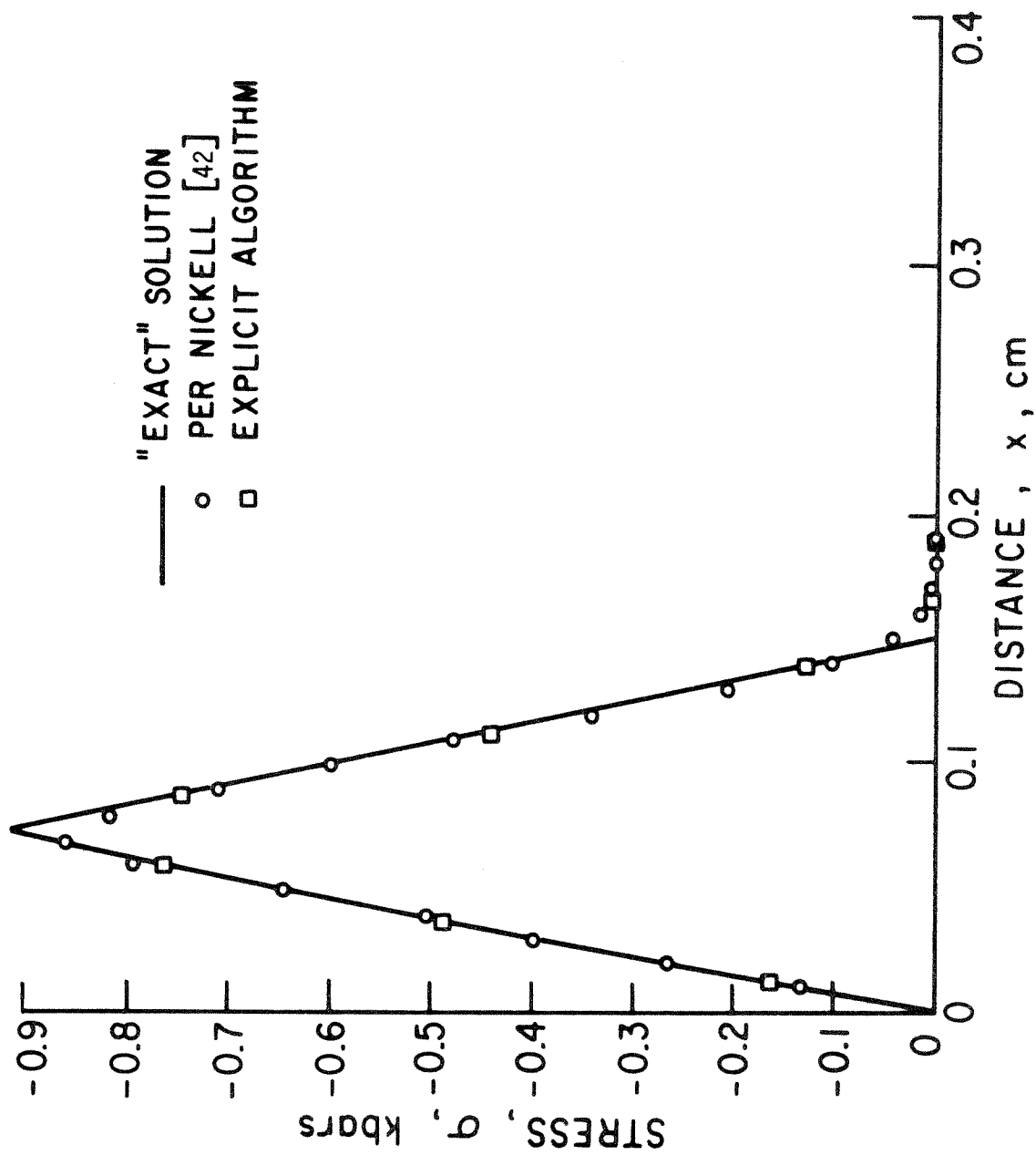FIG. 5.2   STEP STRESS ON A VISCOELASTIC HALF SPACE

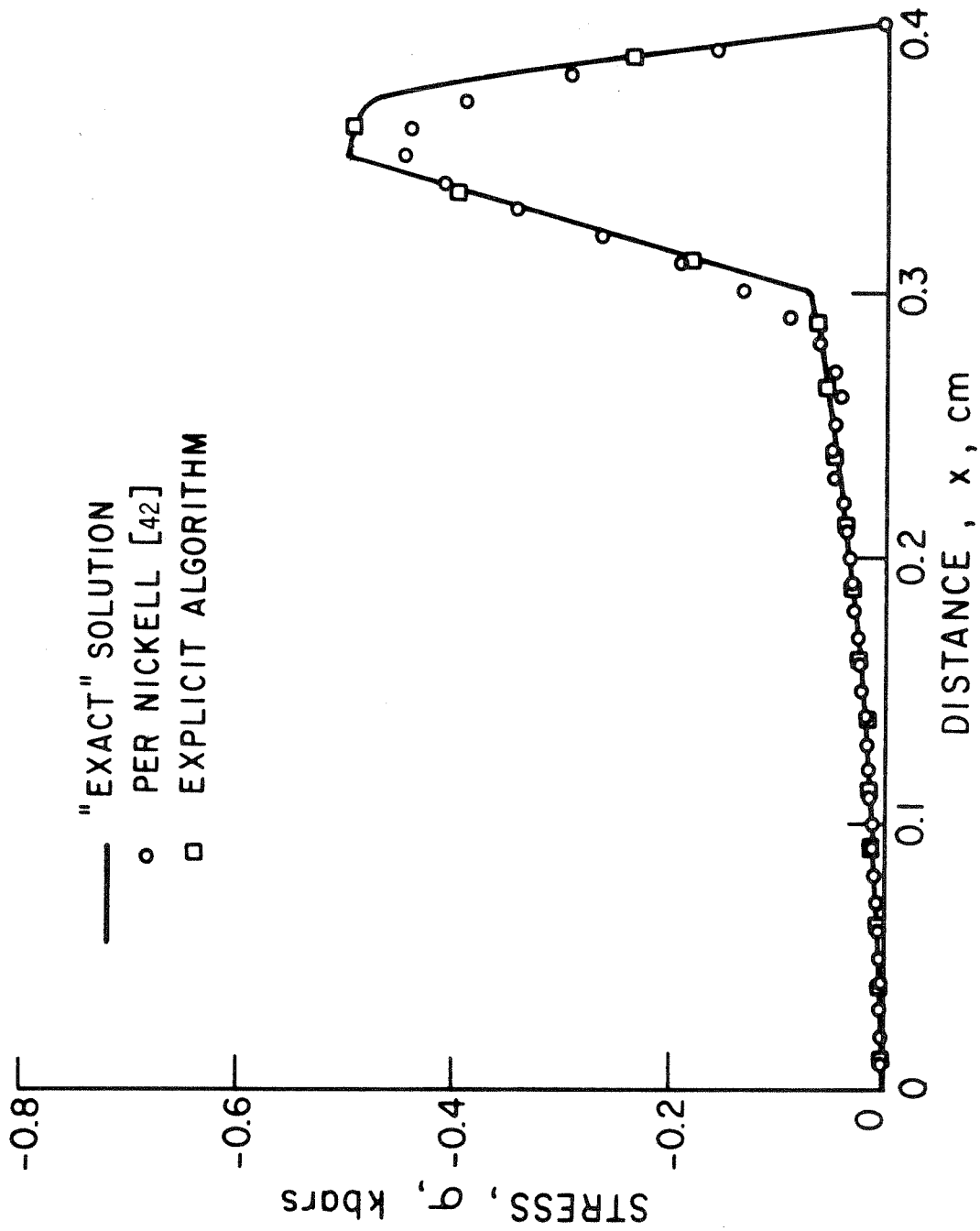FIG.5.3 RESPONSE TO TRIANGULAR PRESSURE PULSE, STRESS FOR 1 μsec

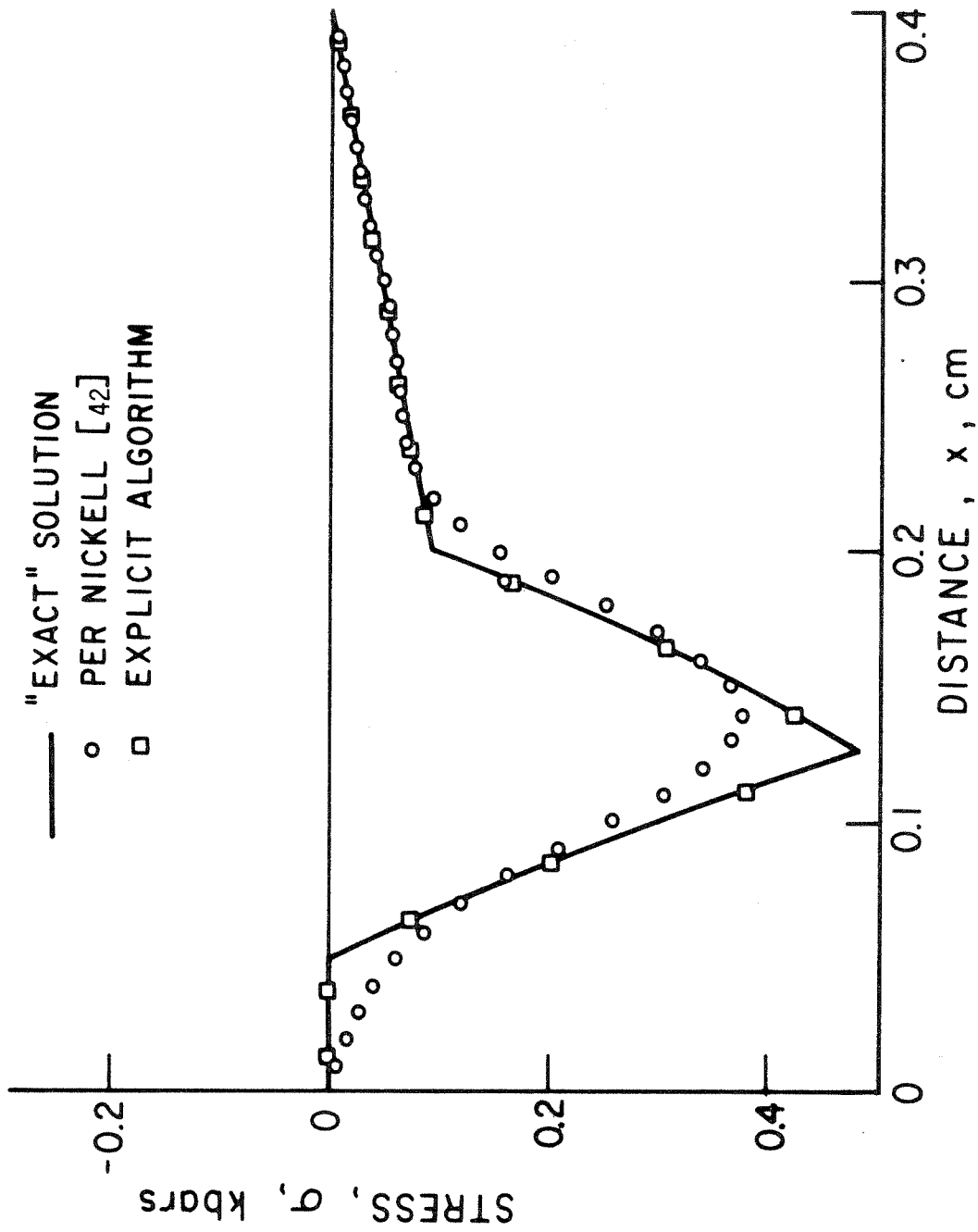FIG. 5.4 RESPONSE TO TRIANGULAR PRESSURE PULSE, STRESS FOR $t = 3 \, \mu sec$

FIG. 5.5 RESPONSE TO TRIANGULAR PRESSURE PULSE, STRESS FOR t = 5 μsec
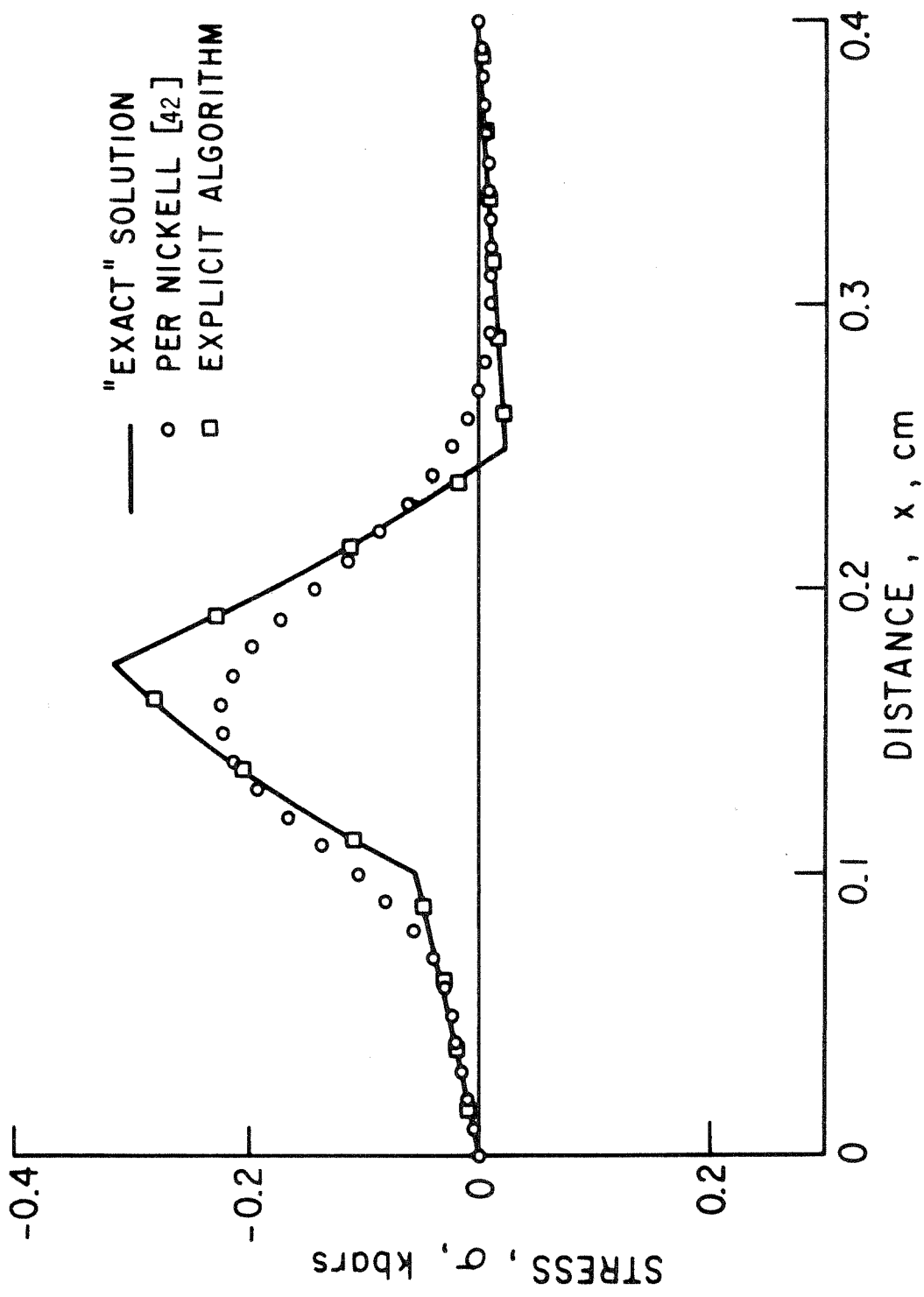
FIG. 5.6 RESPONSE TO TRIANGULAR PRESSURE PULSE, STRESS FOR t = 1 μsec

with Nickell's exact and finite element results. While the former results show no detectible error for a coarse mesh, the results of Nickell with a finer mesh show the geometric dispersion of the finite degree of freedom model and the damping of the time integration algorithm.

This and the previous example show the significance of the discontinuity property of the operator. It is elastic wave propagation which presents the principal challenge to approximation theory. Once that is achieved, viscoelasticity is easily accommodated.

3. Others

Efficient approximations are also obtained for the one dimensional elastic and viscoelastic cylindrical, spherical and shear waves. In particular, the propagation of plane waves through a layered half space (or simple bar) can be captured exactly, if the acoustic impedances, $\sqrt{(\lambda + 2\mu)\rho}, (\sqrt{E\rho})$, of the layers are in the ratio of rational numbers. In that case an integral number of elements can be found for each layer such that for all layers the propagation velocity of the algorithm matches the corresponding continuum velocity. If the impedance ratios are not rational, the true solution can be bracketed by the solutions for adjacent rational impedance ratios. Since subdivision of a mesh with rational ratios preserves the ratios, this bracketing can be made as tight as desired.

For all these one dimensional problems no stability problems arise, as long as the characteristic ratio is ensured.

D. Two Dimensional Examples

1. Higher Order Bar

A particular higher order bar theory, defined by one radial finite element, was introduced in the previous chapter. The solid curves
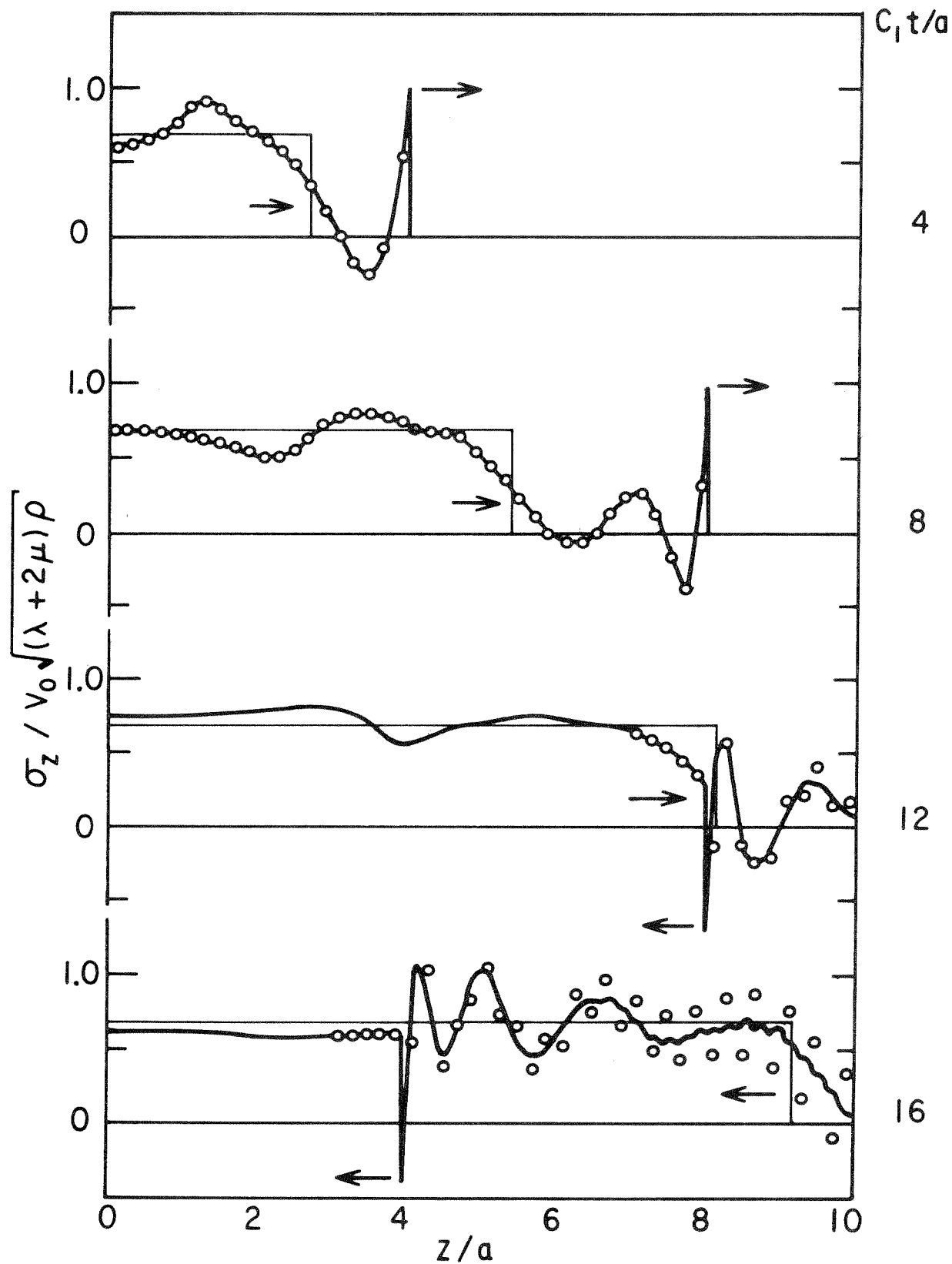
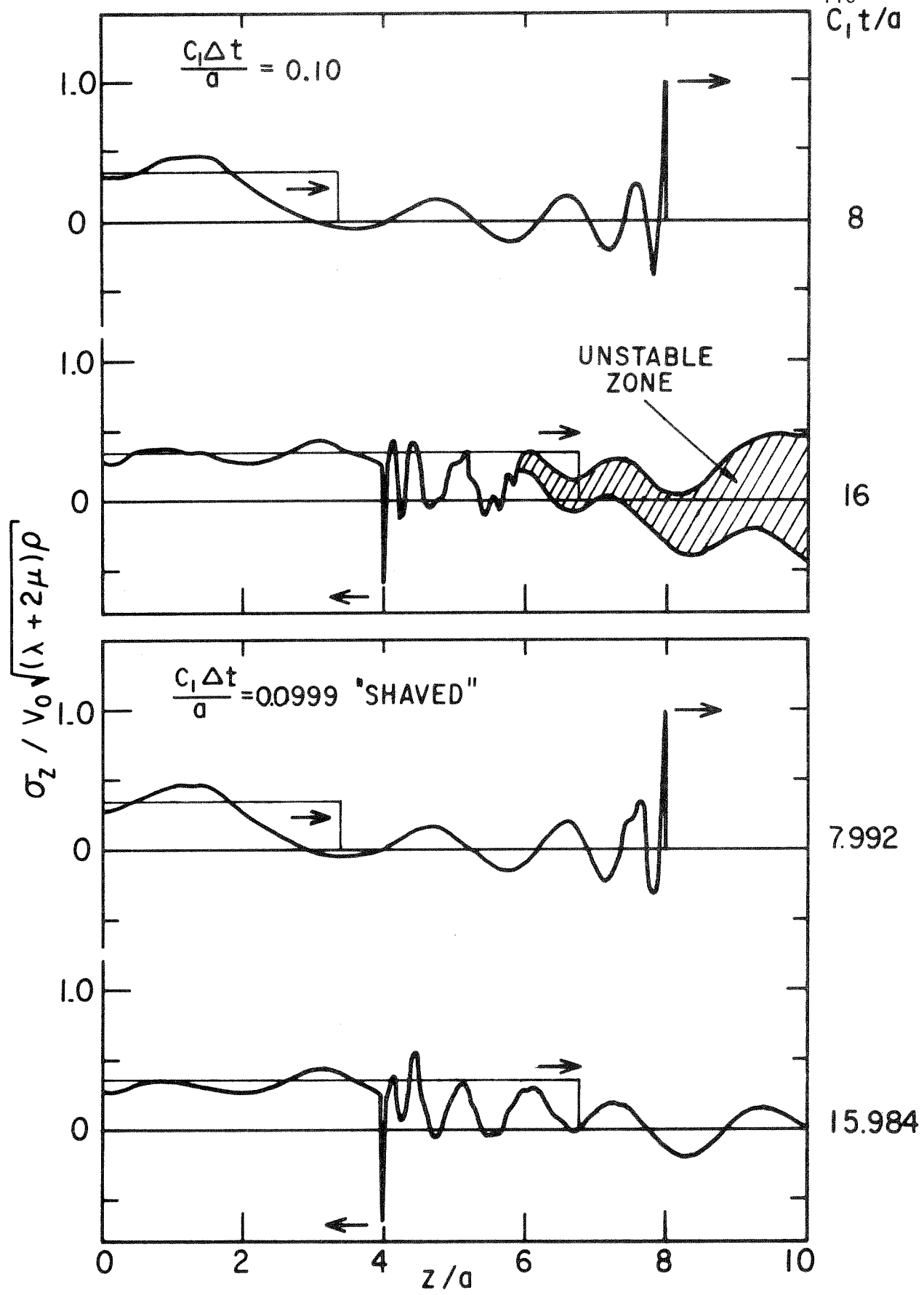FIG. 5.7 RIGID IMPACT OF HIGHER ORDER BAR
($\nu = 0.4$, $C_0/C_1 = 0.68$)

FIG. 5.8   RIGID IMPACT OF HIGHER ORDER BAR
($\nu = 0.48$, $C_0/C_1 = 0.34$)

expect that the use of a time step within the stable region should result in the bounded mesh induced oscillations of the finite degree of freedom model discussed in the previous two chapters. Yet they do not arise. The explanation for this is seen in Figure 4.3. As long as the shaving is small the algorithm lies on the vertical portion of the $\beta = 0$ curve and retains the character of the hyperbolic solution. If the time step is decreased too much, the solution will take on the character of the lumped mass model.

An explanation of the instabilities of this algorithm exhibited in Figures 5.7 and 5.8 would require the determination of the spectrum of the discrete model by the methods of Chapter 3, and will not be attempted here. The essential fact is that the characteristic time step used exceeds the stability limit of the highest frequency of the system which is one other than the highest longitudinal mode.

2. Two Dimensional Bar

An attempt to account for the full radial effect of an elastic bar during longitudinal wave propagation was presented by Bertholf [57]. He used a conventional finite difference discretization of both space and time. With his time step less than the characteristic one, that algorithm corresponds to the stable regime of the $\beta = 0$ method. Bertholf studied several examples of a uniform step stress applied to the end of a bar and exhibited the axial strain at the lateral surface. Since at the surface that strain does not suffer any finite discontinuity, he achieved accurate values with a mesh of ten radial elements and about thirteen per bar radius of length. The discussion of his paper by Tang and Yen and Bertholf's closure [58] acknowledged the mesh induced oscillations in the values of axial strain near the wave front in the interior of the bar.

Figure 5.9 shows that region, defined by the plane dilatational front and the circular unloading wave emanating from the outer surface boundary point at the impact end of the bar. This second front combines with the first at the intersection of the plane wave front with the surface to satisfy continuity of the axial strain at that point. The solution in this region is that of the one dimensional strain theory. It does not attenuate but the region itself shrinks in size as the radius of the arc from the initial outer edge more nearly equals the axial distance down the bar. Behind this second front the influence of the free lateral surface significantly complicates the otherwise simply defined problem. For long times the solution away from the end of the bar becomes more uniform in the radial coordinate and is adequately represented by higher order bar theories. It is evident that the dilatational spike shown in Figures 4.7 and 4.8 is a proper limit of the true solution and not an aberation of the approximate theory as frequently speculated [60, 61].

The explicit characteristic algorithm was applied to Bertholf's finite bar of one diameter length, using a mesh of eight radial and fifty axial elements. It captures the exact location of the dilatational discontinuity. Because the curvature of the second unloading front varies with time, it is not possible to capture the unloading discontinuity with a fixed mesh. However, since the unloading discontinuity is of second order (i.e., the strain is continuous), the constant value of the plateau region is only slightly perturbed.

For long bars, or even short bars at long time, the region near the dilatational front contains ever less energy and need not be well approximated. In early time behavior (where peak response is most likely

to occur) it is difficult to infer the true solution from the mesh induced oscillations when using a general method not accounting for the characteristics of the problem. In this case some account of the characteristic surfaces seems imperative if meaningful results are to be obtained at reasonable expense.
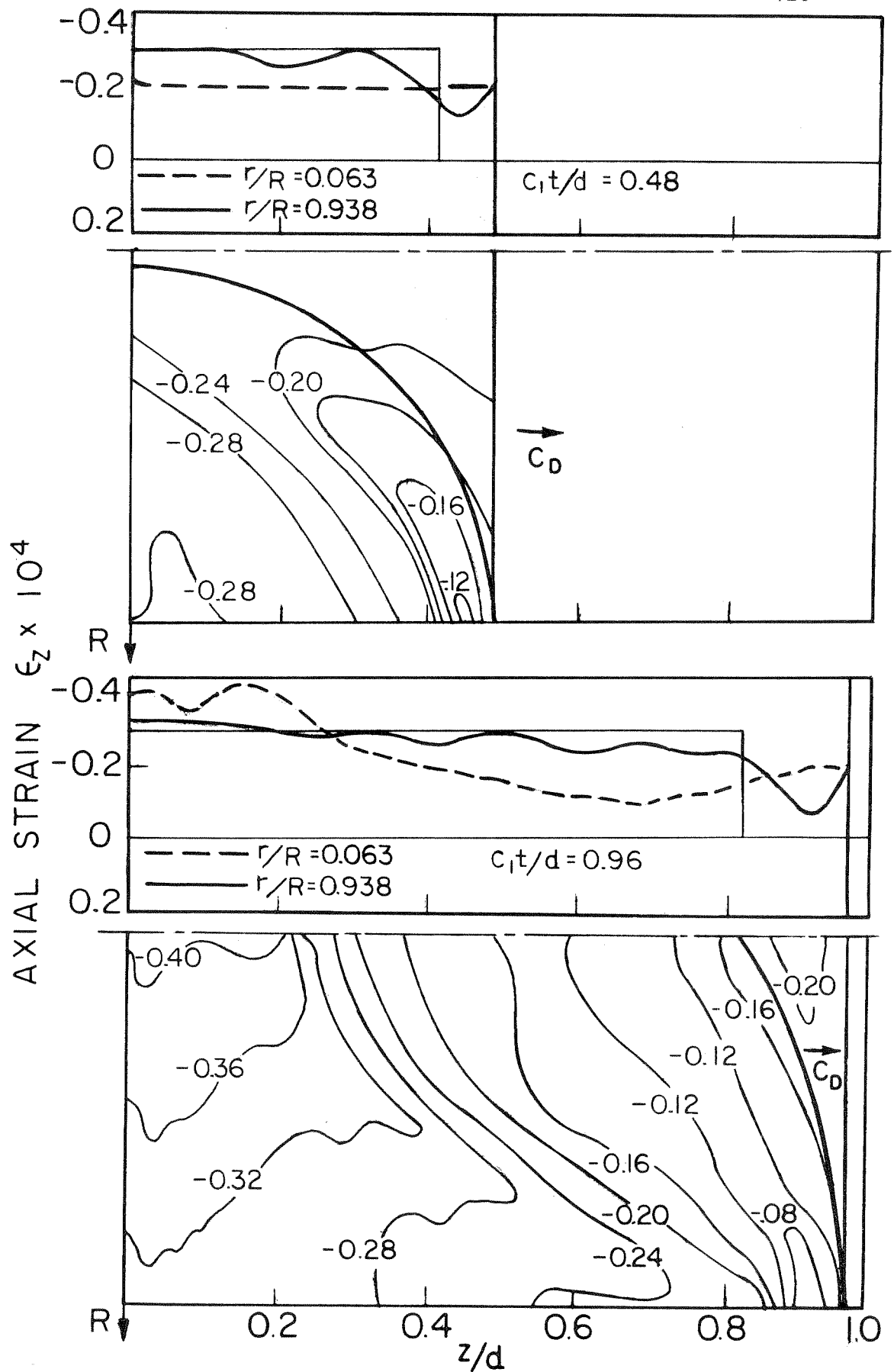
FIG 5.9 STEP STRESS ON BERTHOLF BAR
(ν = 0.3125), (8 × 50 GRID)

REFERENCES

1. S. H. Crandall, Engineering Analysis, McGraw-Hill (1956)

2. R. Courant, Methods of Mathematical Physics, V2, Interscience (1966), Chapters 5 - 6.

3. R. L. Taylor, "Problems in Thermoviscoelasticity," University of California Berkeley, Inst. Engr. Res. Rept. Ser. 199-1, January (1963) pp. 58 - 59.

4. M. E. Gurtin, "Variational Principles for Linear Elastodynamics," Arch. Rat. Mech. Anal. V16, N1 (1964) pp. 35 - 50.

5. M. J. Leitman, "Variational Principles in the Linear Dynamic Theory of Viscoelasticity," Quart. Appl. Math. V24, N1, April (1966) pp. 37 - 46.

6. R. Courant, "Variational Methods for the Solution of Problems of Equilibrium and Vibrations," Bull. American Math. Soc. V49 (1943) pp. 1 - 23.

7. M. J. Turner, R. W. Clough, H. C. Martin, and L. J. Topp, "Stiffness and Deflection Analysis of Complex Structures," J. Aeron. Sci., V23, N9 (1956), pp. 805 - 823.

8. J. H. Argyris, Energy Theorems and Structural Analysis, Butterworths, (1960) (Reprinted from Aircraft Engr. 1954 - 1955).

9. R. Courant, Methods of Mathematical Physics, V1, Interscience (1966) Chapter 4.

10. I. S. Sokolnikoff, Mathematical Theory of Elasticity, McGraw-Hill, (1956) Chapter 7.

11. C. A. Felippa and R. W. Clough, "The Finite Element Method in Solid Mechanics," presented at the AMS Symposium on Numerical Solutions of Field Problems in Continuum Mechanics, Durham, North Carolina, April, (1968).

12. S. G. Mikhlin, The Problem of the Minimum of a Quadratic Functional, Holden-Day, (1965).

13. R. W. Clough, "The Finite Element Method in Structural Mechanics," Chapter 7, of Stress Analysis, ed. by O. C. Zienkiewicz and Hollister, Wiley (1965).

14. Proceedings of the Conference on Matrix Methods in Structural Mechanics, Wright-Patterson Air Force Base, Ohio, October (1965).

15. O. C. Zienkiewicz and Y. K. Cheung, The Finite Element Method in Structural and Continuum Mechanics, McGraw-Hill (1967).

16. W. C. Hurty and M. F. Rubinstein, Dynamics of Structures, Prentice-Hall (1964), Chapter 8.

17. R. W. Clough and A. K. Chopra, "Earthquake Stress Analysis in Dams," Proc. ASCE, V92, EM2, (1966) pp. 197-211.

18. A. J. Carr, "A Refined Finite Element Analysis of Thin Shells Structures Including Dynamic Loads," SESM Report 67 - 9, University of California (Berkeley), June (1967).

19. R. W. Clough and C. A. Felippa, "A Refined Quadrilateral Element for Analysis of Plate Bending," Proceedings of the Second Conference on Matrix Methods in Structural Mechanics, Wright-Patterson Air Force Base, Ohio, August (1969)

20. J. S. Archer, "Consistent Mass Matrix for Distributed Systems," Proc. ASCE, V89, ST4, (1963) pp. 161 - 178.

21. Lord Rayleigh, Theory of Sound, MacMillan, London (1894)

22. K. Washizu, "Some Remarks on Basic Theory for Finite Element Method," Japan - U.S. Seminar on Matrix Methods of Structural Analysis and Design, August 25 - 30, (1969), Tokyo, Japan.

23. F. A. Leckie and G. M. Lindberg, "The Effect of Lumped Parameters on Beam Frequencies," Aeron. Quart. V14, August (1963) pp. 224 - 240.

24. R. D. Mindlin and G. Herrmann, "A One Dimensional Theory of Compressional Waves in an Elastic Rod," Proc. 1st U.S. Natl. Cong. Appl. Mech. (1950) pp. 187 - 191.

25. R. D. Mindlin and H. D. McNiven, "Axially Symmetric Waves in Elastic Rods," J. Appl. Mech., March (1960) pp. 145 - 151.

26. M. E. Gurtin and Eli Sternberg, "On the Linear Theory of Visco-elasticity," Arch. Ratl. Mech. Anal., V11, N4 pp. 291 - 356.

27. D. R. Bland, The Theory of Linear Viscoelasticity, Pergamon, 1960.

28. L. W. Morland and E. H. Lee, "Stress Analysis for Viscoelastic Material with Temperature Variations," Trans. Soc. of Rheology, V4 (1960).

29. R. L. Taylor, K. S. Pister, G. L. Goudreau, "Thermomechanical Analysis of Viscoelastic Solids," SESM Rept. 68 - 7, University of California, Berkeley, June (1968), (accepted for publication by Int. J. Num. Meth. Engr.)

30. F. Schwarzl and A. J. Staverman, "Time Temperature Dependence of Linear Viscoelastic Behavior," J. Appl. Phy., V23, N8, August (1952).

31. W. Stuiver, "On the Application of Variational Methods to Initial Value Problems in Dynamics," Trans. ASME, June (1962) pp. 242 - 246.

32. W. Stuiver, "A new Variational Approach to the Solution of Initial Value Problems," 4th U.S. Natl. Cong. Appl. Mech., (1962), pp. 401 - 409.

33. J. L. Sackman and I. Kaya, "On the Determination of Very Early-Time Viscoelastic Properties," J. Mech. Phys. Solids, V16, p. 121.

34. J. L Sackman, privale communication (1969).

35. R. E. Nickell, "Thermal Cycling Stress Analysis of the SPRINT Second Stage Motor," Bell Telephone Lab. Mem. 69-4116-8, April (1969).

36. C. Lanczos, "Separation of Exponentials," Applied Analysis, Prentice-Hall (1956), pp. 272 - 280.

37. N. Distefano and K. S. Pister, "On the Identification Problem for Thermorheologically Simple Materials" (to be published).

38. R. Kono, "The Dynamic Bulk Viscosity of Polystyrene and Polymethyl Methocrylate," J. Phy. Soc. Japan, V15, N4, April (1960) pp. 718-725.

39. F. B. Hildebrand, Finite Difference Equations and Simulations, Prentice-Hall (1968).

40. H. F. Weinberger, "Upper and Lower Bounds for Eigenvalues by Finite Difference Methods," Comm. Pure Appl. Math, V9 (1956) pp. 613 - 623.

41. H. F. Weinberger, "Lower Bounds for Higher Eigenvalues," Pac. J. Math, V8 (1958), pp. 339 - 368.

42. R. E. Nickell, "Stress Wave Analysis in Layered Thermoviscoelastic Materials by the Extended Ritz Method," Technical Report S-175, VII, Rohm & Haas Co., Redstone Research Laboratories, Huntsville, Al., October (1968), p. 24.

43. E. L. Wilson and R. E. Nickell, "Application of the Finite Element Method to Heat Conduction Analysis," Nuclear Engr. Design 4 (1966) pp. 276 - 286.

44. C. A. Felippa, "HQRW - General Eigenvalue Routine for Real Symmetric Matrices," SESM Computer Programming Series, University of California (Berkeley), February (1967).

45. C. A. Felippa, "BANEIG - Eigenvalue Routine for Symmetric Band Matrices," SESM Computer Programming Series, University of California (Berkeley), July (1966).

46. H. Rutishauser, "On Jacobi Rotation Patterns," <u>Proc. Symposia in Appl. Math.</u>, AMS, V60, pp. 219 - 240.

47. N. M. Newmark, "A Method of Computation for Structural Dynamics," <u>Proc. ASCE</u>, V85, EM3, July (1959).

48. R. E. Nickell, "On the Stability of Approximation Operators in Problems of Structural Dynamics," (submitted for publication to the Int. J. Solids and Structures).

49. L. Fox and E. T. Goodwin, "Some New Methods for the Numerical Integration of Ordinary Differential Equations," <u>Proc. Cambridge Phil. Soc.</u> V49, pp. 373 - 388.

50. E. L. Wilson, "A Computer Program for the Dynamic Stress Analysis of Underground Structures," <u>SEL Rept. 68-1</u>, University of California (Berkeley), January (1968).

51. I. Farhoomand, "Non-Linear Dynamic Stress Analysis of Two-Dimensional Solids," Ph.D Dissertation, University of California, (Berkeley) June 1970.

52. R. E. Nickell and J. L. Sackman, "Approximate Solutions in Linear Coupled Thermoelasticity," <u>J. Appl. Mech</u>, V34, N2, <u>Trans. ASME</u>, V89, Ser. E, June (1968).

53. M. G. Salvadori and M. L. Baron, <u>Numerical Methods in Engineering</u>, Prentice-Hall, Inc. (1961).

54. R. D. Richtmyer and K. W. Morton, "Difference Methods for Initial-Value Problems, Sec. Ed., <u>John Wiley and Sons, Inc.</u>, (1967).

55. P. K. Mehta and N. Davids, "A Direct Numerical Analysis Method for Cylindrical and Spherical Elastic Waves," <u>J. AIAA</u>, V4, N1, January (1966), pp. 112 - 117.

56. P. C. Chou and R. W. Mortimer, "Solution of One-Dimensional Elastic Wave Problems by the Method of Characteristics," JAM, September (1967) pp. 745 - 750.

57. L. D. Bertholf, "Numerical Solution for Two-Dimensional Elastic Wave Propagation in Finite Bars," JAM, September (1967), pp. 725 - 734.

58. S. C. Tang and D. H. Y. Yen, Discussion of [57], JAM, March (1968), p. 199.

59. H. A. Koenig and N. Davids, "Dynamical Finite Element Analysis for Elastic Waves in Beams and Plates," <u>Int. J. Solids and Struct.</u> V4 (1968), pp. 643 - 660.

60. J. Micklowitz, "The Propagation of Compressional Waves in a Dispersive Elastic Rod," <u>JAM</u>, June (1957), pp. 231 - 244.

61. Y. Mengi and H. D. McNiven, "Method of Characteristics for Solving Problems of Axisymmetric Wave Propagation," <u>SEL Rept. 69-6</u>, University of California (Berkeley), May (1969).